Resource Allocation in Cellular Networks with Coexisting Femtocells and Macrocells

Yongsheng Shi

Dissertation submitted to the Faculty of the
Virginia Polytechnic Institute and State University
in partial fulfillment of the requirements for the degree of

Doctor of Philosophy
in
Electrical and Computer Engineering

Allen B. MacKenzie, Chair
Charles W. Bostian
Claudio da Silva
Luiz A. DaSilva
Anil Vullikanti

November 18, 2010
Blacksburg, Virginia

Keywords: Resource allocation, femtocells, cellular networks, graph theory, random graph, genetic algorithm

Resource Allocation in Cellular Networks with Coexisting Femtocells and Macrocells

Yongsheng Shi

(ABSTRACT)

Over the last decade, cellular networks have grown rapidly from circuit-switch-based voice-only networks to IP-based data-dominant networks, embracing not only traditional mobile phones, but also smartphones and mobile computers. The ever-increasing demands for reliable and high-speed data services have challenged the capacity and coverage of cellular networks. Research and development on femtocells seeks to provide a solution to fill coverage holes and to increase the network capacity to accommodate more mobile terminals and applications that requires higher bandwidth.

Among the challenges associated with introducing femtocells in existing cellular networks, interference management and resource allocation are critical. In this dissertation, we address fundamental aspects of resource allocation for cellular networks with coexisting femtocells and macrocells on the downlink side, addressing questions such as: How many additional resource blocks are required to add femtocells into the current cellular system? What is the best way to reuse resources between femtocells and macrocells? How can we efficiently assign limited resources to network users?

In this dissertation, we develop an analytical model of resource allocation based on random graphs. In this model, arbitrarily chosen communication links interfere with each other with a certain probability. Using this model, we establish asymptotic bounds on the minimum number of resource blocks required to make interference-free resource assignments for all the users in the network. We assess these bounds using a simple greedy resource allocation algorithm to demonstrate that the bounds are reasonable in finite networks of plausible size. By applying the bounds, we establish the expected impact of femtocell networks on macrocell resource allocation under a variety of interference scenarios.

We proceed to compare two reuse schemes, termed shared reuse and split reuse, using three social welfare functions, denoted utilitarian fitness, egalitarian fitness, and proportionally fair fitness. The optimal resource split points, which separate resource access by femtocells and macrocells, are derived with respect to the above fitness functions. A set of simple greedy resource allocation algorithms are developed to verify our analysis and compare fitness values of the two reuse schemes under various network scenarios. We use the obtained results to assess the efficiency loss associated with split reuse, as an aid to determining whether resource allocators should use the simpler split reuse scheme or attempt to tackle the complexity and overhead associated with shared reuse.

Due to the complexity of the proportionally fair fitness function, optimal resource allocation for cellular networks with femtocells and macrocells is difficult to obtain. We develop a genetic algorithm-based centralized resource allocation algorithm to yield suboptimal solutions for such a problem. The results from the genetic algorithm are used to further assess the performance loss of split reuse and provide a baseline suboptimal resource allocation. Two distributed algorithms are then proposed to give a practical solution to the resource allocation problem. One algorithm is designed for a case with no communications between base stations and another is designed to exploit the sharing of information between base stations. The numerical results from these distributed algorithms are then compared against to the ones obtained by the genetic algorithm and the performance is found to be satisfactory, typically falling within 8% of the optimum social welfare found via the genetic algorithm. The capability of the distributed algorithms in adapting to network changes is also assessed and the results are promising.

All of the work described thus far is carried out under a protocol model in which interference between two links is a binary condition. Though this model makes the problem more analytically tractable, it lacks the ability to reflect additive interference as in the SINR model. Thus, in the final part of our work, we apply conflict-free resource allocations from our distributed algorithms to simulated networks and examine the allocations under the SINR model to evaluate feasibility. This evaluation study confirms that the protocol-model-

based algorithms, with a small adjustment, offer reasonable performance even under the more realistic SINR model.

This work was supported by the National Institute of Justice, Office of Justice Programs, U.S. Department of Justice under Award No. 2005-IJ-CX-K017 and the National Science Foundation under Grant No. 0448131. Any opinions, findings, and conclusions or recommendations expressed in this dissertation are those of the author and do not necessarily reflect the views of the National Institute of Justice or the National Science Foundation. The NSF/TEKES Wireless Research Exchange Program also contributed to this work by funding a summer study.

Acknowledgments

When it finally comes to this moment, my great praise goes to my wife. Thanks for her support, encouragements, and patience during last the 4 years. When I first proposed the idea of going to America to pursue a Ph.D., I was amazed that she was so supportive, though she knew it would be a hard time ahead of us for separation in two counties. Fortunately, she ended up coming to Blacksburg in my second year of the Ph.D. study. I promised to her that I would obtain my degree within 4 years. I have always been guilty because I am going to finish the study in a longer time. During my toughest time of the study, when I was struggling with finding the right research direction and spending hours, days and nights, and weeks solving problems, her encouragements and and patience gave me endless strength and hope. My sincere thanks will also go to parents. Their selfish support and sacrifice have fueled me to chase my dream.

I would like to thank all my friends and they have made my life in Blacksburg colorful. I would also like to thank all my colleagues for their contributions and help to my work. I would especially like to mention Dr. Daniel Friend and Dr. Mustafa El-Nainay for sacrificing their time and efforts helping my research work. I spent two times of totally 10 month working with Qualcomm as an Intern. The work conducted at Qualcomm inspired the idea behind this dissertation.

I would like to thank all my committee members. Dr. Bostian and Dr. Luiz DaSilva both directly worked on part of my work. Their expertise and wisdom helped me through the Ph.D. study. Dr. Claudio da Silva and Dr. Anil Vullikanti gave valuable comments on

my research work.

Ultimately, I will express thanks to my advisor, Dr. Allen MacKenzie. He recruited me to Virginia Tech and gave me a great platform to work on. He did not set a specific research topic for me and instead, he would let me to explore and find my own interest. This is a very different way of advising compared to my previous student experience. I had difficulties at first and had not found a good kick-off point to start the research work. Now eventually, I have tasted the sweet part of his advising. The Ph.D. study instructed by him has trained me to successfully formulate, approach, and solve a problem. I believe these attributes will help me to build my future career. Once I am into my research and meet problems, his insightful and sharp instructions have guided me over many obstacles. Dr. MacKenzie's concern on his students' life and family is also greatly appreciated. Definitely, he is the best academic advisor I have ever worked with.

Contents

List of Figures

List of Tables

Chapter 1

Introduction

1.1 Overview

With the proliferation of mobile computing and communication platforms, such as cell phones, laptops, and various hand-held digital devices, the information society is being driven from the personal computer age to the ubiquitous computing age. A user may want to utilize several electronic platforms to access all required information whenever and wherever needed. Thus, we have experienced rapid development and growth in wireless communications and wireless networks in the past decade. Various new ideas and technologies have been proposed and studied to cater to modern telecommunication networks.

Heterogeneity and complexity are two remarkable characteristics of modern wireless networks. The two features make current wireless networks difficult to configure and operate manually. In some cases, the complexity of wireless networks far exceeds the capability of users and operators to optimally handle them. The network has to incorporate a great degree of intelligence to perform autonomously or at least with little human intervention. Also, it is well known that the operational environment of wireless networks is dynamic. The network should be able to perceive and adapt to different network conditions by itself. A potential

solution to meet these challenges is a cognitive radio that observes the surrounding network environment and reconfigures to adapt to network changes.

Cellular networks are one of the most important commercial applications of wireless networks, offering both voice and data services to end users. As the network scale increases, user's demands diversify, and new applications appear, cellular networks also become more complex and heterogeneous. Usually, the network is tuned by teams of skilled professionals and runs in a relative static way. Each base station's (BS's) parameters, frequency reuse pattern, and core network configurations are preset and remain constant until they are adjusted manually, normally driven by network condition changes, such as deploying new BSs, changing current BSs' positions, adding new spectrum bands, and so on. Under this kind of operation, the cellular network is blind to the surrounding network environments. When there are changes in network conditions, the network is not able to react and must await human intervention. Cellular networks need to become more dynamic and autonomous.

In addition, emerging new technologies, such as customer owned femtocells, make manual operation by operators almost impossible. Driven by the continued worldwide growth in demand for mobile communications, mobile operators are evaluating and deploying technologies that deliver voice and data services to users' homes and workplaces. According to [3], 50% of phone calls and 70% of data services will take place indoors in the next years. However, traditional cellular networks often have inadequate building penetration and thus cannot offer high quality services to indoor users. Research shows that only two percent of buildings are currently equipped with purpose-built indoor coverage solutions [4]. This issue becomes more critical with increased popularity of smart phones, which have many applications requiring high data rate. With the growing demand for these new services, most industry observers see significant potential for the use of new technology in the form of femtocells. Femtocells operate in the same spectrum as the macrocell network, enabling high quality services to be delivered to indoor mobiles. A femtocell BS (fBS) creates a small coverage area and uses broadband Internet service as the backhaul to connect to the core network. Unlike macrocell BSs, fBSs are owned by customers and are deployed in an ad hoc

fashion. This ad hoc deployment makes it almost impossible for mobile operators to manually configure cellular networks with coexisting femtocells and macrocells. Future cellular networks must be self-organized and self-optimized.

This dissertation applies cognitive radio concepts to cellular networks with macrocells and femtocells, particularly on resource allocation. Cognitive radio technology, first proposed by Mitola in [5], is defined by a cognitive cycle: observe, orient, decide, and act. The network senses and gathers useful information locally or externally. Based on this information, the network uses algorithms, its past experience, or external instructions to make appropriate decisions under current network conditions. Once these decisions are applied, the network enters a new cycle. The cognitive cycle can thus help make cellular networks smarter and more autonomous on resource allocation.

1.2 Femtocells

1.2.1 Development of Cellular Networks

Currently, cellular networks are the most used wireless coverage and data transmission networking technology. While earlier Global System for Mobile communications (GSM) and IS-95 standards begin to be phased out, Universal Mobile Telecommunications System (UMTS) and cdma2000 are two main standards behind current cellular networks. User demand for both high data rate service and good voice communication coverage in wireless networks continues to increase. Several new data-oriented standards have been actively discussed and developed in recent years to address this growing demand. Influential standards include: the 3rd Generation Partnership Project's (3GPP) High Speed Packet Access (HSPA), High Speed Packet Access Plus (HSPA+), Long Term Evolution (LTE), and LTE Advanced standards; 3GPP2's Evolution Data Optimized (EVDO) and Ultra Mobile Broadband (UMB) standards; and Worldwide Interoperability for Microwave Access (WiMAX) (IEEE 802.16).

Another notable technology is Wireless-Fidelity (WiFi), or IEEE 802.11 series, networks. Although WiFi networks are not able to offer the same level of Quality of Service (QoS) that WiMAX, 3GPP, and 3GPP2 standards could offer and lack support for mobility, they achieve great flexibility by using licence-free channels and customer deployment, which make WiFi networks suitable for home and home office applications.

Indoor coverage and service are a vulnerability of cellular networks because wireless transmissions are greatly affected by fading and shadowing. To compete with WiFi networks, cellular systems must keep their advantage of guaranteed QoS while offering indoor services comparable to WiFi networks.

Martin Cooper of Arraycomm observed that the wireless capacity has doubled every 30 months over the last 104 years. This corresponds to about one million times capacity increase in past 50 years. If we break down the capacity gains, there has been a 25x improvement from wider spectrum, a 5x improvement by dividing the spectrum into smaller slices, a 5x improvement by designing better modulation schemes, and a 1600x gain through reduced transmit distance (i.e. reduced cell sizes) [6]. With smaller cell sizes, spectrum is reused more efficiently, causing the enormous gains shown above.

One of the most effective ways to increase network capacity and improve wireless coverage is to get the transmitter and receiver closer to each other. Cell size flexibility is a feature of cellular networks and is a significant factor in improving the capacity of such networks. Power controls implemented on networks make it possible to prevent interference from neighboring cells using the same frequencies. By subdividing cells and creating more cells to serve high density areas, a cellular operator can optimize the use of spectrum and ensure the capacity can grow. Thus, in addition to original macrocells, microcells, pictocells, and relaycells have also been proposed.

Microcells and picocells are smaller cells compared to macrocells. They are equipped with a lower-power BS that provides coverage and adds network capacity in areas with dense cellular phone usage, such as one or two street blocks, a shopping mall, or a transportation

hub. Sometimes, they are deployed temporarily during sporting events and other occasions in which extra capacity is known to be needed at a specific location ahead of time. Microcells and picocells allow the operator to either load balance users [7–9] or preferentially assign high data rate cellular users [10–12].

Relaycells do not have a wired connection to the backhaul network and are connected to a macrocell BS via wireless link. They are used to help increase network coverage in suburban areas where deploying a macrocell BS is economically infeasible. Various works have shown that relay technologies can effectively improve service coverage and system throughput, and relaycells can also be successfully applied in areas suffering from high path loss [13–16]. The macrocell BS and relaycell BS form a multi-hop wireless network. Relaycells have been a research focus recently as the concept of multi-hop cellular networks has arisen, for example, in the multi-hop relay specification for WiMAX. Wireless Regional Area Networks (WRANs), based on IEEE 802.22, also adopts the idea of relaycells. Relaycells can be used to fix coverage holes in existing cellular systems, normally at the cell edge, or sometimes to provide temporary coverage like microcells and picocells do. From a communications perspective, a relaycell BS needs to synchronize with its upstream macrocell BS to ensure coherent reception and improved signal strength for the cellular phone user [17]. Also, implementing relaycells require careful design of signaling and data packet routing between relaycell BS and macrocell BS. Efficiently sharing spectrum between macrocells and relaycells is another potential problem. Figure 1.1 shows a cellular networks with relaycells.

There are common problems associated with the above ideas. First, all these cells are operator deployed and maintained. Although this makes it easier for the operator to plan, deploy, and control the cells, it increases the effort and cost required to run the network. Second, though the cell size is greatly reduced in microcell and picocell, they still may be unable to offer high data rate services to home and office users because they are mainly designed to increase capacity in a dense area rather than to provide good indoor coverage. To meet these challenges, the concept of femtocells has become an intensive research topic.

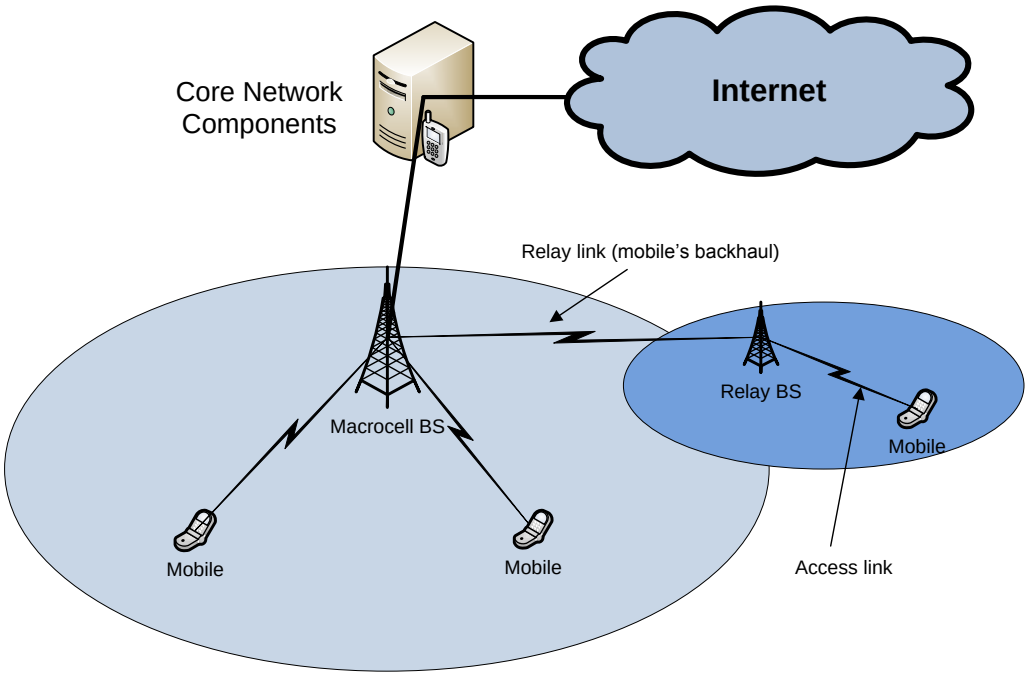

Figure 1.1: A cellular networks with relaycells

1.2.2 Concept of Femtocells

A femtocell is a small low power cellular BS, typically designed for use in a home or small business. It connects to the operator's network via broadband internet, which could be provided via DSL or cable modem. It is normally designed to support 2 to 4 active mobile users in a residential setting, although some investigation of office and enterprise deployment is underway. A femtocell allows an operator to extend service where access would otherwise be limited or unavailable. The femtocell incorporates the functionality of a typical BS but allows simpler, customer deployment. The concept is applicable to all cellular standards. For a mobile user, the attractions of a femtocell are improvements to coverage and capacity, especially indoors. For a cellular network operator, besides increased capacity and indoor coverage, there may also be opportunities for new services and reduced cost. Operators do not need to spend money maintaining femtocells. A femtocell allows the operator to deliver the benefits of fixed-mobile convergence while taking advantage of existing handsets. Figure

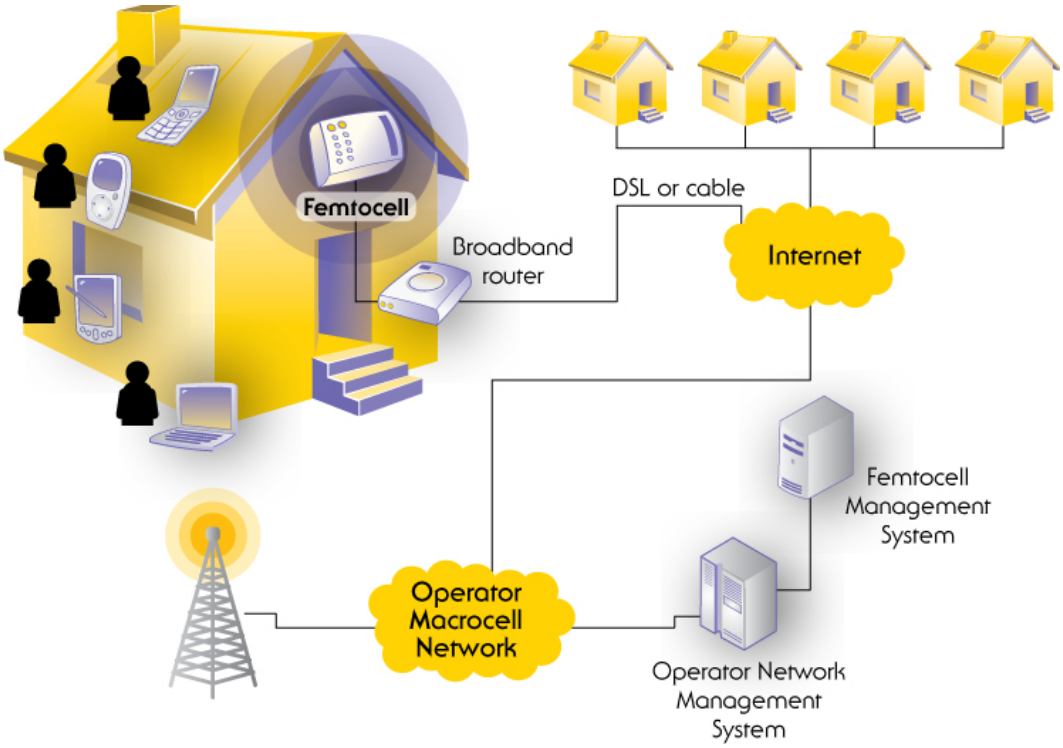

Figure 1.2: Typical femtocell deployment scenario [1] ©May 2008 Femto Forum, used by permission.

1.2 shows a typical femtocell deployment scenario.

Femtocells have following distinguishing features:

- **Overlay on top of current cellular networks**

  Femtocells use current cellular standards over the air to communicate with user equipment. Those standards could include: GSM, IS-95, UMTS, cdma200, LTE, and WiMAX. The International Telecommunication Union has estimated that mobile cellular subscriptions worldwide reached approximately 4.1 billion by the end of 2008 [18]. Thus femtocells deployments compatible with existing cellular networks will have a huge potential market.

- **Spectrum efficiency**

  Spectrum is a precious resource. In some countries, operators have to pay billions of

dollars to acquire access to spectrum. Femtocells operate on the mobile operator's own spectrum. The spectrum may be either already allocated to the operator but not being used or in use in macrocells. With fine controls on transmit power and effective coordination between femtocells and macrocells, the spectrum can be efficiently reused and hence could serve a greater number of users without requiring more spectrum. Simulation results show a significant gain in spectrum efficiency in both uplinks and downlinks when femtocells are correctly deployed [19, 20]. In addition, with femtocells, it is possible to make use of higher frequencies, at which the transmission range limits wide-area operation.

- **Customer owned and deployed**

  Femtocells are purchased, installed, and operated by customers and thus are deployed in an ad-hoc mode. Femtocells extend the operator's high data rate service to a customer's apartment or house. Though limits on femtocell operational parameters, such as power level and channel selection, are still set by the operator, femtocells may have autonomy to set some parameters automatically. The control on femtocells from operators is much less than on macrocells.

- **Improved access**

  Femtocells offer users truly broadband access using existing mobile devices. In addition, mobile users will experience better indoor access to cellular networks. In certain areas, it is difficult and costly to build a macrocell BS. Femtocells can be an easy way to get customers in those areas access to mobile services.

- **Operate in licensed spectrum and use internet as backhaul**

  Unlike WiFi networks, which use free wireless channels to provide data transmission, femtocells use operator owned or licensed spectrum over the air and thus can provide assured QoS. However, femtocells will use broadband Internet as backhaul and this may limit QoS because the operator cannot control the backhaul.

- **Reduce operator's cost and reduce load on macrocells**

Femtocells connect to an operator's core network via broadband Internet and thus the operator avoids the cost of femtocells' backhaul. It is expected that many users will use femtocells while at home or in their offices. This will reduce macrocell traffic and allow macrocells to offer better service to macrocell users. A comprehensive analysis of the femtocell business model is given in [21].

1.3 Current Deployment and Challenges

1.3.1 Business Challenges

The femtocell market opportunity, estimated to be as high as $22.5 billion by 2013, has caught the attention of incumbents and start-ups alike [22]. The problem for mobile operators is how quickly they can overcome challenges and gain market acceptance for femtocells as the technology of choice for in-home wireless access.

A direct competitor to femtocells is WiFi, which has achieved great success all over the world. In developed countries, many families already use WiFi to access Internet from their homes. Today, a WiFi chipset costs only a couple of dollars, and the price of WiFi access points has dropped below $20. More importantly, WiFi users are accustomed to using wireless access for free once they purchase and install the access point (except for the monthly payment to the Internet Service Provider). Although technically WiFi networks do not guarantee any QoS and sometimes their connections drop, most customers are still satisfied with their performance.

For femtocells, the cost is of paramount concern to most industry watchers. The market simply will not open unless femtocells are affordable to end users. At least for now, with a small number of femtocell users, the price of a femtocell BS is much higher than a WiFi access point. For example, Sprint customers are be able to purchase the Airave femtocell, which is made by Samsung, at Sprint stores nationwide for $99.99. To get the additional coverage,

they must pay an extra $4.99 per month. This could give customers the impression that the operator is asking the subscriber to pay for its lack of investment in providing sufficient indoor coverage. The implication is that the subscriber would be reluctant to pay to remedy the operator's shortcoming. Currently, even the most optimistic market growth estimates suggest that femtocells will take years to approach WiFi access point volumes and price points.

Operators may be forced to subsidize customers who are willing to purchase a femtocell BS in order to keep the price low and encourage early adopters. At the same time, the operator must find other ways to lower the price. For example, operators may charge a lower rate to use femtocells or work with manufactures to integrate femtocell BS with other home networking equipment. For example, it might be a good idea to integrate femtocell components into a set-top box or a cable/DSL modem to provide further opportunities for cost reduction.

WiFi devices cover a much broader range than just phone services. Today, WiFi is embedded in an extraordinary range of consumer devices, from the personal computer, which is now by default equipped with the WiFi interface, to digital cameras, game consoles, scanners, and printers. This is due to the ubiquity of WiFi home access points, interoperability guaranteed by strong standards, and the low cost of equipment due to huge volume production. In addition, some cellular phones now include a WiFi interface, for example, the Apple iPhone and many smartphones running the Android operating system. Thus the increased application of WiFi has squeezed the potential market for femtocells.

Another strong point of WiFi is that its access point interface is clearly defined, allowing multi-vendor interoperability and driving designers to seek novel and profitable new applications. It is difficult to see this happening in the femtocell community where each device will be vendor/operator specific. Thus it is necessary to develop an open standard for femtocells to assure product interoperability.

Consequently, cost, application and interoperability are three major business challenges

for femtocells. It is known that two important resources that a mobile operator has are information about subscribers, which is helpful to customize applications for different users, and a cellular network with a nationwide coverage, which establishes a high threshold for other technologies that want to enter the market. To compete with WiFi networks, mobile operators must use their strengths, come up with good business models, and cooperate with each other. In addition to Sprint, Verizon Wireless has launched their femtocell service. T-mobile, AT&T, and some European and Asian operators have conducted tests but have not yet entered the market. Verizon Wireless's entrance may be of most interest since Verizon also provides broadband Internet service and this dual-role may help them to operate femtocells more efficiently and develop good applications.

1.3.2 Technical Challenges

Though the concept of a femtocell is straightforward and femtocells are compatible with existing cellular networks, several technical challenges remain to be addressed.

1.3.2.1 Interference Management

Interference management is the first problem facing mobile operators. Interference management, in fact, is a two-fold problem: spectrum allocation and interference control. The macrocell base station is operator owned and maintained. The spectrum reuse policy is well defined to avoid intra-cell interference and mitigate inter-cell interference. If unexpected interference occurs, the operator can take steps to address the interference. However, the femtocell base station is customer owned and ad-hoc deployed. In some areas, thousands of femtocell base stations may be deployed in a single macrocell. The deployment could severely impact the operator's planned spectrum allocation. Various works show that without careful spectrum planning, macrocell users and femtocell users could suffer from severe interference problems on both uplink and downlink [23–26]. Figure 1.3 shows typical interference sce-

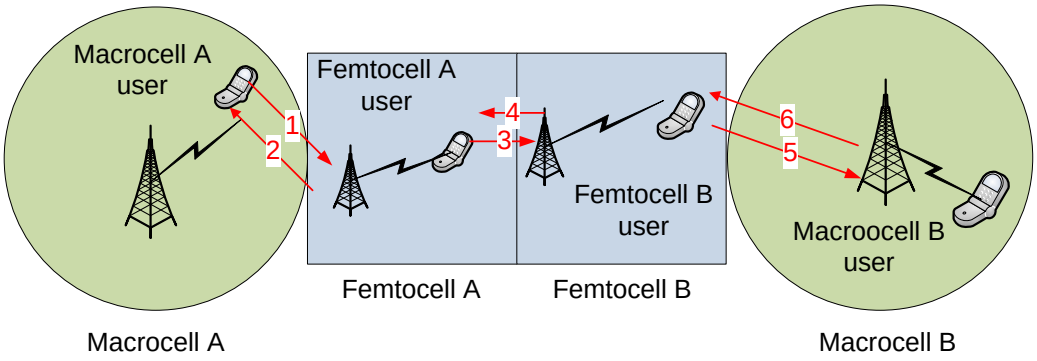

Figure 1.3: Typical interference scenarios between femtocell users and macrocell users. ©2010 IEEE. Reprinted with permission from [2].

narios between femtocell users and macrocell users.

In the figure, there are three sets of interference scenarios, including interference from a macrocell user to a femtocell user, interference from a femtocell user to a macrocell user, and interference between two femtocell users. Interference 1, generated by macrocell A user, will affect the uplink of femtocell user A; interference 2, generated by femcoell A BS, will affect the downlink transmission of macrocell A user; interference 3, generated by femtocell A user, will affect uplink of femtocell user B; interference 4, generated by femtocell B BS, will affect femtocell A user's downlink; interference 5, generated by femtocell user B, will affect uplink of macrocell user B; and interference 6, generated by macrocell B BS, will affect downlink of femtocell user B. Usually interference between femtocells is relatively small compared to other interference scenarios due to low transmit power and penetration losses.

Allocating existing spectrum between femtocells and macrocells is an open topic. We can easily see two ways to allocate spectrum. One is that femtocells share some portion of the spectrum with macrocells. The other is that femtocells are allocated spectrum for exclusive use. However, we need to determine how to optimally separate spectrum between femtocells and macrocells, with respect to different situations. Another research problem is to design a fully or partly decentralized algorithm and protocol to allocate spectrum, owing to the limited coordination between macrocells and femtocells and between femtocells.

1.3.2.2 Handoff

Handoff for femtocells includes two sub-topics. The first question is whether femtocells are open for public access. A closed access femtocell offers only offer service to a small set of users, including the femtocell owner and others they allow (e.g. friends and visitors). Two issues must be considered for closed femtocells are: i) interference between femtocells and macrocells must be controlled so that a passing macrocell user, who is not allowed to perform handoff to the femtocell, can still maintain the call to the macrocell without being dropped because of femtocell's interference; ii) authorized users must be able to seamlessly handoff between a macrocell and the femtocell without being dropped. There is limited coordination between macrocells and femtocells creating potential problems when a user does handoff between them. This has been a common customer complaint with Sprints Airave service. Analysis of different femtocell access strategies and case studies are provided in [27, 28].

If a femtocell allows open access to public, this causes more challenges. Although open access will reduce traffic in macrocells, it increase usage of the femtocell owner's backhaul. The backhaul is normally paid by femtocell owners and they may not want their internet service degraded by allowing too many cellular users access via their backhaul. There are also privacy concerns. In addition, most femtocell services currently use a flat rate monthly charge to their users. Thus open access femtocells must differentiate between a home user and a pay-per-minute (or other charging method) passing user. Operators probably need to reward femtocell users for offering open access to public by, for example, giving credits or more minutes to encourage open access in poor coverage areas. In current femtocell deployments, operators are pursuing a hybrid approach with femtocells configured for open access, by default, but allowing femtocell owners to select closed access, if desired.

Handoff from a femtocell to a macrocell is much easier than the other direction since usually a femtocell has only one neighboring strong-signal macrocell. However, for handoff from a macrcell to a femtocell, it is difficult for the macrocell to maintain an up-to-date neighbor list. This could greatly reduce successful handoff probability. Another problem

is when a cellular user passes several femtocells, the user may be repeatedly handed over between the macrocell and multiple femtocells, causing a "ping-pong" handoff. Several techniques for handoff between macrocells and femtocells are proposed in [29–31].

1.3.2.3 Backhaul QoS, Security, and Scalability

For femtocells, the air interface is on licensed spectrum and controlled by the operator. If we do not consider intra-system interference, guaranteed QoS is offered over the air. However, unlike macrocells, which connect to the core network using a dedicated connection, femtocells communicate with the core network via broadband Internet. This backhaul, in most cases, is not controlled by the operator and is paid for by the femtocell owners. Thus the offered data rate varies depending on the ISP, and the femotcell owner's data plan, how many users are sharing the same cable, and so on. Even if the backhaul belongs to the operator (e.g. Verizon might be both the cellular operator and ISP serving a femtocell owner), best-effort internet service cannot guarantee QoS. Given a QoS requirement from the core network, it is difficult for the femtocell to judge whether or not this QoS requirement can be satisfied. To overcome this challenge, we need to develop algorithms, protocols, or models to predict backhaul performance and dynamically adjust offered QoS, and applications need to be designed to accommodate varying QoS.

Security, of course, is challenging on the internet because of its open nature. If home computers can suffer attacks from the internet, then femtocell BSs will be attacked as well. Though the relatively small number of femtocells, relative to PCs, might make them a less attractive target, the air interface operating in (and potentially interfering with) operator-licensed spectrum might make them a more attractive target. In [32], the authors analyze several key aspects of network security of femtocell.

Femtocell scalability is also a concern to operators. The relevant components in the core network are designed to work with at most hundreds of cells. The protocols and interfaces between BSs and the core network are not designed to scale to thousands of femtocells. Thus

the current system must be modified to accommodate appropriate numbers of femtocell BSs.

1.4 Motivation

The motivation behind this research is to address resource allocation and interference management in cellular networks with coexisting femtocells and macrocells.

As we mentioned in section 1.3.2.1, there are two major spectrum allocation schemes. One is that femtocells share spectrum with macrocells and the other is femtocells use exclusive spectrum. It is intuitive that the former can give better network performance through maximizing spectrum reuse. However, we need to examine the cost to acquire this performance gain. Femtocells have limited ability to coordinate with macrocells, and sharing the same spectrum requires a mechanism to coordinate spectrum usage. The overhead introduced by the coordination mechanism will include computational overhead and additional message exchange. One may ask whether shared reuse will always be better if we include these overheads. If not, when should we use shared reuse and when should we use split reuse? Further, in either reuse scheme, can we find an optimal split point to separate spectrum that balances femtocell and macrocell requirements?

In addition to studying spectrum allocation schemes, a more important problem is how to efficiently assign resources to femtocell and macrocell users. Clearly, if a central allocator could gather all needed information from the network instantly and costlessly, it could allocate resources to each user optimally, given sufficient computational resources. In practice, gathering complete real time network information in a large scale network is almost impossible and finding the optimum resource allocation in wireless network is often NP-hard. Nevertheless a centralized allocator, though not practical, can act as a reference in simulation and be compared with possible decentralized allocation methods.

The characteristics of femtocells require that resource allocation be done in a decentralized or a hybrid way with minimal central aids. Each femtocell is only able to access local

information in the network and sometimes this information is inaccurate. A femtocell needs to make decisions based on the limited knowledge that it has, considering both its own requirements and network performance. Because of the dynamic nature of wireless communications and the ad-hoc style of femtocell deployment, femtocells need to evaluate their decisions constantly and make necessary adaptations to the current network environment.

The autonomous behaviors of femtocells motivate us to apply the cognitive cycle to address resource allocation. The cognitive cycle consists of four phases: observe, orient, decide, and act. The work cycle of a femtocell (on the resource allocation problem) is similar to the cognitive cycle: a femtocell and its mobiles scan the spectrum (observe); gather useful information, both locally and externally (orient); apply algorithms to determine resource allocation (decide); and enact these decisions (act). Ideally, femtocells should be forward-looking and attempt to adjust to problems before they occur [33].

1.5 Related Work

1.5.1 Resource Allocation in Macrocell only Networks

Resource reuse has been an important research topic since the emergence of cellular networks. The initial goal of cellular networks is to separate the coverage areas into many small cells such that resources can be reused and system capacity can be enhanced. Several well-known ways to reuse resources in cellular networks include frequency-division multiple access (FDMA), time-division multiple access (TDMA), code-division multiple access (CDMA), and orthogonal frequency-division multiple access (OFDMA). GSM was the most successful second generation (2G) standard, using a combination of FDMA and TDMA. An important parameter in GSM is the frequency reuse factor (FRF). It is easy to understand that two neighboring cells could generate interference to each other if they use the same frequency. To mitigate the inter-cell interference, it is natural to let nearby cells use different frequencies.

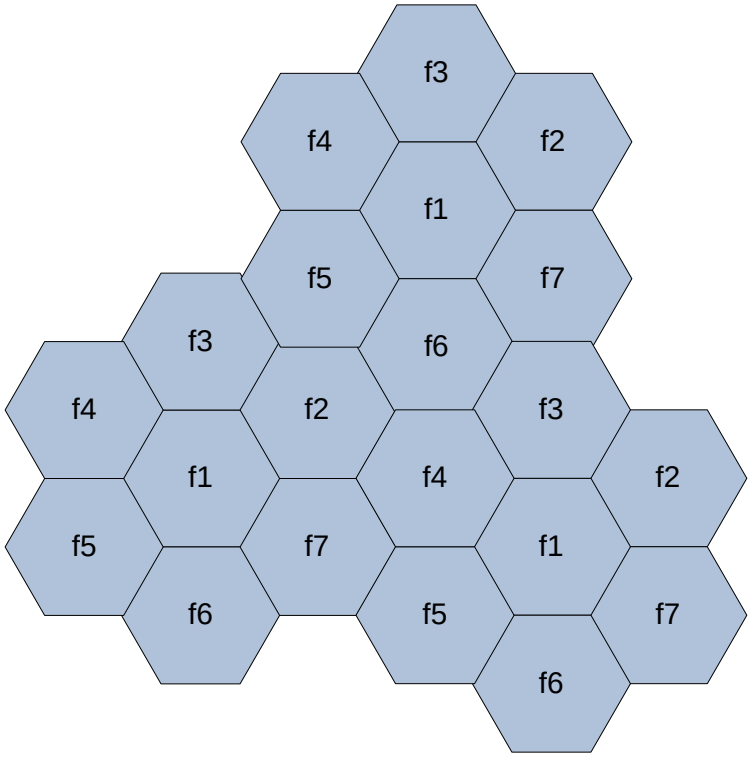

Figure 1.4: A frequency reuse pattern with a frequency reuse factor (FRF) of 7.

FRF is defined as the number of cells in a cluster in which each cell uses a unique set of frequency channels without causing co-channel interference to each other [34]. A higher FRF provides better isolation between cells (and potentially reduces inter-cell interference) but makes for poor spectrum reuse. Common FRFs include 3, 4, and 7. Figure 1.4 shows a FRF of 7.

There are various work that discusses static frequency assignment in cellular networks in terms of different FRFs. In [35], a cellular network is modeled as a subgraph of a triangular lattice. In the static frequency assignment problem, each vertex of the graph is a base station (BS) in the network, and has associated with it an integer weight that represents the number of calls that must be served at the vertex by assigning distinct frequencies per call. The edges of the graph model interference constraints for frequencies assigned to neighboring stations. The static frequency assignment problem can be abstracted as a graph multicoloring

problem. The authors of [36] propose a framework for studying distributed online frequency assignment in cellular networks and present several distributed online algorithms for static frequency assignment. Some other work discusses dynamic frequency assignment by applying frequency hopping [37,38]. The results in this work show that by combining frequency reuse with frequency hopping, an increase in the network capacity in terms of carried traffic per cell is achieved. In addition, random frequency hopping introduces interference diversity on the transmission link, which improves the system performance. In [39], the optimal reuse scheme for a GSM system with random frequency hopping is presented and the optimal FRF is found to be 3. The simulation results show a significant reduction in the percentage of dropped calls when frequency hopping is applied. The authors in [40] consider the need for microcells and picocells and aim to provide an easy way of performing frequency planning for the system operator. The results of system simulations show that slow frequency hopping makes it possible to decrease FRF while maintaining system performance.

CDMA is the main resource reuse technique behind the third generation (3G) cellular networks. In CDMA systems, channels are defined not by time or frequency but by code. Spread spectrum systems rely on pseudo-random spreading codes to create noise-like transmission and each user is assigned an unique code to access the physical channel [41]. Clearly in a CDMA cellular network, FRF is 1. Comparing against GSM, power control plays a key role in CDMA systems because all users work on the same band of spectrum and every other transmission link is treated as noise of the targeted receiving transmission. The authors of [42] discuss power control and resource management in a CDMA system. They formulate resource management as a constrained optimization problem. Two objective functions are defined: minimum power and maximum rates; bounds are developed on the total number of users of each class (in terms of the QoS requirement) that can be supported simultaneously while meeting resource constraints. The work in [43] addresses radio resource allocation for UMTS systems. A set of resource allocation algorithms is proposed that consists of resource estimation and power and rate allocation. The simulation results show that resource estimation is essential to achieve a good power and rate allocation. A distributed

dynamic resource allocation strategy for a hybrid TDMA/CDMA system is proposed in [44]. This strategy is evaluated in a system that consists of Manhattan-like microcells covered by hexagonal-shaped cells and compared against the fixed resource allocation strategy.

LTE is to be the next generation of cellular networks and uses OFDMA. OFDMA has been widely used in standards such as Institute of Electrical and Electronics Engineers (IEEE) 802.11a/b/g, 802.16, Digital Video Broadcast (DVB), and Digital Audio Broadcast (DAB). OFDMA uses a large number of narrowband sub-carriers for multi-carrier transmission. The basic LTE downlink physical resource can be seen as a time-frequency grid. In the frequency domain, each sub-carrier uses 15 kHz. One resource element (corresponding to one sub-carrier and one OFDM symbol) carries QPSK, 16QAM, or 64QAM modulated bits. The resource elements are grouped into resource blocks (RB), which spans 12 sub-carriers in the frequency domain and 7 symbols (0.5 ms) in the time domain. 3GPP specifications usually requires each user to receive at least 2 RBs. In this dissertation, for simplicity, we consider one RB per user is sufficient. An LTE radio frame has length of 10 ms. Therefore, a 5 MHz LTE system could accommodate up to 250 active data clients (2 RBs per user). The more RBs a user receives and the better modulation used in the resource elements, the higher the achieved bit-rate. A scheduler at the BS determines which and how many RBs are assigned to a user. Scheduling of resources can take place as often as every millisecond, that means 2 RBs. Note that in the uplink, LTE uses a pre-coded version of OFDMA called Single Carrier Frequency Division Multiple Access (SC-FDMA).

In an OFDMA-based LTE system, resources are divided into RBs that are essentially a combination of time and frequency domain resources. So LTE can be seen as a return of FDMA and TDMA and thus FRF needs to be addressed again. 3GPP does not indicate any specific values of FRF. Most proposals of resource reuse pattern propose a FRF of 1, assuming that better resource allocation techniques (by taking advantages of OFDMA) would be applied in LTE. However, seeing potential vulnerabilities with a FRF of 1, most work focuses on fractional frequency reuse (FFR). A system with a FRF of 1 achieves a high resource reuse efficiency, while suffering from heavy inter-cell interference in the cell edge

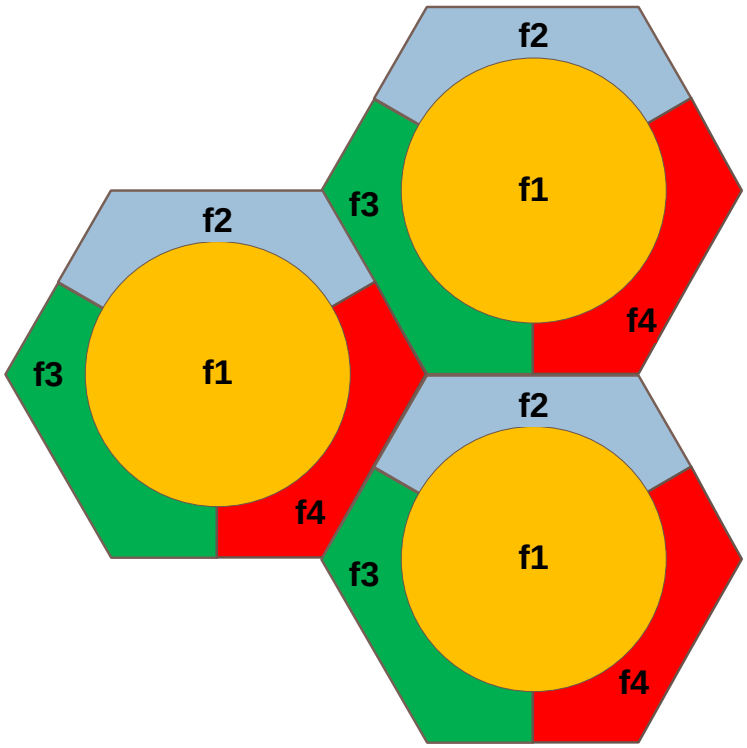

Figure 1.5: Illustration of fractional frequency reuse

areas. As we have seen in [39], a FRF of 3 system achieves acceptable interference at the cell edge, but has a resource reuse efficiency of 1/3. Thus a possible solution is FFR, in which a FRF of 1 is applied in areas close to BS, and a higher FRF is used in areas closer to the cell border [45]. This idea was proposed for GSM networks and has been adopted in the 3GPP LTE standardization [46]. Figure 1.5 gives a simple example applying FFR.

In [47], the author improves on static FFR with a distributed algorithm for interference coordination, which enhances cell edge performance with global information provided by a cental coordinator. The simulation results show that the communication delays with the central coordinator are on the order of seconds and the algorithm yields good system performance. In particular, throughput of the cell edge users is greatly improved and the spectral efficiency is enhanced about 50%, compared to a classical FFR system. [48] presents a dynamic channel allocation (DCA) and opportunistic scheduling scheme for multicell OFDMA

networks. The scheme proposes a dynamic FFR architecture where the cell is divided into two overlapping geographical regions and orthogonal subcarriers are allocated to the regions. The so-called "super group" of subcarriers covers the whole cell rather than covering the center of a cell in the traditional FFR, and the frequencies in this group experience interference from all the neighboring cells. There are three so-called "regular groups" serving three sectors of a cell. The proposed scheme consists of two algorithms such that one runs at the core network to define the groups and the other one runs at BS where an opportunistic scheduling decisions are made. The results show that opportunistic scheduling greatly improves the system performance. Similarly in [49–53], the authors study different varieties of FFR in OFDMA systems and propose new schemes showing improvement compared to the static FFR with respect to different aspects of system performance. Unlike most FFR work, which is doing optimization or simulation, the work in [54] analyzes the theoretical capacity and outage probability of an OFDMA cellular system employing FFR by using a proportional fair scheduler. The results show that FFR is effective in achieving both high capacity and low outage rates.

In terms of a full FRF of 1 (without FFR), most work assumes a centralized coordinator which has global information and manages resource allocation for all cells in the system. Thus the problem becomes an optimization problem (mostly to maximize user throughput) with various constraints. Normally this kind of problem belongs to nonlinear integer optimization and is NP-hard without computational efficient algorithms to obtain the optimal solution [55]. Some work uses well-know branch-and-bound algorithms to approach the optimal [56, 57], while other work proposes heuristic algorithms to address this problem [58, 59].

1.5.2 Resource Allocation for Femto -and Macrocell coexistence

Femtocell resource allocation and interference management have gained much attention recently, and there is a large body of work trying to address this problem. Current 3G cellular networks are CDMA-based and CDMA-based femtocells are initially investigated. As we

have discussed, each user in CDMA uses the whole bandwidth of a carrier. Normally, a mobile operator only has a limited number of carriers. In UMTS networks, the system bandwidth is 5 MHz, with the result that femtocells may have to use the same carrier that macrocells use. In cdma2000 systems, the situation is better because the system bandwidth is 1.25 MHz, which means femtocells could use different carriers from macrocells. However, in cdma2000 voice and data traffics require different carriers. Therefore, in most cases, a mobile operator needs to use a number of carriers only for macrocells and to use the remaining carriers for both macrocells and femtocells. In any case, in a CDMA-based system, co-channel interference avoidance must be addressed. This can be achieved by power control and a carrier selection mechanism.

In [60], the authors provide a simulation study of UMTS femtocells. Their analysis with the dense urban model shows that single carrier allocation to femtocells would be sufficient in most cases. On the downlink side, if multiple carriers are available, the interference can be well controlled by using carrier selection and femtocell BS (fBS) power control. In addition, coverage and capacity analysis are provided by system-level simulations showing that femtocells eliminate indoor outage without noticeable impact on the coverage for macrocell users and with a significant capacity improvement. These results reveal that the capacity benefits of femtocells are due to two factors. On one hand, the femtocell users can achieve high data rates. On the other hand, macrocell users benefit from the capacity offload since more macrocell network resources are available for them. The work in [61] addresses several key aspects of system design of cdma2000 femtocells. The work concludes that the larger number of carriers available in cdma2000 systems (compared to UMTS systems) allows more design options to provide excellent femtocell service without mutual interference.

Most research on femtocell resource allocation is on OFDMA-based LTE systems. The work in [62] gives a comprehensive analysis on OFDMA femtocell spectrum allocation and interference mitigation. First, the resource allocation problem is categorized into two aspects, namely orthogonal channel and co-channel assignment. Second, under each aspect, the mechanisms of static/dynamic assignment and centralized/distributed assignment can be

applied to the problem. The femtocell self-optimization process is divided into sensing and turning phases, partly inline with the cognitive cycle. Similar to [62], some work discusses the "big picture" of femtocell resource allocation and interference management [6, 63, 64].

As to the algorithm development and simulation study, the authors in [65] provide resource management solutions for femtocell networks along with performance guarantees. They propose a contention-based distributed algorithm to address resource allocation between femtocells and a location-based algorithm allowing femtocells to share resources with macrocells. Performance evaluations indicate that with proper resource management solutions, femtocells can increase the system throughput. The work in [66] presents a simulation study of the self-organization of femtocells, in which the femtocell dynamically senses the air interface and tunes its resource assignment to reduce inter-cell interference and enhance system capacity. A frequency planning algorithm for femtocells in cellular networks using FFR is proposed in [67]. This work mainly considers the interference between macrocells and femtocells and proposes to assign unused frequencies to the femtocells located in the areas covered by a macrocell frequency. The authors in [68] propose and analyze an optimum decentralized spectrum allocation policy for two-tier networks. The proposed allocation is optimal in terms of Area Spectral Efficiency (ASE), which is defined as the network-wide spatially averaged throughput per unit area over which the transmissions take place.

1.6 Organization and Contributions

1.6.1 Organization

This chapter explains why femtocells have garnered such interest from academic and industry researchers, identifies the main research challenges associated with the deployment of femtocells, and reviews the relevant literature on femtocells and resource allocation in macrocell cellular networks. Chapter 2 applies knowledge of graph theory to analyze upper and lower

bounds on the number of resources required for a network with femtocells and macrocells. Two ways to describe interference scenarios, denoted a random model and a specific observation, are used. A heuristic algorithm is developed for comparison with the bounds. In Chapter 3, we define three different social welfare functions and use them to analyze split reuse and shared reuse. We run simulations to find the optimum resource split point for the reuse schemes and make comparisons. In Chapter 4, a genetic algorithm-based centralized algorithm is developed to attempt to obtain best-known resource allocations. The results in this chapter also provide a baseline to be compared to by the later introduced distributed algorithms in Chapter 5. Other than developing two distributed resource allocation algorithms, in Chapter 5, we apply conflict-free resource allocations obtained from the protocol model to simulated networks and examine the allocations under the SINR model to evaluate feasibility. Finally, in Chapter 6, we summarize the work and give conclusions.

1.6.2 Contributions

The major contributions of this dissertation:

- By applying a random conflict graph model, we analyze properties of the split, shared, and universal reuse schemes and give upper and lower bounds on the minimum number of resource blocks required for the network.
- We analyze the optimum resource split point, which separates femtocell users from macrocell users, for split and shared resource reuse schemes.
- We define different fitness functions representing the utility of different resource allocation regimes. Two represent extremes of utilitarianism and egalitarianism; the third, based on the Nash Bargaining Solution or proportional fairness, represents a compromise between fairness and utility maximization.
- We present simulation results based on simple, greedy heuristics optimizing the three

fitness functions. These results verify our analysis and provide guidelines on resource reuse and allocation for different fitness functions and network environments.

- We develop two practical, distributed resource allocation algorithms. One supports the case of no communications between BSs and the other utilizes shared information between BSs. The algorithms' performance is comparable to a GA-based centralized algorithm.

- We apply the developed resource allocation solutions to a simulated cellular network and examine their performance under the SINR model.

Chapter 2

Bounds on Number of Resource Blocks

This chapter provides upper and lower bounds on the number of RBs required to support a cellular network with femtocells and macrocells. We define a random graph model and also discuss requirements for specific observed conflict graphs. Graph theory is applied to assist with this analysis, and a simple heuristic algorithm is developed to verify the theoretical upper and lower bounds. All results are presented for both shared reuse and split reuse of spectrum.

2.1 Introduction

When femtocells are introduced into existing cellular networks, the first question operators might ask is what resources will be required to support them. If femtocells use the same spectrum as the existing macrocells, will current spectrum be able to support these newly-added femtocells? If not, how much additional spectrum does the operator need? If femtocells use exclusive spectrum, how much spectrum do they require?

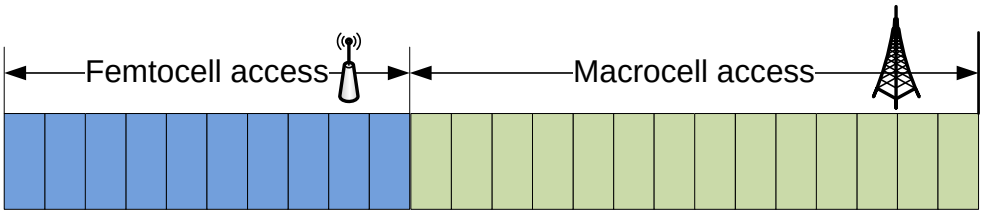

(a) Case I: Split reuse

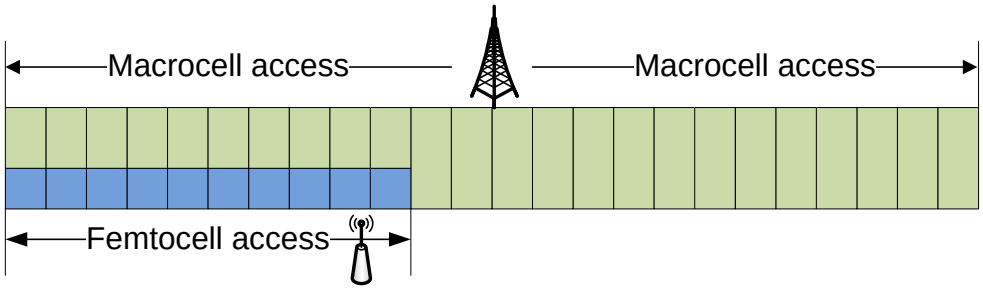

(b) Case II: Shared reuse

Figure 2.1: Resource allocation schemes for OFDMA-based cellular networks with femtocells and macrocells. ©2010 IEEE. Reprinted with permission from [2].

In our work, we consider two commonly used methods for resource reuse, as illustrated in Figure 2.1. In split reuse, shown in Figure 2.1(a), the resources are separated such that some of the RBs are solely used by femtocell users and the remaining resource blocks are only for the macrocell users. In shared reuse, shown in Figure 2.1(b), macrocells are able to access all the resource blocks while femtocells are permitted to access only some of the resource blocks. Split reuse naturally avoids interference between femtocells and macrocells and thus reduces the complexity of the resource allocation algorithm. However, it decreases the resource reuse efficiency. Shared reuse is expected to result in better performance but may require a more complex algorithm to handle interference between femtocell and macrocell users. Note that when the split point moved to the far right in the figure 2.1(b), femtocells can share all spectrum with macrocells and this special case of shared reuse is termed universal reuse.

2.2 Related Work

The authors of [6] provide a survey of femtocells, comparing several different ways to extend network coverage and enhance service quality in terms of capacity gain, coverage area, indoor coverage, cost, and operator benefit. They also describe key technical challenges, including spectrum allocation, timing and synchronization, femtocell access policies, and network architecture. Research directions in interference management are also presented.

The majority of work on channel allocation for OFDMA-based cellular networks focuses on macrocells and proposes various methods to mitigate inter-macrocell interference with frequency reuse factor of 1 [69–71]. The study of interference management in femtocell deployment is a recent research area. In [72] and [73], Claussen and Ho study co-channel interference management for CDMA-based femtocells and macrocells. Simulations are performed for a residential femtocell scenario to determine the potential effects on macrocell users with and without self-provisioning of femtocell power. The results show that the increase in call drop probabilities due to the deployment of these femtocells would be low if power adaptation techniques were implemented, but unacceptably high otherwise. The work also shows that, despite low transmit power, the short distance between the fBS and the femtocell user results in high achievable femtocell throughput for both uplink and downlink in most covered femtocell areas.

In the context of OFDMA-based systems, López-Pérez *et al.* [62] provide and interference analysis and some guidelines on how the spectrum allocation and interference mitigation problems can be approached. Self-configuration and self-optimization techniques are used for interference avoidance. In addition, these authors study how to share the resources and avoid interference for different femtocell access mechanisms, namely open access, closed access, and hybrid access in [66]. The authors of [65] address optimal resource allocation between macrocells and femtocells. They also propose a location-based resource management solution for maximizing spatial reuse by femtocells. The work in [74] presents a procedure for performance evaluation of a multi-carrier cellular system with femtocells using the same

carrier as the macrocells.

For macrocell/femtocell networks, the above related work either provides guidelines on resource reuse, or addresses optimum resource allocation under various assumptions, but does not address the following basic questions: Without significant degradation to existing users' performance, what is the impact on resource allocation of introducing femtocells into macrocells with respect to both split reuse and shared reuse? How many additional RBs are required to accommodate femtocells under different resource reuse schemes? This chapter addresses these questions and makes the following contributions:

- By applying a random conflict graph model, we analyze properties of the different reuse schemes and derive upper and lower bounds on the minimum number of RBs required for the network.
- We develop a simple heuristic algorithm for resource allocation between femtocell and macrocell users. In the majority of cases, the heuristic algorithm results tightly track the upper bound derived in split reuse and the lower bound in shared reuse.

2.3 System Model

2.3.1 Parameter Description

There are two widely used models to characterize interference scenarios in wireless networks, namely, signal-to-interference-plus-noise-ratio (SINR) model and the protocol model. The SINR model is based on real transceiver design and treats interference as noise. In such a model, a transmission is successful if the SINR at the receiver exceeds a threshold so that the received signal can be correctly decoded. However, the difficulty associated with the SINR model is the computational complexity because a SINR calculation results in a non-convex function. Further, under the SINR model, the additive interference makes it difficult to

theoretically analyze the interference scenarios in a large-sized network. Consequently, most of the work employing the SINR model ties to find sub-optimal solutions for a particular optimization function, rather than giving theoretical bounds. Another concern about the SINR model is that this model will introduce many simulation parameters, such as node distribution, the transmit power, the propagation model, the modulation schemes, and so on. So the results obtained may not be generalized and could only reflect particular simulated network scenarios.

Thus, we formulate our problem using the protocol model [75] of interference to simply the mathematical characterization. Although less expressive than the SINR model, the protocol model allows us to study resource allocation analytically. Under this model, interference is a binary condition: either a pair of links interfere with each other or they do not.

2.3.2 Conflict Graph

A conflict graph is a graph G with vertex set V and edge set E. Each vertex $v \in V$ in the conflict graph represents a communication link in the network. Two vertices u and v are connected by a non-directional edge $(u, v) \in E$ if and only if their associated communication links will interfere. In other words, the communication links represented by two adjacent vertices in the conflict graph cannot share the same channel simultaneously.

An example conflict graph is shown in Figure 2.2. Figure 2.2(a) illustrates communication activities in a macrocell/femtocell network while figure 2.2(b) shows the generated conflict graph. Macrocell user links 1 , 2, and 3 naturally interfere with each other and the corresponding nodes in conflict graph are connected. Femtocell user links 4 and 5 are close enough to interfere with each other. Links 2 (due to the long distance from the macrocell BS to mobile user 2) and 3 (due to the proximity of mobile user 3 to the femtocells) also interfere with femtocell links 4 and 5.

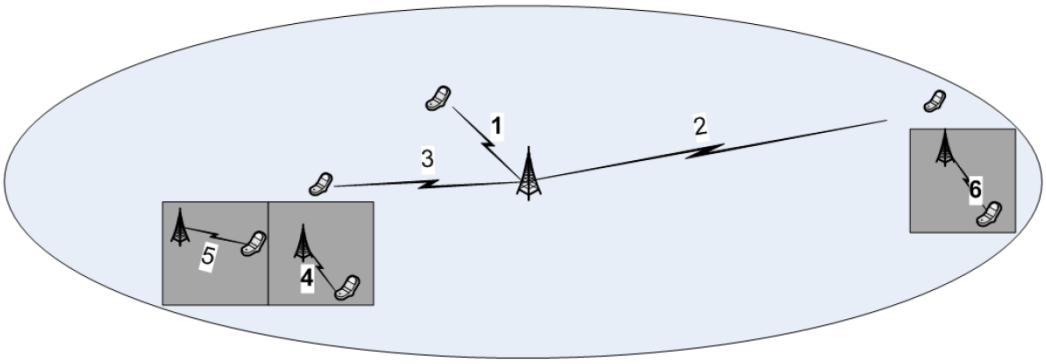

(a) A Network with a mix of macrocell and femtocells

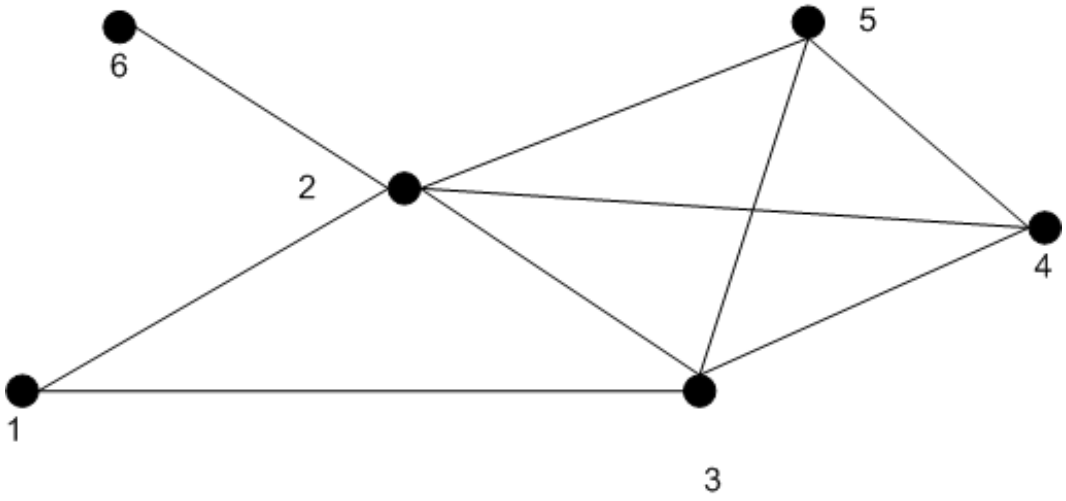

(b) Conflict graph based on network scenario in (a)

Figure 2.2: An Example of Conflict Graph ©2010 IEEE. Reprinted with permission from [2].

2.3.3 Problem Formulation

We focus on the downlinks to all femtocell and macrocell users within one macrocell in a cellular network. The macrocell has M macrocell users and F femtocells inside. Each femtocell has one active femtocell user. We assign one user to each femtocell for convenience and ease of analysis; our model is easily adapted to an arbitrary number of users in each femtocell by modifying the conflict graph accordingly. The number of available RBs is N.

A resource allocator builds a conflict graph G to represent interference. A link i in the cellular system is represented as a vertex $i \in V$. There is an undirected edge $(i, j) \in E$ if and only if link i and link j conflict. Based on the constructed conflict graph, the resource allocation problem is to build an $(M + F) \times N$ binary resource assignment matrix $\mathbf{A}$. An element in $\mathbf{A}$, $a_{i,k}$, is 1 when RB k is assigned to link i and 0 otherwise. Two links i and j cannot use the same RB if they conflict, that is if $(i, j) \in E$. A resource assignment matrix $\mathbf{A}$ that satisfies this condition is said to be *feasible* and represents an interference-free resource assignment, i.e. $a_{i,k} \times a_{j,k} = 0$ if $(i, j) \in E$. We denote the set of feasible resource assignment matrices as $\mathcal{A}$

For the purpose of analysis, we adopt the idea of a random graph from graph theory to construct sample conflict graphs. Four parameters are needed to construct such a random femtocell conflict graph: M (the number of macrocell users), F (the number of femtocell users), p_{ff} (the probability that two arbitrarily chosen femtocell links interfere) and p_{mf} (the probability that an arbitrarily chosen femtocell link interferes with an arbitrarily chosen macrocell link).

The conflict graph G is then constructed with $M+F$ vertices. The M vertices representing the macrocell links are fully connected because a RB cannot be shared by two macrocell users in the same macrocell. The existence of an edge between arbitrarily chosen macrocell and femtocell links is a Bernoulli random variable with probability p_{mf}. The existence of an edge between two arbitrarily chosen femtocell links is a Bernoulli random variable with probability p_{ff}.

Note that in the case of split reuse, there will be no conflicts between macrocell and femtocell users. In that case, we can focus on the subgraph G_m, which consists of M vertices that are fully connected, and G_f, which is a Bernoulli graph with F vertices and connection probability p_{ff}.

Another way to construct a conflict graph is via specific observation of a cellular system, or a simulation model. In this method, we use simulation to construct a conflict graph that attempts to reflect interference scenarios in a real network, though this reflection depends on certain assumptions such as how to drop network nodes in the area and how to decide whether two communication links interfere with each other. We drop a random number of femtocell users and macrocell users in the area covered by a macrocell. Unlike most protocol models that determine the interference based on distance, however, our model determines interference based on SINR. The difference between our specific observation model and the SINR model is that we do not account for additivity of interference. We have the following assumption: each user is able to track channel quality, e.g. SINR, and feedback the instantaneous value to their BS with insignificant delay. Although we acknowledge that imperfect feedback and channel quality estimation have a potentially large impact on system performance, we do not account for these effects for sake of analytical tractability. To construct a conflict graph, if the measured SINR value at a user is higher than a pre-defined threshold when only the two link are simultaneously active, we consider that the corresponding two links to interfere with each other. This is a widely used model to determine link conflicts [76, 77].

2.4 Problem Analysis

2.4.1 Graph Theory Preliminaries

It is useful to introduce some basics of graph theory before we proceed with the resource allocation problem.

Any feasible matrix $\mathbf{A} \in \mathcal{A}$ results in conflict free transmission for all links in the network. Such an $\mathbf{A}$ assigns different RBs to any adjacent vertices in the conflict graph G. This motivates us to apply graph coloring to analyze this problem. Graph coloring tries to find the minimum number of colors that can color a graph such that any adjacent vertices are assigned different colors. The following definitions and propositions will be useful:

Definition 2.4.1. *The **chromatic number** of a graph G, written $\chi(G)$, is the minimum number of colors needed to label the vertices so that adjacent vertices receive different colors [78].*

Definition 2.4.2. *If vertex v is an endpoint of edge e, then v and e are incident. The **degree** of vertex v, written $d(v)$ is the number of edges incident to v. The **maximum degree** of a graph G is $\Delta(G) = max_{v \in V} d(v)$ [78].*

Definition 2.4.3. *A **complete graph** is a graph whose vertices are fully connected with each other [78].*

Definition 2.4.4. *The **complement** $\overline{G}$ of a graph G is the graph with the same vertex set as G and edge set defined by $uv \in E(\overline{G})$ if and only if $uv \notin E(G)$. A **clique** in a graph is a set of fully connected vertices. An **independent set** in a graph is a set of vertices are not connected to each other; $S \subseteq V$ is an independent set if there do not exist $u, u \in S$ such that $(u, v) \in E$ [78].*

Definition 2.4.5. *The **clique number** of a graph G, written $\omega(G)$, is the maximum size of a set of fully connected vertices (clique) in G. The **independence number** of a graph G, written $\beta(G)$ is the maximum size of an independent set of vertices. Thus $\beta(G) = \omega(\overline{G})$ [78].*

2.4.2 Random Model

We use the model $\mathscr{G}\{n,p\}$ to describe Bernoulli random graphs, where $0 < p < 1$. The model consists of all graphs with vertex set $V = \{1, 2, ..., n\}$ such that the probability that a particular graph with edge set E is observed is $p^{|E|}(1-p)^{(n(n-1)/2)-|E|}$. That is, edges are chosen independently with probability p.

Definition 2.4.6. *Let Ω_n be the set of Bernoulli random graphs of order n with connection probability p. We shall say that **almost every** (**a.e.**) graph in Ω_n has a certain property $\mathcal{Q}$ if $P(\mathcal{Q}) \to 1$ as $n \to \infty$ [79].*

Most graph properties of random graphs, such as clique number, independence number, and chromatic number, are based on the concept of **almost every** because the graph properties are not deterministic. In a conflict graph generated for femtocell users, the number of vertices is not infinite, but for a typical case, the number of femtocell users may easily reach hundreds. Thus we believe applying properties derived from the random graph model is reasonable.

To find the lower and upper bounds on the chromatic number of a random graph, we begin by determining the independence number. For $r \in \mathbb{N}$, let X_r denote the number of independent sets with r vertices of a graph G. Let Y be the independence number of G. By definition $Y = \max\{r : X_r > 0\}$.

If G is chosen according to $\mathscr{G}\{n,p\}$ then X_r is a random variable. For any integer r, the expected number of independent sets of size r in G is

$$E(X_r) = \binom{n}{r}(1-p)^{r(r-1)/2}. \tag{2.1}$$

According to [79], for small values of r and n sufficiently large, $E(X_r)$ is large and the variance is fairly small. As the value of r increases, $E(X_r)$ drops below 1 rather suddenly. For some r_0, we have $E(X_{r_0}) \gg 1$ and $E(X_{r_0+1}) \ll 1$. We are interested in this value of r_0,

as we have $Y = r_0$ with high probability.

We can re-write Equation 2.1 using Stirling's approximation:

$$n! \approx \sqrt{2\pi n}\left(\frac{n}{e}\right)^n.$$

This yields

$$E(X_r) \approx \frac{n^{n+\frac{1}{2}}(n-r)^{-n+r-\frac{1}{2}}r^{-r-\frac{1}{2}}(1-p)^{\frac{r(r-1)}{2}}}{\sqrt{2\pi}}. \tag{2.2}$$

Notice that if we could find a real number $\bar{r}_0 \geq 2$ that makes the right hand side of Equation 2.2 equal to 1, then we would expect $Y = r_0 = \lfloor \bar{r}_0 \rfloor$ with high probability (again for sufficiently large n). Matula solved an equivalent problem in [80], finding an approximate solution, which we denote $\hat{r}_0$,

$$\hat{r}_0 = 2\log_b n - 2\log_b \log_b n + 2\log_b\left(\frac{e}{2}\right) + 1 \tag{2.3}$$

where $b = 1/(1-p)$.

In any proper graph coloring, every color class must be an independent set. Every color class thus contains at most roughly $\hat{r}_0$ vertices, resulting in following lower bound for chromatic number of **a**.**e**. G:

$$\chi(G) \geq \frac{n}{\hat{r}_0}. \tag{2.4}$$

An upper bound on the chromatic number of G is more difficult to obtain. The best bound we can find is from [81] and is given by

$$\chi(G) \leq \frac{n}{2\log_b n}\left(1 + \frac{3\ln\ln n}{\ln n}\right). \tag{2.5}$$

Combining Equation 2.4 and 2.5 and considering $\hat{r}_0 \leq 2\log_b n$ (according to Equation 2.3 while n is sufficiently large), we have the following bounds for the chromatic number for **a**.**e**. G:

$$\frac{n}{\hat{r}_0} \leq \chi(G) \leq \frac{n}{\hat{r}_0}\left(1 + \frac{3\ln\ln n}{\ln n}\right). \tag{2.6}$$

Note that as $n \to \infty$, the lower and upper bounds in Equation 2.6 converge. That is $\chi(G) \to n/\hat{r}_0$ for **a.e.** G.

2.4.2.1 Split Reuse of Resource

Now we map the random graph model to split reuse of RBs. The lower bound and upper bound of the number of resource blocks required to serve F femtocell users (the random graph G_f) are

$$\frac{F}{\hat{r}_0} \leq \chi(G_f) \leq \frac{F}{r_0'}\left(1 + \frac{3\ln\ln F}{\ln F}\right) \tag{2.7}$$

where

$$\begin{aligned}\hat{r}_0 =& \max\left(2, 2\log_b F - 2\log_b\log_b F + 2\log_b\left(\frac{e}{2}\right) + 1\right)\\ b =& 1/(1-p_{ff}).\end{aligned}$$

Let us denote the lower bound and the upper bound as $\chi_{lower}(G_f)$ and $\chi_{upper}(G_f)$. Obviously, the minimum number of RBs required to guarantee no macrocell user outage is M and the number of resource blocks for femtocell users is roughly $N_f = \chi_{upper}(G_f)$. Hence the total number of resource blocks required for whole network is $N_{\min} = M + N_f$.

2.4.2.2 Shared Reuse of Resource

Although it is challenging to allocate the resources to users, a possible benefit of shared reuse is that this scheme potentially requires fewer RBs to support the same size network or, from another prospective, is able to serve more users with the same amount of resources. In the shared reuse scheme, another factor that needs to be considered is where to split the resource blocks such that part of them are shared by macrocell and femtocell users, and part of them

is exclusively for macrocell users. Clearly, sharing all resources among all users allows for the most efficient allocation. This would be the case where the split point in Figure 2.1(b) is at the far right, a reuse scheme known as "universal reuse." In this section, we focus on the analysis of such a universal reuse scenario. Other locations of the split point may result in slightly less efficient results.

Proposition 2.4.1. *In random model with M macrocell users and F femtocell users; with interference parameters p_{ff} and p_{mf}, under shared reuse of resource the minimum number of required RBs, N_{min}, follows:*

$$max\{M, N_f\} \leq N_{\min} \leq M + N_f. \tag{2.8}$$

The left-hand part is easy to check. It is also intuitive that the right-hand part holds because graph G is formed by graph G_m and graph G_f. The worst case (most number of colors needed) of G is that every vertex in G_m connects to every vertex in G_f, i.e. $p_{mf} = 1$. Thus any color used in G_m cannot be reused in G_f and the total number of colors for G is at $M + N_f$.

This confirms that shared reuse of resource is more efficient than split reuse. However, the upper bound of $N_{\min}$ shown in equation 2.8 is pessimistic. We attempt to tighten this upper bound. One potential tighter bound is given by:

$$N_{min} \leq M + \min\{Fp_{mf}, N_f\}, \text{if } M + Fp_{mf} \geq N_f \tag{2.9}$$

A macrocell user interferes with Fp_{mf} femtocell users on average. The extreme case is that all macrocell users interfere the same set of Fp_{mf} femtocell users and this set of femtocell users forms a clique in conflict graph G_f. This case will lead to the minimum number of resources as $M + Fp_{mf}$.

Equation 2.9 gives a strict upper bound on the number of RBs, but it is still pessimistic. We would like to have a further investigation and try to derive a more reasonable upper

bound. The mentioned Fp_{mf} femtocells actually are unlikely form a clique. The subgraph formed by the Fp_{mf} femtocells is also a random graph following the interference probability p_{ff}. If we can find an upper bound on the minimum number of resource blocks required for the set of Fp_{mf} femtocell users, by adding this number to M can give a reasonable upper total number of RBs required in shared reuse. Thus by Equation 2.6, an upper bound on the minimum required number of RBs in shared reuse is

$$N_{\min} \leq \max\left(M + \frac{Fp_{mf}}{\hat{r}_0}\left(1 + \frac{3\ln\ln(Fp_{mf})}{\ln(Fp_{mf})}\right), N_f\right) \tag{2.10}$$

where

$$\begin{aligned}\hat{r}_0 =& \max\Big(2, 2\log_b(Fp_{mf}) - 2\log_b\log_b(Fp_{mf}) + 2\log_b\left(\frac{e}{2}\right) + 1\Big)\\ b =& 1/(1-p_{ff}).\end{aligned}$$

2.4.3 Specific Observation

To bound the number of required RBs for a specific conflict graph, we use the following propositions [78]:

Proposition 2.4.2. *For every graph G,*

$$\chi(G) \leq \Delta(G) + 1.$$

Proposition 2.4.3. *If we denote d_i as degree of node i, and a graph G has degree sequence $d_1 \geq d_2 \geq ... \geq d_n$, then*

$$\chi(G) \leq 1 + \max_i \ \min\{d_i, i-1\}.$$

Proposition 2.4.4. *If a graph G has clique number $\omega(G)$, then*

$$\chi(G) \geq \omega(G).$$

Generally speaking, the upper bound given by Proposition 2.4.2 is the worst bound (giving the biggest number) and the bound in Proposition 2.4.3 is better. As to the lower bound, since both finding the clique number of a graph and finding its chromatic number are NP-complete problem, acquiring a practical lower bound is not easy.

To simulate real conflict graphs, we randomly drop a number of femtocells BSs and macrocell users in an area. Then we drop femtocells users within a small distance (10 m) of each femtocell. The simulator then constructs the conflict graph based on the simulated SINR values of each links, requiring appropriate propagation models. We use the following models:

- **Outdoor propagation model**

We use the 3GPP outdoor propagation model [82]:

$$PL_{out}(\text{dB}) = 15.3 + 37.6 \log_{10} d + \text{Log}F$$

where d is the distance between transmitter and receiver in meters and Log$F$ is normally distributed with standard deviation of 10 dB.

- **Indoor propagation model**

We use the Keenan-Motley model [83] to describe the indoor environment:

$$PL_{in}(\text{dB}) = 20 \log_{10} \frac{4\pi f d}{c} + pW$$

where f is the carrier frequency in Hz, p represents the number of walls between transmitter and receiver, W is wall attenuation factor.

- **Outdoor-to-indoor propagation model**

For outdoor-to-indoor propagation model, we use a simplified model described in [84]. The model is given by:

$$PL_{oti}(\text{dB}) = \max\left(PL_{out}, 20\log_{10}\frac{4\pi fd}{c}\right) + pW + PL_{building}$$

where $PL_{building}$ is building penetration loss.

- **Indoor-to-outdoor propagation model**

The indoor-to-outdoor model is given by:

$$PL_{ito}(\text{dB}) = \max\left(PL_{out}, 20\log_{10}\frac{4\pi fd}{c}\right) + pW + PL_{building}$$

While applying the propagation models, the indoor model is for the link between a femtocell user and femtocell BS, the outdoor model is for the link between a macrocell user and the macrocell BS, and the outdoor/indoor models are for links between macrocell BS/users and femtocell BSs/users. According to pre-defined threshold SINR value, the resource allocator can obtain a conflict graph that describes interference among users. The analysis is similar to random model. Let $\chi_{upper}(G_f)$ be the upper bound on the chromatic number of G_f given by Proposition 2.4.3. Then, for split reuse the total number of required RBs will be $N_{min} = M + \chi_{upper}(G_f)$. For shared reuse, we have $\max\{M, \chi_{upper}(G_f)\} \leq N_{min} \leq M + \chi_{upper}(G_f)$.

2.5 Numerical Results

A single coloring algorithm can be used to solve the RB allocation problem, i.e., for a given network, we find the minimum number of RBs required to serve all users. The optimal single coloring problem is known to be NP-hard and thus is intractable in a large scale network. In this section, we use a simple greedy algorithm to solve the resource allocation problem

and compare results to the lower and upper bounds developed in previous sections. This algorithm sorts all network links in descending order based on the number of conflicting links. The algorithm goes through the link list from top, assigning each link with the lowest numbered eligible color (based on the conflict matrix).

2.5.1 Random Model

In the random model, for split reuse, we are interested in the relationship between the lower and upper bounds and the heuristic algorithm results. Figure 2.3 gives the results. From the figure, the number of RBs required by the heuristic algorithm tracks the upper bound closely. The number from the heuristic algorithm is slightly larger than the upper bound when p_{ff} is large. This can be explained in two ways. In our random model, all bounds are under the umbrella of *almost every* as $n \to \infty$. Though the number of hundreds is large, it is not guaranteed that all graph realizations are covered by the upper bound. Second, the heuristic algorithm is not optimal. When p_{ff} is increasing, the performance of the heuristic algorithm degrades fast. On the other hand, the figure suggests that when p_{ff} is not large, the upper bound gives a good estimate of the number of RBs required by the heuristic algorithm.

For shared reuse, we randomly generated G for a large number of instances and found that in most cases, N_{min} is close to $\max\{M, N_f\}$, particularly when M is large or p_{mf} is small. There are 200 femtocell users and values of p_{ff} are 0.1, 0.3 and 0.5 shown in Figure 2.4, 2.5 and 2.6, respectively. The upper surface is the bound we derived and well covers the other surfaces. The two lower surfaces represent the number of required RBs calculated using a heuristic algorithm and the lower bound given by $\max\{M, N_f\}$. As shown, the heuristic algorithm results are approximately equal to the lower bound in most cases, especially when p_{mf} is small and M is large. In every case, the lower bound gives a better estimate on the required number of resource blocks than the upper bound. As p_{mf} increases, the gap between the upper bound and the heuristic algorithm become so large that the upper bound becomes almost irrelevant. With a larger p_{mf}, the gap between the lower bound and heuristic

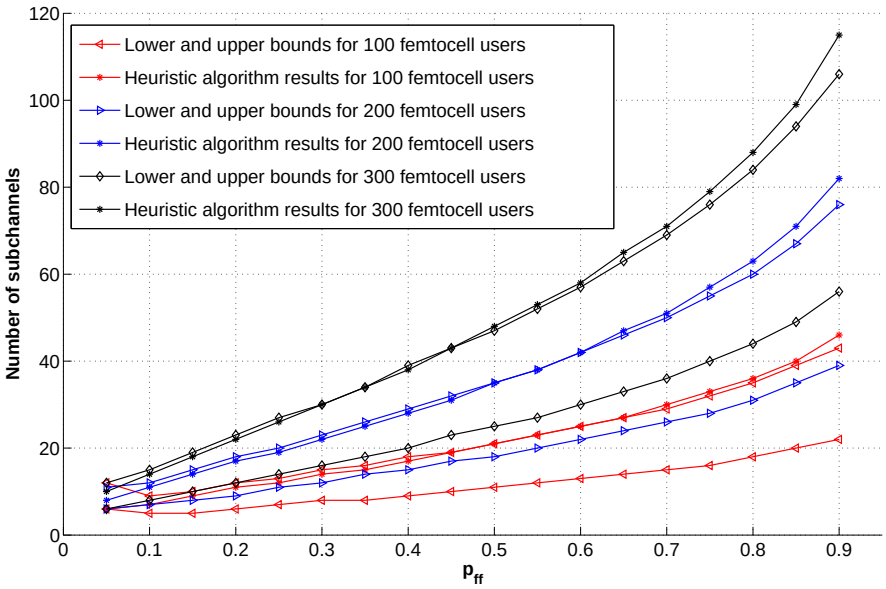

Figure 2.3: The number of RBs for femtocell users in random model. ©2010 IEEE. Reprinted with permission from [2].

algorithm becomes much larger than with a smaller p_{mf}. This can be explained because if p_{mf} is larger, there are more conflicts between the femtocell users and the macrocell users so that fewer resource blocks can be reused in the other group. In shared reuse, if M is large, it is likely that the clique number is M. In [85], it is shown that in a graph, the chromatic number is at most within 1.21 times of the clique number.

In practice, it is not likely that p_{ff} and p_{mf} are close to 1 or even larger than 0.5. We try to use reasonable estimates of p_{ff} and p_{mf}. We assume an inter-site (macrocell BS) distance of 1 km for dense urban areas. In this case, the area of a sector of a hexagonal macrocell will be 0.289 km^2. Population density in dense urban areas is $10,000$ to $20,000$ per km^2. We take the upper bound of $20,000$ and assume there are 7692 household units (2.6 persons per household) per km^2. This corresponds to 2223 household units per macrocell. Furthermore, we assume cellular phone penetration of 80%, operator penetration of 40%, and femtocell penetration of 30%. Thus we have approximately 213 femtocells in one macrocell located in dense urban areas. We randomly drop 200 femtocells in the coverage area of one macrocell.

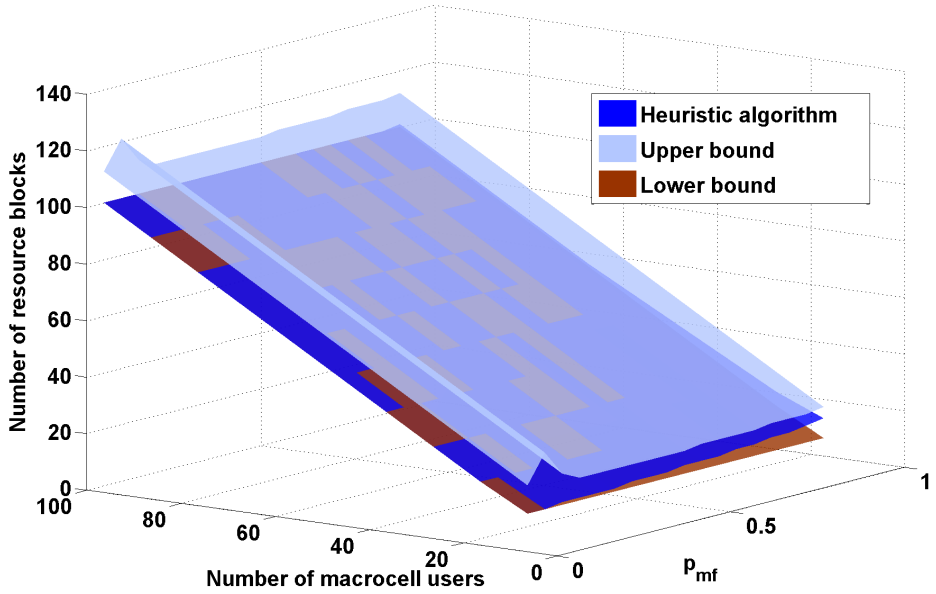

Figure 2.4: Number of RBs required in shared reuse for random model with p_{ff} of 0.1.

By applying propagation models introduced in section 2.4.3, p_{ff} is about 0.2 on average and p_{mf} ranges from 0.2 to 0.3 depending on the number of macrocell users.

Figure 2.7 shows the results using the above parameters. The heuristic algorithm results closely track the lower bound given by $\max\{M, N_f\}$. In fact, they are equal in most cases. This indicates that with a small p_{mf} (light interference between macrocell users and femtocell users), the lower bound is tight. In such a case, most RBs used by macrocell users can be reused by femtocell users.

Figure 2.8 gives a surface showing the number of RBs required in shared reuse for a network with 200 femtocell users and 30 macrocell users in different interference scenarios.

Figure 2.9, 2.10 and 2.11 give other scenarios of 200 femtocell users and increasing number of macrocell users (from 50 to 100) under different p_{mf} and p_{ff}. Clearly, as the number of macrocell users increases, the number of resource blocks required for the whole network is dominated by the number of resource blocks required by the macrocell users, as

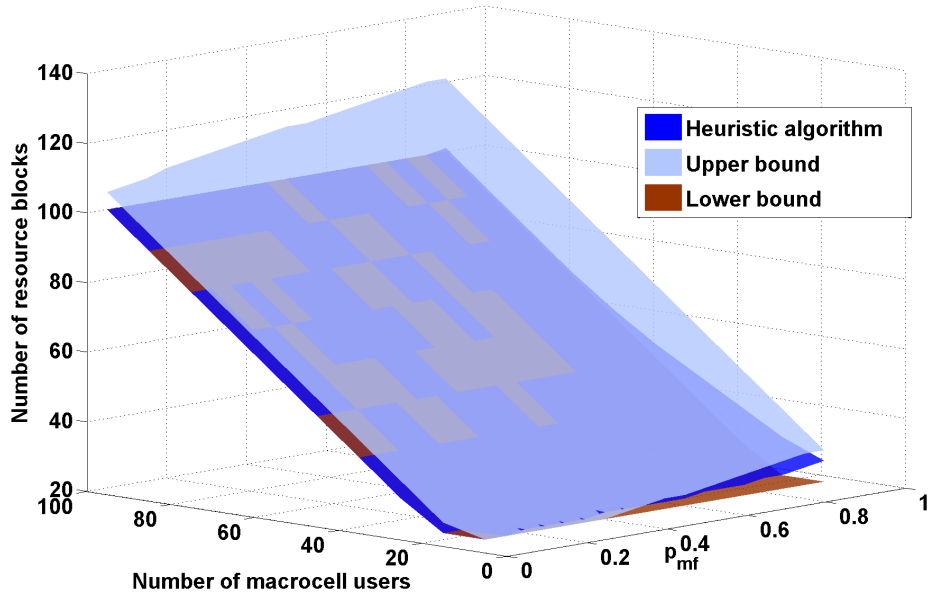

Figure 2.5: Number of RBs required in shared reuse for random model with p_{ff} of 0.3.

long as fBSs use sufficiently low transmit power (possibly through power control) to insure that p_{ff} and p_{mf} are not exceptionally high.

2.5.2 Specific Observation

In specific observation, we use the parameters obtained in Section 2.5.1 such that 200 femtocell users and 50 macrocell users are dropped in a macrocell, which is one third of a hexagonal cell with 500m radius, shown in Figure 2.12. In the figure, we give each femtocell base station an exclusive area of 100m^2 and the associated femtocell user is randomly dropped in this area and macrocell users are dropped outside of this area. Since we do not have a mature source that gives a reliable model on how femtocell and macrocell users are distributed in a cell, for simplicity, we assume this uniform distribution. However, our work can certainly fit other models.

As for choosing a threshold SINR value, according to [86], there are several minimum

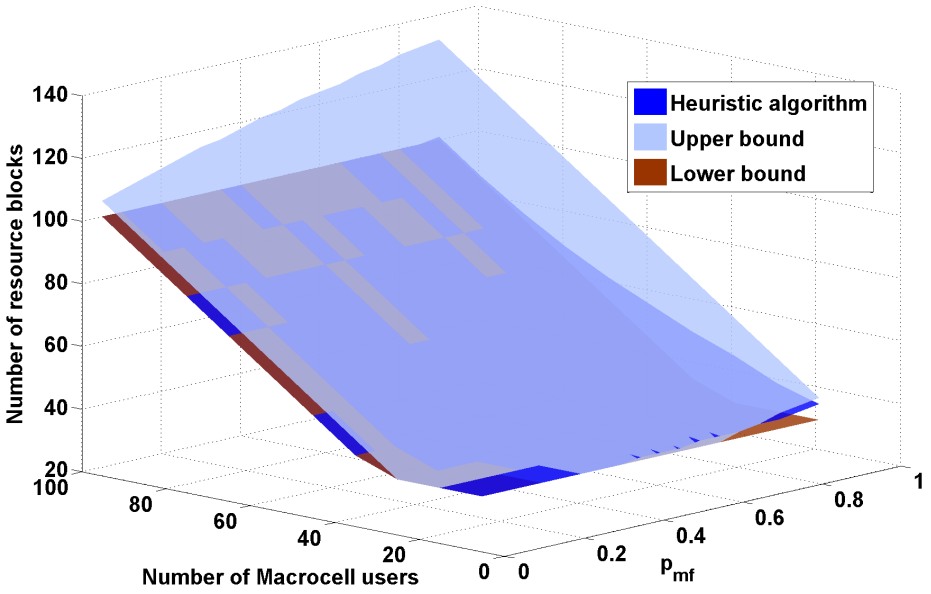

Figure 2.6: Number of RBs required in shared reuse for random model with p_{ff} of 0.5.

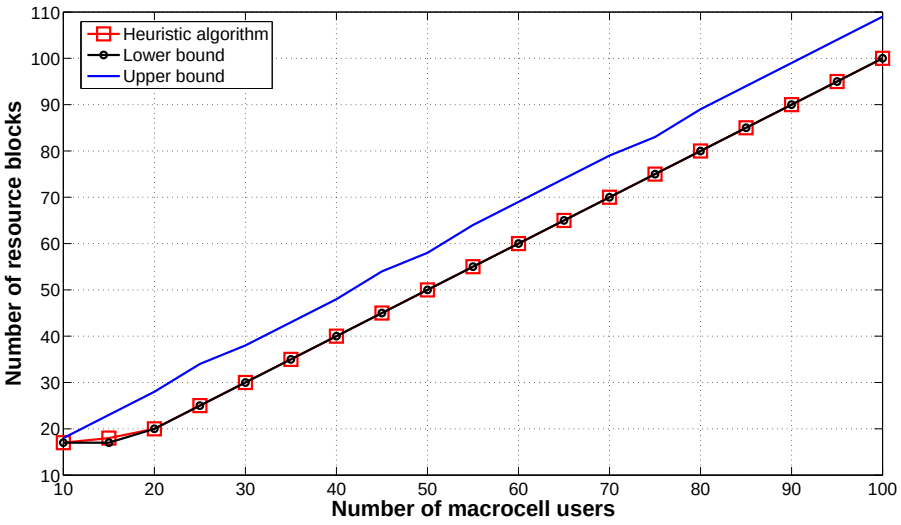

Figure 2.7: The number of RBs required in shared reuse with 200 femtocell users and p_{ff} and p_{mf} of 0.2. ©2010 IEEE. Reprinted with permission from [2].

SINR requirements for different modulation models. We assume that femtocell users need a better SINR and macrocell users only need a basic one. Thus we use the lowest value of 0.9

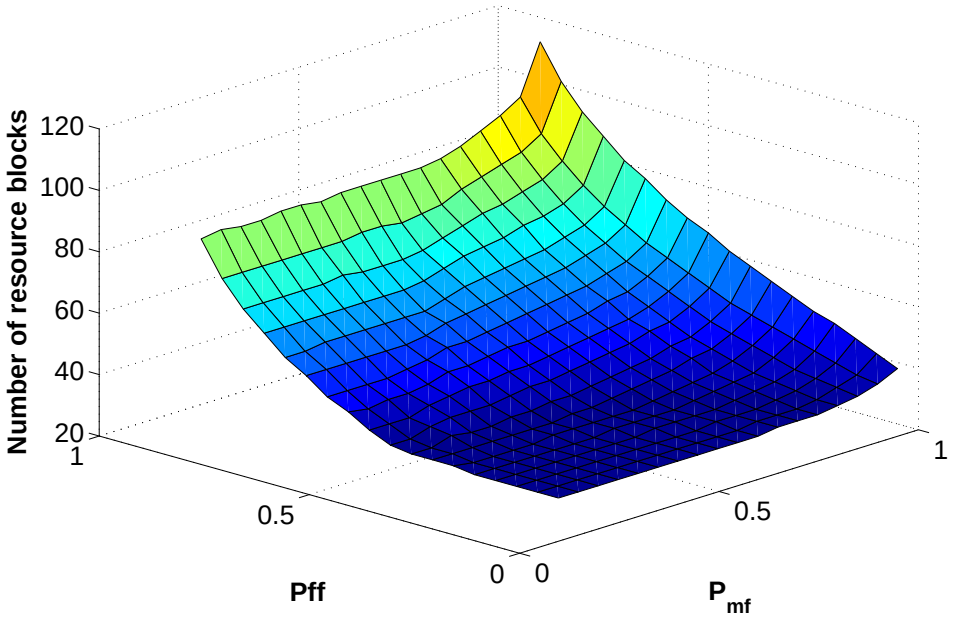

Figure 2.8: The number of RBs for 200 femtocell users and 30 macrocell users in random model.

dB as the SINR threshold for macrocell users, which is able to support QPSK modulation with a rate 1/3 channel code. For femtocell users, we use 18.4 dB as the threshold, which is sufficient to support 64-QAM modulation with a rate 5/6 channel code.

Figures 2.13 and 2.14 show the results for a specific observation from the described simulation model. From the figures, the heuristic algorithm's results are bounded by the upper bound. However, there is a large gap between the heuristic algorithm and the upper bound so the upper bound is not tight. As we mentioned before, clique number as a lower bound may be an appropriate estimate since it is close to the chromatic number in most cases. However, computation of clique number is also a NP-complete problem, which is not suitable for a large network. Thus, we apply the heuristic algorithm, which runs faster than a clique number algorithm, to estimate the number of required RBs, instead of estimating by the upper bound. Since macrocell users naturally form a clique and the clique number of the whole network is at least the number of macrocell users, we use the number of macrocell users as a on the clique number in Figure 2.14 and the results show that the performance

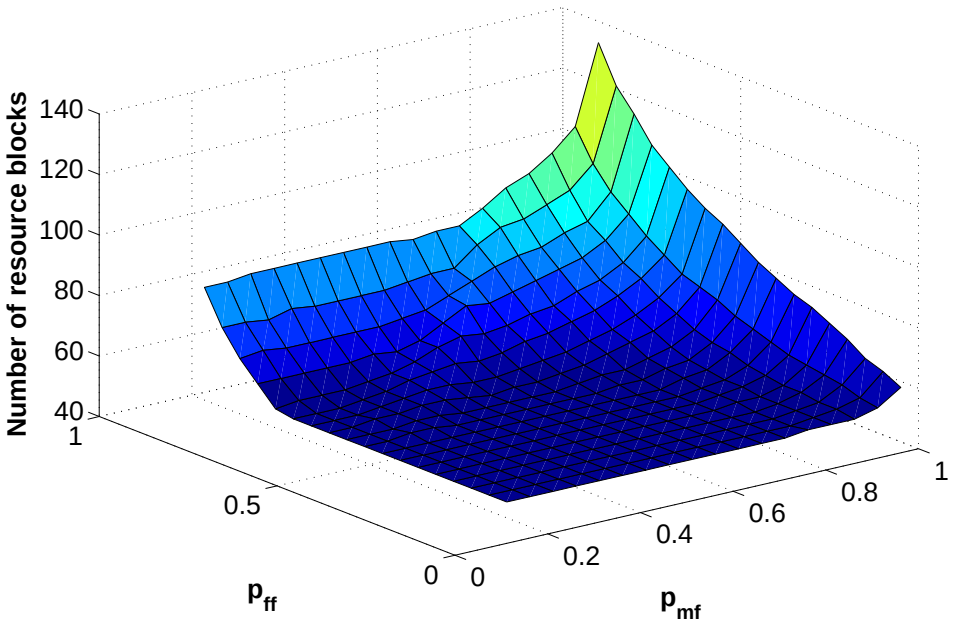

Figure 2.9: The number of RBs for 200 femtocell users and 50 macrocell users in random model. ©2010 IEEE. Reprinted with permission from [2].

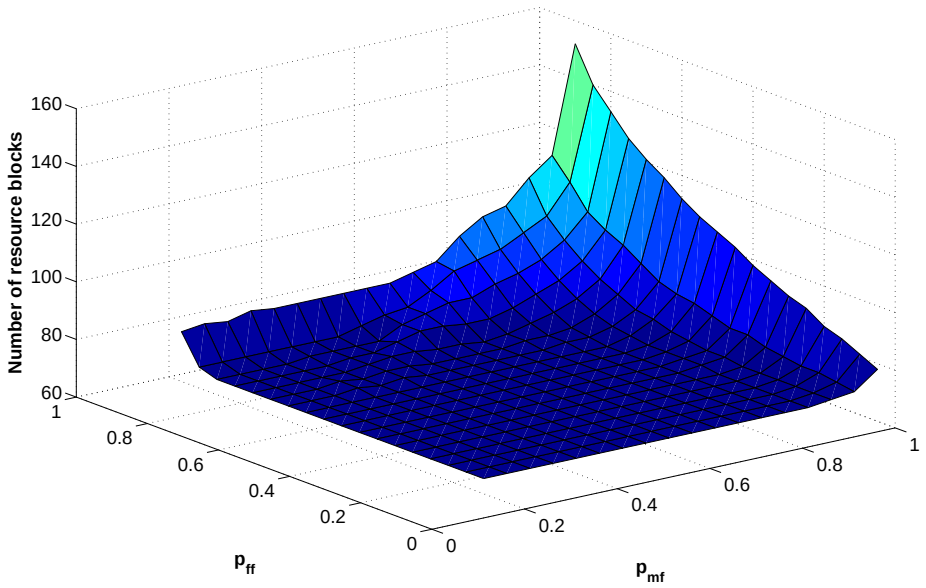

Figure 2.10: The number of RBs for 200 femtocell users and 70 macrocell users in random model.

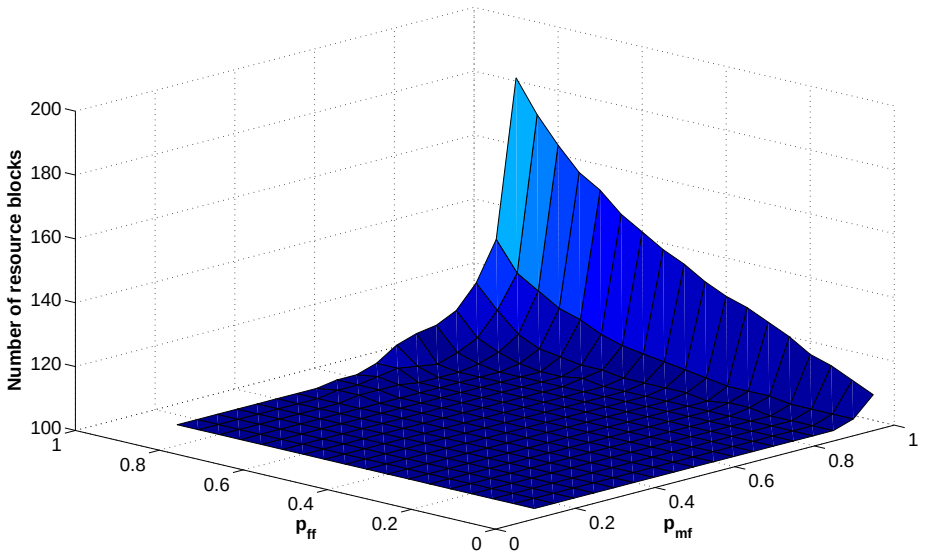

Figure 2.11: The number of RBs for 200 femtocell users and 100 macrocell users in random model. ©2010 IEEE. Reprinted with permission from [2].

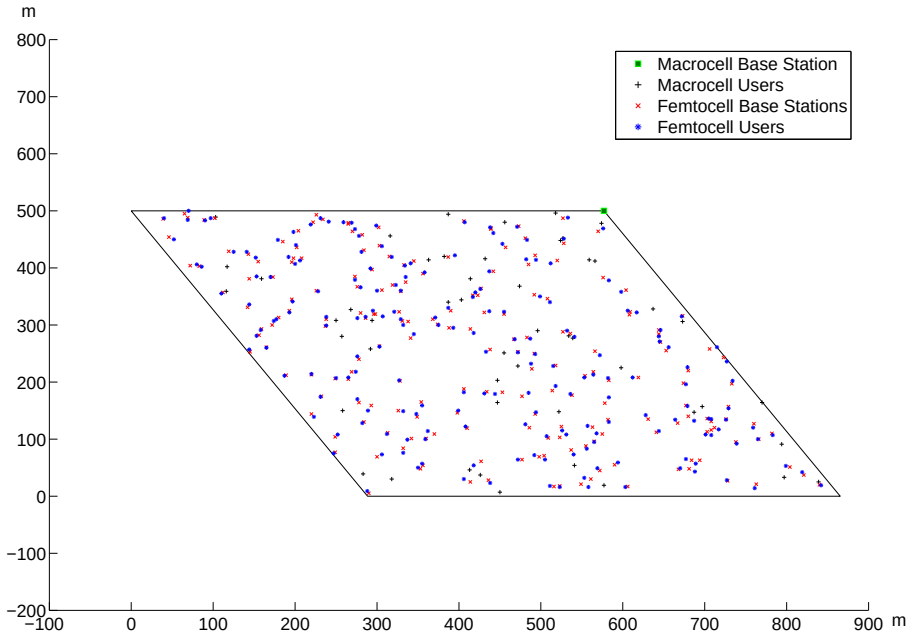

Figure 2.12: Network layout of 200 femtocell users and 50 macrocell users

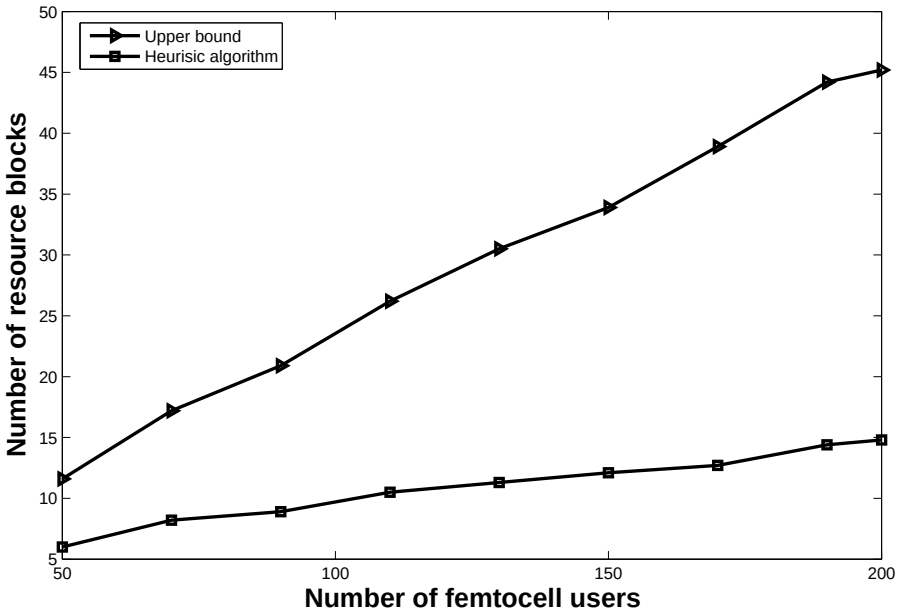

Figure 2.13: The number of RBs for femtocell users in specific observation

of the heuristic algorithm is much closer to this lower bound than to the upper bound. Considering that the actual clique number may be a little larger, we might conclude that the heuristic algorithm's performance is good enough. An alternative solution for specific model is to map it to random model and use random model's upper bound to estimate the number of RBs. This may give us a more accurate and faster result.

2.6 Summary

In this chapter, we have addressed the issue of interference management for cellular networks with macrocells and femtocells. We have described three resource reuse schemes, universal reuse, split reuse, and shared reuse. We have used a protocol model with a conflict graph to address resource reuse problem. Knowledge of graph theory, especially on random graphs, has thus been used to analyze the problem and give upper and lower bounds on the number of RBs required to satisfy minimum assignment requirements for the network. A heuristic

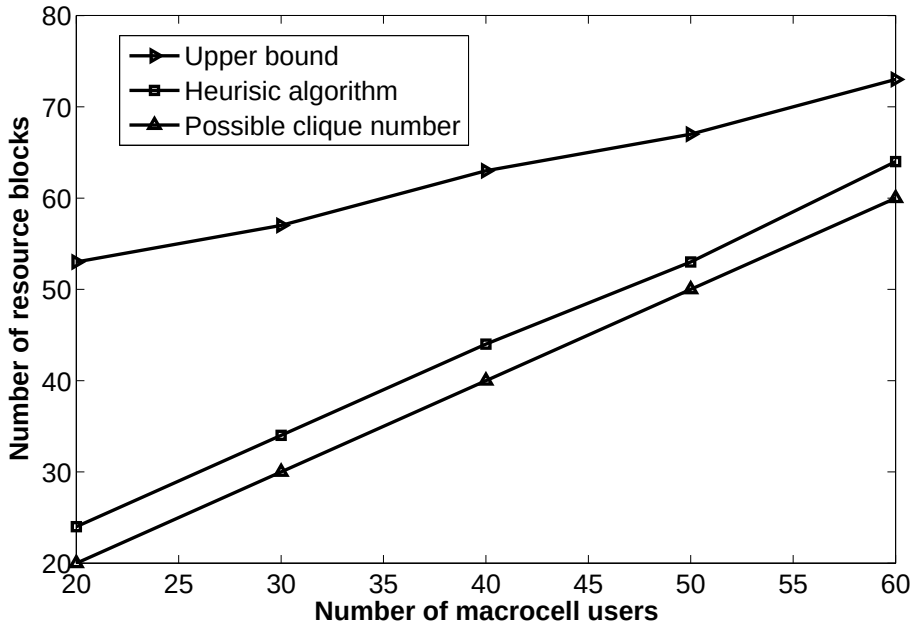

Figure 2.14: The number of RBs for macrocell users and femtocell users in specific observation

algorithm has been developed that yield results that are comparable to theoretical bounds.

Chapter 3

Comparison on Resource Reuse Schemes

In this chapter, our focus is on assigning available RBs to cellular users to maximize social welfare. We first define three network fitness or social welfare functions. Two of them model extremes of utilitarianism and egalitarianism; the third models a compromise between fairness and utility maximization based on proportional fitness. We define resource split points in shared reuse and split reuse to separate resource usage for femtocells and macrocells. As the split points move, we analyze the effect on fitness function values, and we compare fitness between shared reuse and split reuse.

3.1 Introduction

Finding the minimum required number of RBs establishes a baseline on the requirements to operate a network. Another important problem is assigning those RBs among network users (assuming that more than the minimal number of required are available).

Suppose that a network has N RBs, M macrocell users and F femtocells with total of F

femtocell users. For split reuse, we define N_f as the number of RBs that only femtocells can access; thus $N - N_f$ is the number of RBs that only the macrocell can access. We define the split point as $\alpha_{split} = N_f/N$. Similarly, for shared reuse, let N_f be the number of RBs that femtocells are permitted to access; the macrocell is permitted to access all N RBs. We define the split point as $\alpha_{shared} = N_f/N$. Let $N_{f,min}$ denote the minimum number of RBs required to support the femtocell users. Recall that M RBs are required to support the macrocell users, as each must have its own resource block. Then the split point can range from $N_{f,min}/N$ to $(N - M)/N$ in the case of split reuse and from $N_{f,min}/N$ to 1 in the case of shared reuse.

Many works on resource allocation in wireless network use an SINR model as it better reflects reality since an actual system decides channel quality based on the SINR at the receiver. The SINR value further determines the feasible modulation schemes which directly effect the realized throughput. However, there are many challenges associated with using an SINR model in simulation. First, the SINR model depends on many modeling assumptions such as how nodes are distributed in an area, which propagation model is used to evaluate channel attenuation, and how transmit power is selected. Moreover, the SINR is a nonlinear function of the transmit powers, resulting in a complex optimization problem, even without applying a logarithm to covert an SINR value to a capacity. In fact, the work in [87] indicates that resource allocation for an OFDMA system under an SINR model is a nonlinear integer optimization problem. It has been shown in [88] that this problem is NP-hard (i.e. there are no computational efficient algorithms to obtain the optimal allocation). Further, unlike the case where only a few first-tier macrocells generate strong interference, our problem involves a large number of femtocells (e.g. hundreds of them) that interfere with both other femtocell users and macrocell users.

Motivated by this and our work in the previous chapter, we focus on optimal resource allocation within the protocol model. We believe that the protocol model can fairly reflect two things that we are interested in: i) how fitness values vary as the split points move; ii) how split reuse and shared reuse compare.

3.2 Definition of Optimization Functions

At present, we do not consider channel conditions in our optimization formulations of the resource allocation problem. As a result, we assume that RBs are equally valuable to all users. Also we denote a conflict-free resource allocation matrix as $\mathbf{A}$ and $a_{i,j}$ represents the $(i,j)^{th}$ element of $\mathbf{A}$. Intuitively, our first fitness function maximizes reuse efficiency of RBs as follows:

(1) Utilitarian Fitness Optimization

$$\begin{aligned} &\max_{\mathbf{A}\in\mathcal{A}} \left[\sum_{j=1}^{N}\sum_{i=1}^{M+F} a_{i,j}\right] \\ &\text{subject to}: \sum_{j=1}^{N} a_{i,j} \geq 1 \end{aligned} \tag{3.1}$$

This optimization problem seeks to maximize the number of resource block allocations subject to every user receiving at least one resource block. Unfortunately, this formulation tends to lead to unfair resource allocation. Femtocell users are generally more favored by this formulation than macrocell users as the system gets better resource reuse efficiency (more spatial spectrum reuse) if most resources go to femtocells. It can also be expected that most resources will be allocated to those users with better channel conditions, for example, the users close to the BS.

(2) Egalitarian Fitness Optimization

$$\max_{A\in\mathcal{A}} \min_{1\leq i\leq M+F}\left[\sum_{j=1}^{N} a_{i,j}\right] \tag{3.2}$$

This optimization formulation maximizes the number of RBs assigned to the users with the fewest RBs and thus achieves absolute fairness.

(3) Proportionally Fair Fitness Optimization

$$\max_{A \in \mathcal{A}} \left[\sum_{i=1}^{M+F} \log\left(\sum_{j=1}^{N} a_{i,j} \right) \right] \tag{3.3}$$

This formulation reduces the fitness gain associated with possessing a large number of RBs (decreasing returns to scale) and give fairness among all users. This formulation also does not require the the constraint in Equation 3.1 because the log function will force the fitness value to $-\infty$ if any user cannot get at least one RB. Such a resource allocation is commonly called "proportionally fair" and is closely related to the Nash Bargaining Solution in cooperative game theory.

3.3 Optimum Value of Split Points

Similar to single coloring problems, finding the optimum RB allocation for a network with femtocells and macrocells in terms of various optimization functions is at least an NP-hard problem. Therefore it is difficult to determine the optimal value of α_{split} and α_{shared}. Nevertheless, we can derive some useful information about the optimal value by analyzing the resource allocation matrix.

3.3.1 Split Reuse

A typical feasible assignment matrix for split reuse is shown in Figure 3.1. Horizontal lines in the matrix separate users in different cells.

Proposition 3.3.1. *In split reuse, for the utilitarian fitness, as α_{split} increases, the fitness value is non-decreasing. Particularly, as long as G_f is not a complete graph, the fitness value is monotonically increasing.*

We can get this proposition by examining the matrix. Utilitarian fitness optimization aims to maximize the total number of $1s$ in matrix $\mathbf{A}$. If α_{split} increases by a small amount,

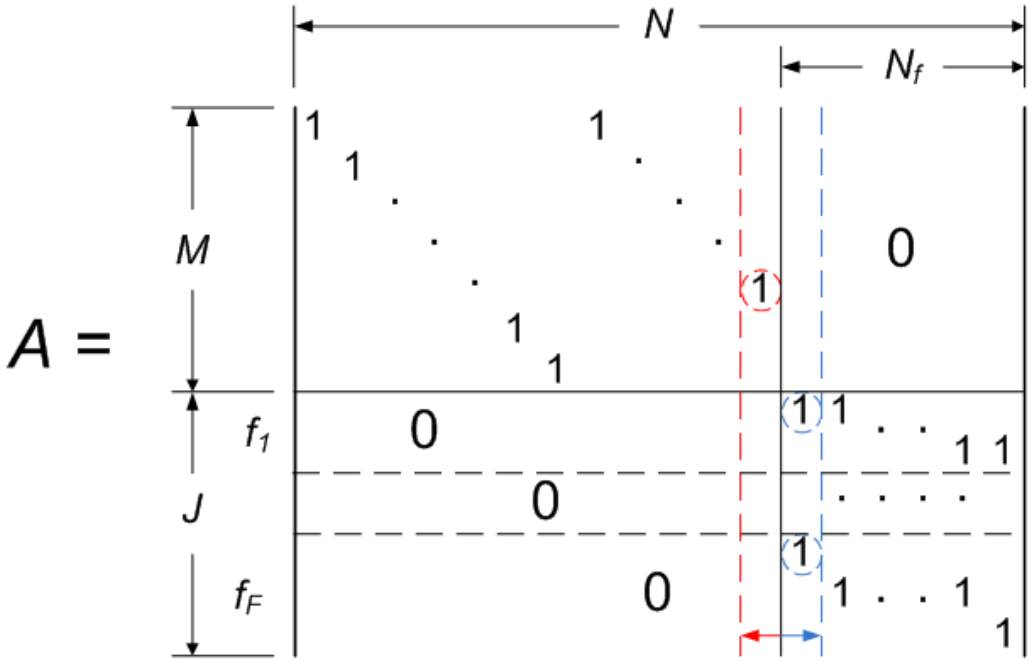

Figure 3.1: A feasible RB assignment matrix for split reuse.

which means the solid vertical line in Figure 3.1 moves to the left by one column (the position of the left vertical dotted line), then one of the 1s from the upper part of the matrix (e.g. the circled 1) has to be removed. Meanwhile, there is an 1 that can be added to at least one position in lower part of the matrix and thus the fitness function value is not decreasing. As long as G_f is not a complete graph, this 1 can be placed at multiple positions in lower part and thus the fitness function value is monotonically increasing.

The proposition is well understood because as long as there are two femtocell users are not conflicting with each other, the RB released from macrocell users can be reused for at least two femtocell users. This result of this proposition is that the optimal value of α_{split} for split reuse under utilitarian fitness is $(N - M)/N$, its upper bound.

For egalitarian fitness, the optimal values of α_{split} is trival to find and it is simply the value of α_{split} at which each user can receive at least $\lfloor N/(N_{f,min}+M) \rfloor$ RBs. Note that $N_{f,min}+M$ is the minimum number of RBs required by the network. Specifically, this means that it is optimal for α_{split} to take on values between $\lfloor \frac{N}{(N_{f,min}+M)} \rfloor \frac{N_{f,min}}{N}$ and $1 - \lfloor \frac{N}{(N_{f,min}+M)} \rfloor \frac{M}{N}$.

For proportionally fair fitness, because of the nature of log function, it is difficult to determine the trend of fitness values when α_{split} is used. We would rather use the algorithms introduced in Section 3.4 to approach the optimum point.

3.3.2 Shared Reuse

Consider the resource allocation matrix for shared reuse shown in Figure 3.2.

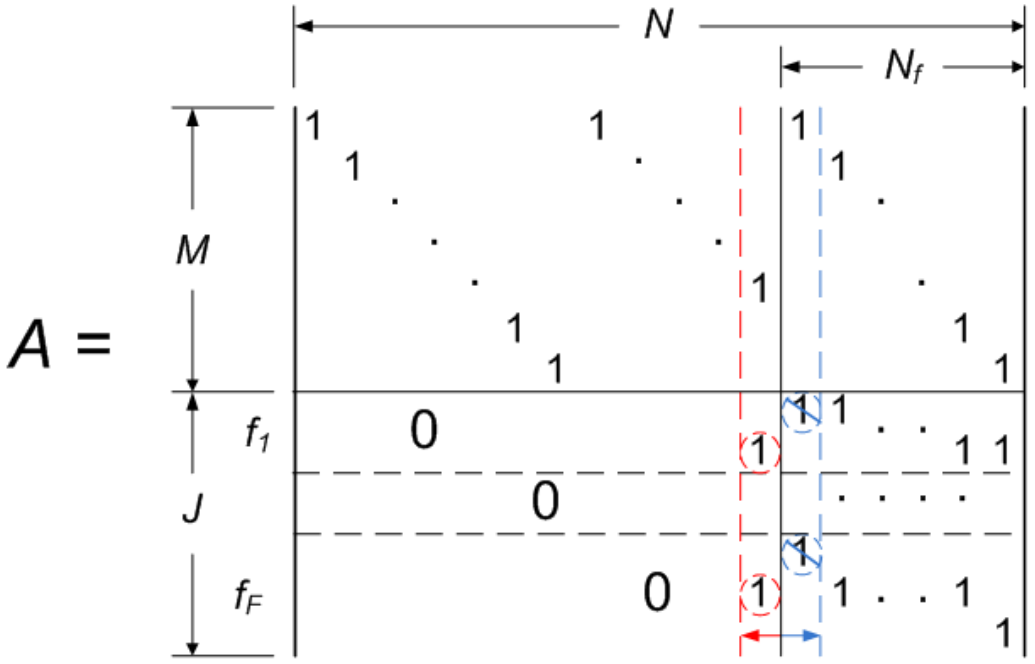

Figure 3.2: A feasible RB assignment matrix for shared reuse.

Proposition 3.3.2. *In shared reuse of resource, as α_{shared} increases, the fitness value is non-decreasing for all fitness functions. Thus the optimal value of α_{shared} from a social welfare point of view is $\alpha_{shared} = 1$.*

This proposition is also easy to understand. When α_{shared} increases by a small amount, the solid vertical line in Figure 3.2 moves to the left by one column (the position of the dotted vertical line on the left), one of the 1s from the upper part of the matrix is opened to access by the lower part of the matrix. If this 1 cannot be put to any position in the lower

part due to conflict graph constraint, the fitness value can at least remain unchanged and thus it is not decreasing.

This proposition shows that, in shared reuse, the optimal value of α_{shared} for all three optimization functions appears at its upper bound 1.

3.4 Numerical Results

Allocation of RBs to network users to optimize certain fitness functions can be mapped to a multi-coloring problem, in which multiple colors are assigned to graph nodes to achieve pre-defined goals. There are several proposed methods for multi-coloring. The work in [89] uses list coloring to allocate multiple colors to nodes. In our work, since we have developed a heuristic algorithm on single RB allocation, our multi-RB allocation method can take advantage of these list coloring methods.

We develop a set of simple algorithms to address different optimization functions. Let $N_{f,heuristic}$ be the number of RBs that the heuristic algorithm requires for single coloring for femtocell users. Thus for split reuse the minimum number of RBs for the whole network is $N_{f,heuristic} + M$. Let $N_{heuristic}$ be the minimum number of RBs that the heuristic algorithm requires for single coloring for the whole network in shared reuse. In general $N_{f,heuristic} \neq N_{f,min}$ and $N_{heuristic} \neq N_{min}$, where N_{min} is the minimum number of RBs required for the network in shared reuse.

For each fitness function, the heuristic function from chapter 2 is first used to partition the users into "color groups" based on a single coloring of the conflict graph. For utilitarian fitness, each color group is given one RB, except for the largest color group which is given all remaining RBs. For egalitarian fitness, every color group is given a set of $\lfloor N/(N_{f,heuristic} + M)\rfloor$ or $\lfloor N/(N_{heuristic})\rfloor$ RBs (depending on split reuse or shared reuse), after which the remaining RBs can be randomly dispersed among the color groups. For proportionally fair fitness, each color group is initially given one RB. Then the remaining RBs are distributed

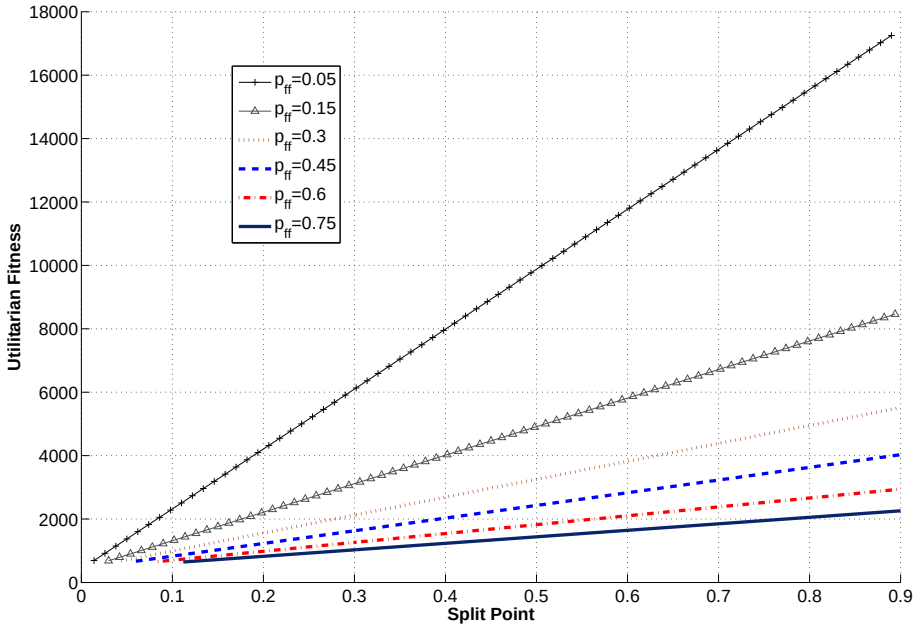

Figure 3.3: Utilitarian fitness optimization for split reuse in random model

one at a time to greedily increase the fitness by giving each RB the the color group that will produce the largest fitness increase.

We simulate conflict graphs constructed using the random model with 200 femtocell users and 50 macrocell users under different values of p_{ff}. We assume there are $N = 500$ available RBs. For split reuse, Figures 3.3, 3.4, and 3.5 show results for utilitarian fitness, egalitarian fitness, and proportionally fair fitness, respectively. Note that in split reuse in the random graph model, p_{mf} does not effect the results.

As expected, utilitarian fitness increases monotonically. In fact the increases are virtually linear. The smaller p_{ff} is, the faster the curve increases due to that RBs freed from macrocell users are allocated only to least conflicted femtocell users. And this allocation leads to extreme unfairness. In egalitarian fitness, the optimum split point actually is the point that every user is allocated with the same number of RBs. As p_{ff} increases, the fitness values drop because with a larger p_{ff}, $N_{f,heuristic} + M$ is larger and this leads to a smaller

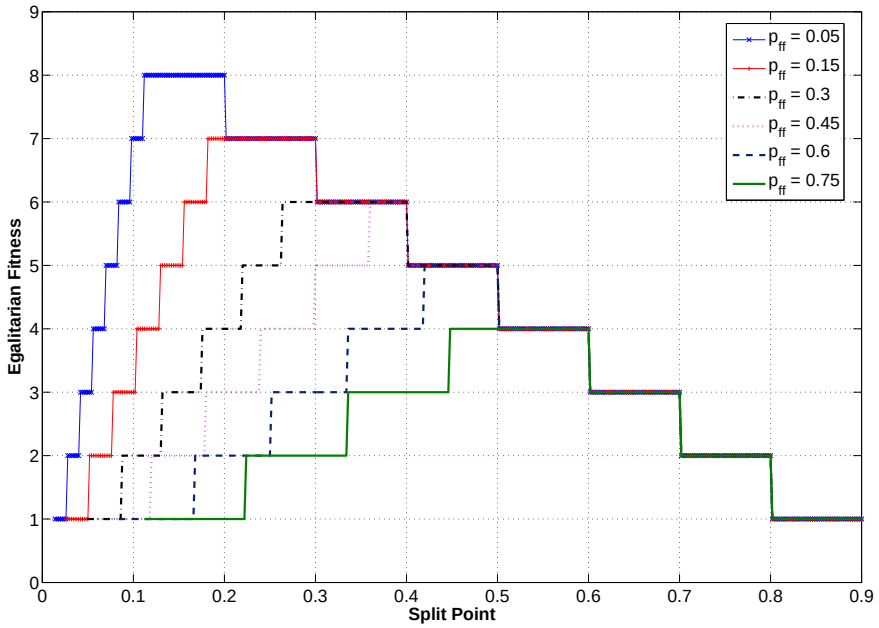

Figure 3.4: Egalitarian fitness optimization for split reuse in random model

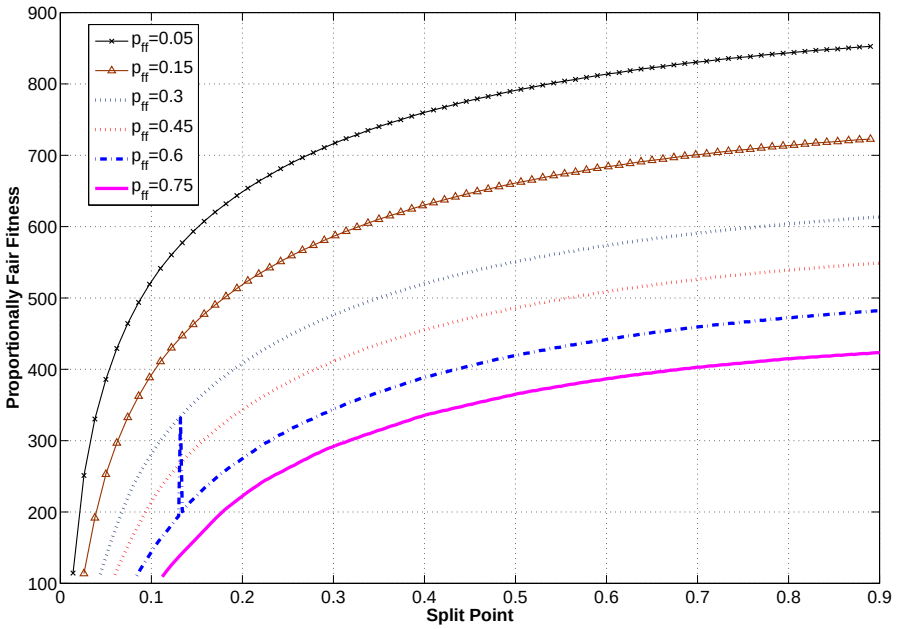

Figure 3.5: Proportionally fair fitness optimization for split reuse in random model

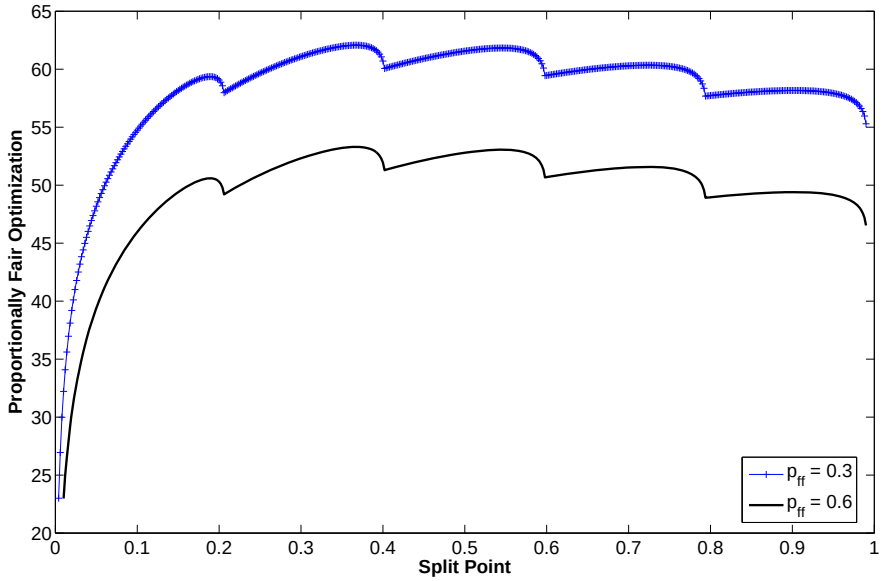

Figure 3.6: An example of proportionally fair fitness optimization for split reuse in random model

$\lfloor N/(N_{f,heuristic}+M)\rfloor$. We also notice that the smaller p_{ff} is, the smaller the optimal α_{split} is. A smaller p_{ff} leads to a smaller $N_{f,heuristic}$. It means we need fewer resources to satisfy femtocell users and this fact can be interpreted as a smaller optimal α_{split}. In addition, this observation verifies our statement in section 3.3.1 that the optimal value of split point happens between $\lfloor \frac{N}{(N_{f,min}+M)} \rfloor \frac{N_{f,min}}{N}$ and $1 - \lfloor \frac{N}{(N_{f,min}+M)} \rfloor \frac{M}{N}$. Curves for proportionally fair fitness function are concave and vary less because they consider fairness among users. Though the curves look monotonically increasing, they are not, and it is hard to tell where the optimum split point is, although it is clearly close to $\alpha_{split} = 0.9$ (which is the upper bound of α_{split} in the simulated scenario). Figure 3.6 gives another example which "amplifies" variation by reducing the number of macrocell users to 5 and the number of femtocell users to 10.

For shared reuse, Figures 3.7, 3.8, and 3.9 illustrate corresponding results of three functions. Curves for all functions increase monotonically and $\alpha_{shared} = 1$ is always the optimum split point. As p_{ff} and p_{mf} increase, all fitness values drop since there are more

conflicts among users.

If we compare shared reuse and split reuse, for egalitarian fitness, shared reuse is always better than split reuse because shared reuse needs fewer RBs to support the same sized network and thus gives each user a larger average number of RBs at the optimum split point. For utilitarian fitness and proportionally fair fitness, shared reuse is always better than split reuse. However, as p_{mf} increases, the advantage of shared reuse becomes smaller, and in some cases, they are very close to each other. This fact can be explained by two aspects. First, the main resource reuse efficiency comes from femtocell users. Thus if a RB is mostly reused within femtocells, the fitness gain associated with switching to shared reuse is the gain associated with assigning one additional macrocell user to the RB, which is not significant. Second, as p_{mf} increases, $N_{heursitic}$ gets closer to $N_{f,heuristic} + M$ (higher p_{mf} implies an increasing need to put femtocell and macrocell users in different RBs). Thus, the fitness gain by allowing reuse of RBs between femtocell and macrocell users is reduced. This also indicates that split reuse may be a better choice than shared reuse for utilitarian and proportionally fair fitness in the case of heavy interference between femtocell users and macrocell users, given that fitness optimization and spectrum management under split reuse is much easier than under shared reuse.

3.5 Summary

In this chapter, we have addressed allocating RBs to femtocell users and macrocell users with respect to three different optimization functions: utilitarian fitness, egalitarian fitness, and proportionally fair fitness. We evaluate the performanc of split reuse and shared reuse on the three optimization functions. Numerical results confirm our analysis and indicate that in the case of heavy interference between femtocell users and macrocell users, split reuse may be a better choice than shared reuse because split reuse offers easier interference control and lower computational complexity while offering comparable performance. In the case of

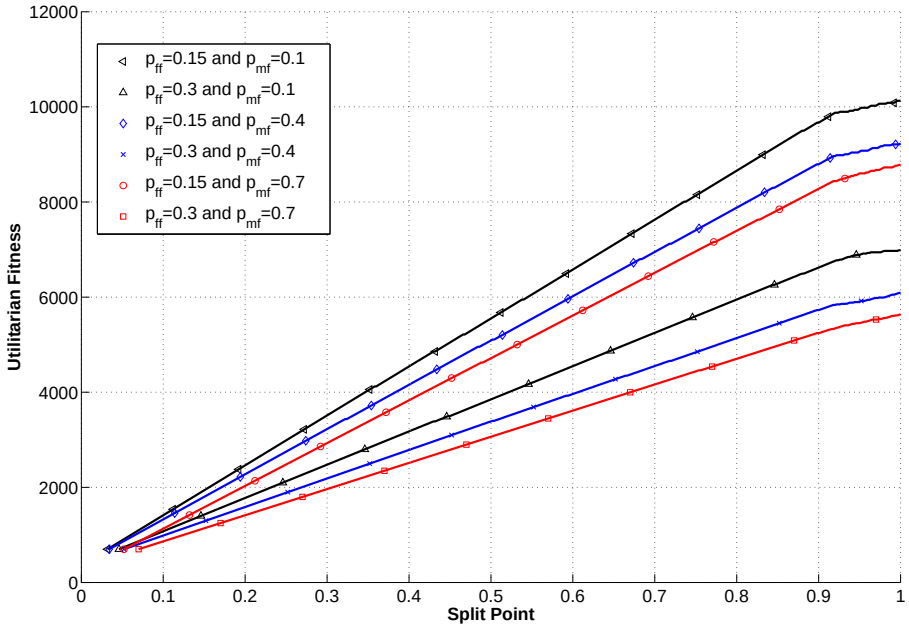

Figure 3.7: Utilitarian fitness optimization for shared reuse in random model

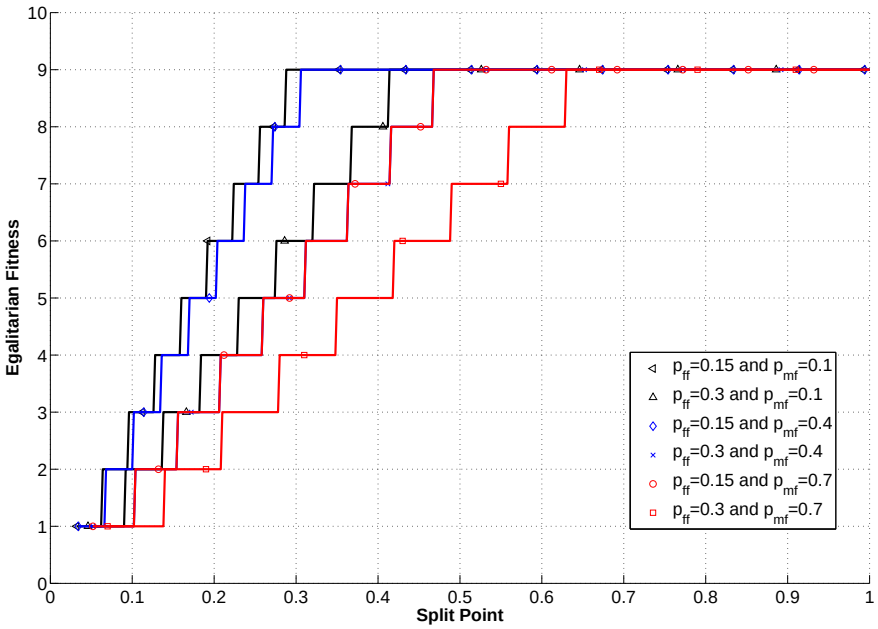

Figure 3.8: Egalitarian fitness optimization for shared reuse in random model

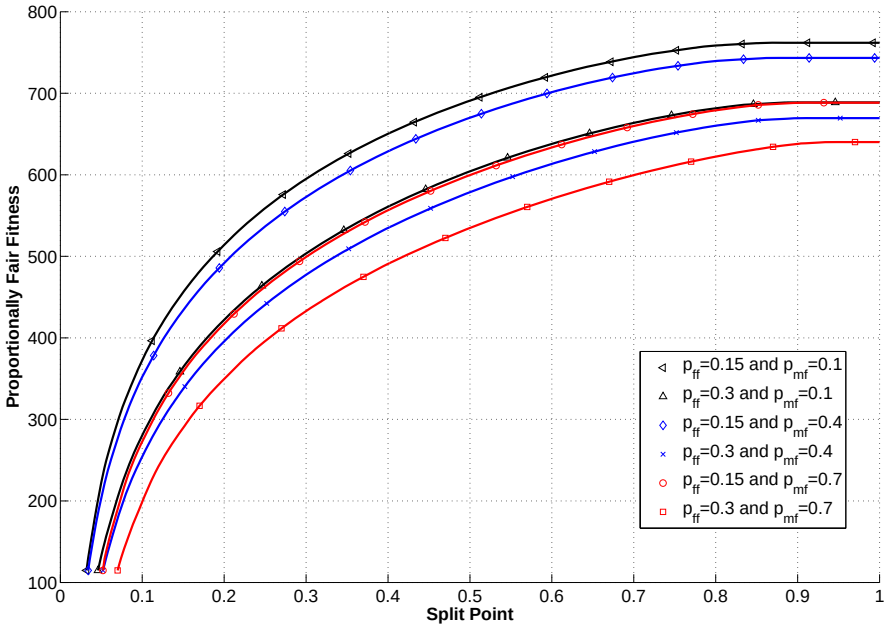

Figure 3.9: Proportionally fair fitness optimization for shared reuse in random model

lighter interference between femtocell users and macrocell users, our results are lass stark. Shared reuse can provide significant fitness benefits, but at potentially high computational and informational cost.

Chapter 4

Genetic Algorithms for Resource Allocation [1]

In last two chapters, we have derived upper and lower bounds for the number of RBs required for cellular networks with coexisting macrocells and femtocells and analyzed the performance of different resource reuse schemes, namely split reuse and shared reuse. In this chapter, a centralized algorithm based on a Genetic Algorithm (GA) is introduced to solve the resource allocation problem. Such a problem is known to be NP-hard. The results of this chapter serve two purposes: First, to demonstrate that GAs can find near-optimal resource allocations for macrocell/femtocell cellular networks. Second, the allocations found by GAs establish baselines that can be compared to the allocations generated by distributed resource allocation algorithms, which will be presented in the next chapter.

[1] This work was completed in cooperation with Fahad Ali, an M.Eng. student, as part of his final project

4.1 Introduction

Resource allocation is a key issue in a network serving multiple users. The basic question is how to efficiently distribute limited resources to users with respect to social welfare. Normally, resource allocation is jointly considered with interference management as they are closely related to each other and may be addressed simultaneously. In the protocol model used in this dissertation, two communication links either interfere with each other or not. Thus, essentially, our resource allocation problem needs to be addressed from two aspects. First, the allocation has to be conflict-free. That is, conflicted links cannot use the same RB. Second, the allocation needs to optimize social welfare.

To achieve an efficient conflict-free resource allocation, in Chapter 2 we mapped the network interference scenario to a conflict graph such that the vertices represent the communication links in the network and an edge between two vertices indicates that these two links cannot use the same RB. Thus the resource allocation problem is mapped to a graph coloring problem such that adjacent vertices cannot be the same color. Then we used a greedy single coloring algorithm to assign colors (in our problem, RBs) to the vertices (communication links). Though the greedy algorithm is not guaranteed to give an optimal solution (in this case, finding the minimal number of RBs required for the network), its results are sufficiently good. However, the single coloring algorithm aims to find as few RBs as possible to achieve a conflict-free allocation, but not to assign a fixed number of RBs, which is usually much larger than the minimal number of required RBs, to the network. In practice, a common problem is, for example, given 100 RBs and 50 users, what is the best way to assign those RBs to the users. Clearly, other algorithms are required to solve this problem.

Assuming a network has F femtocell users, M macrocell users, and N RBs, we denote a resource allocation matrix $\mathbf{A} \in \mathcal{A}$, where $\mathcal{A}$ is the set of all conflict-free resource allocation matrices, and $a_{i,j}$ represents the $(i,j)^{th}$ element of $\mathbf{A}$. Recall three social welfare functions defined in Chapter 3, namely utilitarian, egalitarian, and proportional fairness, expressed as follows:

(1) Utilitarian Fitness Optimization

$$\begin{aligned} &\max_{\mathbf{A}\in\mathcal{A}} \left[\sum_{j=1}^{N}\sum_{i=1}^{M+F} a_{i,j}\right] \\ &\text{subject to}: \sum_{j=1}^{N} a_{i,j} \geq 1 \end{aligned} \tag{4.1}$$

(2) Egalitarian Fitness Optimization

$$\max_{A\in\mathcal{A}} \min_{1\leq i\leq M+F} \left[\sum_{j=1}^{N} a_{i,j}\right] \tag{4.2}$$

(3) Proportionally Fair Fitness Optimization

$$\max_{A\in\mathcal{A}} \left[\sum_{i=1}^{M+F} \log\left(\sum_{j=1}^{N} a_{i,j}\right)\right] \tag{4.3}$$

One way to optimize the above functions is to use the result of a single coloring algorithm, shown in Figure 4.1. If we assume the single coloring algorithm results are optimal then it is relatively easy to derive the resource allocations that optimize the utilitarian and egalitarian fitness functions. For utilitarian fitness, one simply copies the usage pattern of the most used RB to all unused RBs. (Technically, one should identify a maximal independent set and assign all unused RBs to it. But in many cases the largest color family in the optimal single coloring will be a maximal independent set.) In the egalitarian fitness case, the single coloring result is repeated across all RBs. However, it is not trivial to find the optimum for proportionally fair fitness function. In Figure 4.1, the illustrated is one allocation that is optimal by an exhaustive search. As the problem is NP-hard [90], it is impossible to find a computationally efficient algorithm that achieves the optimal proportionally fair resource allocation for a large network.

In reality, utilitarian fitness is rarely used as it tends to result in unfair allocations.

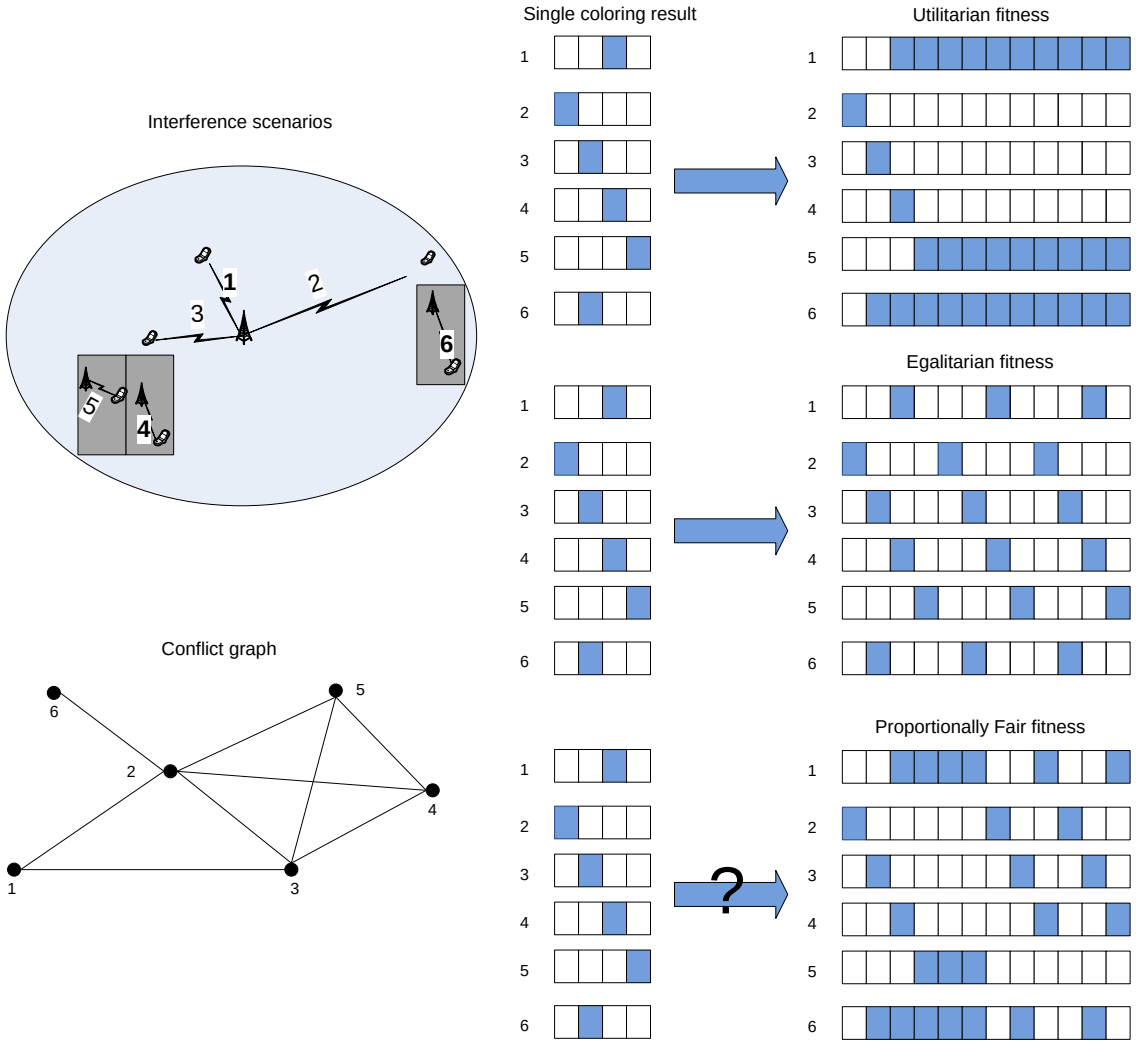

Figure 4.1: Resource allocations for a macrocell/femtocell network.

Most practical resource allocators strive for proportional fairness (or a related concept) as it achieves a degree of fairness among all users, but does not lose much resource reuse efficiency. In this chapter, we will use a GA to address the resource allocation problems in macrocell/femtocell networks with respect to proportional fairness. Other published works show that GA is a good tool to address such a problem [91–94]. In one of our previous works, an island-GA is used to solve channel allocation problem in an ad hoc network and yields satisfactory results [95].

4.2 Genetic Algorithms

4.2.1 Overview

The GA is an optimization and search technique based on principles of genetics and natural selection [96]. A GA allows a population composed of many individuals (individuals are feasible solutions) to evolve under specified selection rules in an attempt to identify the individual that optimizes the fitness. The method was developed by Holland [97] over the course of the 1960s and 1970s and popularized by one of his students, Goldberg, who was able to solve a difficult problem involving the control of gas-pipeline transmission [98]. A GA is not guaranteed to find the optimal solution in finite time, but is proven to yield good solutions if it runs with sufficient iterations.

Once the problem variables and other feasibility constraints are converted into elements of natural selection, the GA will use the problem variables to create solutions. The GA will then evolve of these solutions by crossover and mutation. Unwanted solutions are rejected or down weighted at every stage of the evolution on the basis of a fitness function. Two types of genetic algorithms are binary genetic algorithms and continuous genetic algorithms [96]. Binary genetic algorithms work with variables after encoding them as binary vectors while a continuous genetic algorithm deals directly with continuous variables. Note that in our

resource allocation problem, binary genetic algorithms are applied.

4.2.2 Procedures of Genetic Algorithms

Figure 4.2 briefly describes the procedures of a GA. The components and terminologies used in the GA are explained below.

- Fitness function

  The fitness function (also called the objective function) is usually defined as an objective to measure the "quality of the obtained solution" [96]. The fitness function is problem dependent and needs to be as simple as possible because the evaluation of the fitness function is one of the most time consuming stages of the GA procedure. Equations 4.1, 4.2, and 4.3 are examples of the fitness function.

- Chromosomes

  Chromosomes are a fundamental element of the GA. A chromosome is a set of variables that are source of good or bad traits in an individual. Offspring inherit these traits from the parents.

- Individuals

  An individual is a candidate solution consisting of chromosomes.

- Initial population

  GA begins by creating an initial population of individuals. The general rule of creating an initial population is to distribute individuals as evenly as possible throughout the search space. This allows the GA to cover many regions in the search space and helps to avoid the algorithm becoming trapped a local optimum.

- Natural selection

  Natural selection retains only a percentage of the population in the next generation. Normally, only the best individuals (according to the fitness function) are selected to

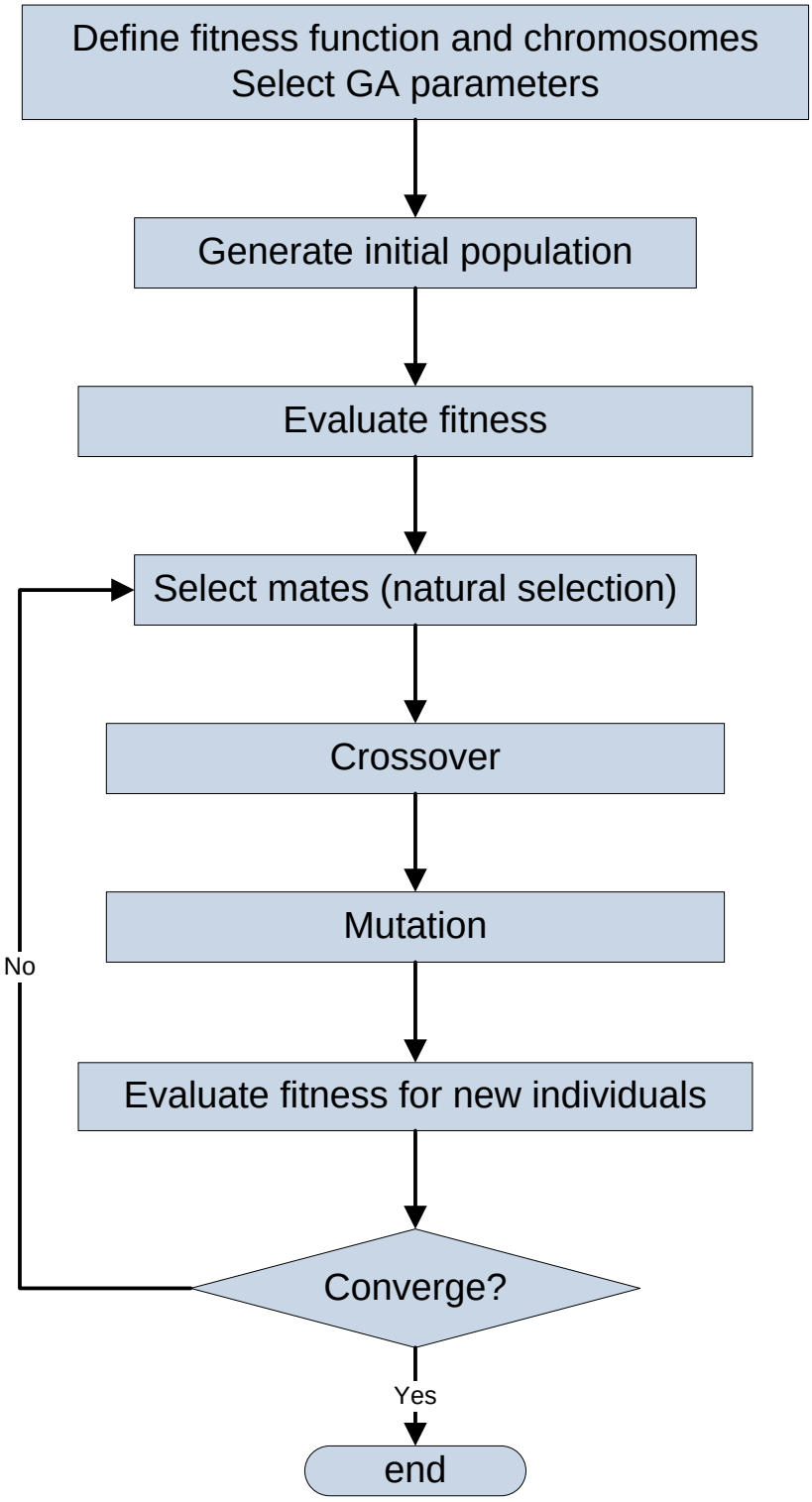

Figure 4.2: Flowchart of A Genetic Algorithm.

survive. Remaining individuals are removed from the population. Sometimes, a small number of individuals of bad fitness are also retained to maintain population diversity. The percentage of population discarded is one important parameter in a GA. If the percentage is too low, then many bad individuals will stay, preventing quick evolution of a GA; if the percentage is too high, there will be a lack of good individuals in the next generation.

- Crossover

  Once natural selection is done, mating is performed among these parents to generate one or more offspring. The most common form of mating is crossover that uses two parents to produce two offspring. One or more crossover points are randomly selected to split the parents' genes into pieces, and the pieces of different parents are then combined to form new offspring.

- Mutation

  Crossover may lead to a next generation that explores more areas of the search space. However, it is still tied to the previous generation because it does not introduce any new gene values. Mutation is introduced to explore areas of search space that cannot be explored by crossover. Random mutations alter a certain percentage of chromosomes of an individual. Mutation help to prevent the GA from converging to a local optimum. Note that usually the best individuals in a generation are categorized as elite individuals and excluded from mutation. In a binary GA, mutations happen by mutating a 1 to 0 or vice versa. Figure 4.3 shows examples of crossover and mutation.

4.3 Problem Formulation

To map our resource allocation problem to the format that the GA can address, chromosomes and individuals have to be defined. Assuming there are M macrocell users, F femtocell users,

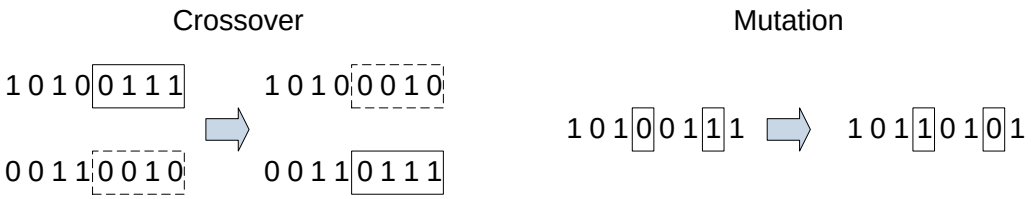

Figure 4.3: Examples of crossover and mutation.

and N RBs, the resource allocation problem is to build a $(M+F)\times N$ matrix, $\mathbf{A}$, such that element $a_{i,j}$ is 1 if the i^{th} user uses the j^{th} RB. This matrix should represent a conflict-free RB allocation and should optimize social welfare. Note that in this chapter, we only focus on proportional fairness because it is widely used in practical systems and challenging to optimize.

4.3.1 Chromosomes

Chromosomes are basic elements in the GA. We define each column of the resource allocation matrix as a chromosome. Thus, a chromosome reflects how a RB is reused among macrocell users and femtocell users. In a conventional binary GA, chromosomes are usually randomly set. For example, one could let the computer program randomly generate binary vector as a chromosome. However, this will have a problem in our setting as the achieved resource allocation matrix must be conflict-free. If a randomly selected chromosome is used, it is likely that this chromosome will be "infeasible", i.e. the usage pattern of the RB is not allowed by the conflict constraint. Thus the resource allocation matrix composed of such infeasible chromosomes will also be infeasible. If such infeasible matrices are allowed in the population, it may take a long time, or be impossible, to evolve to feasible allocation. In our GA, an algorithm that is pseudo random in nature is developed to formulate feasible chromosomes. This algorithm will be described in Section 4.3.3.

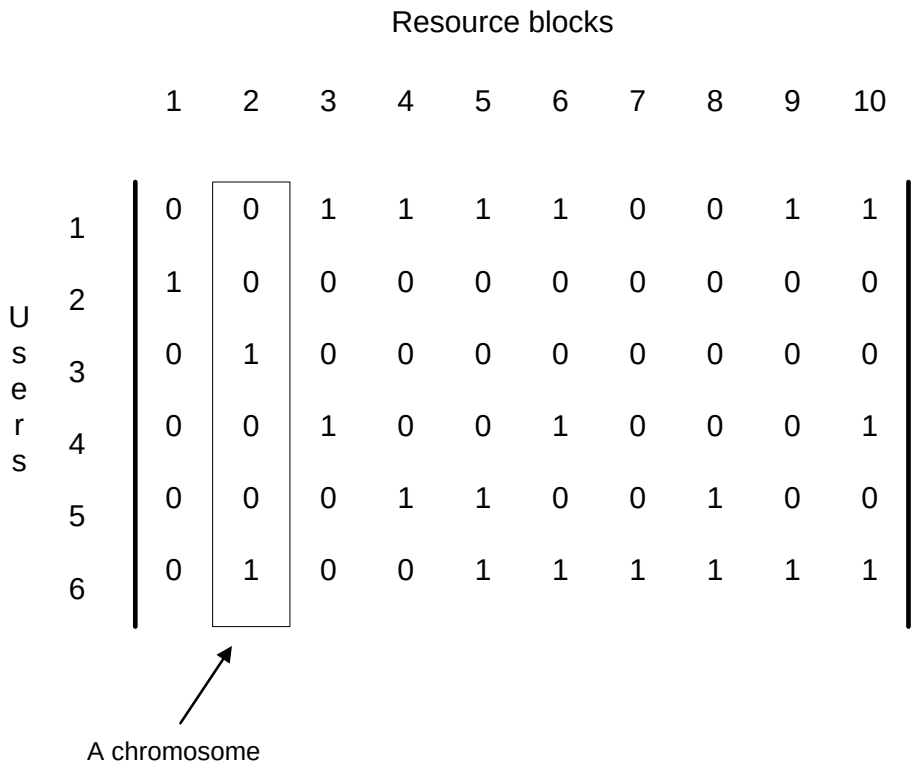

Figure 4.4: An Example of an individual and chromosomes in it.

4.3.2 Individuals

An individual is a set of chromosomes and represents a feasible resource allocation. Note that if a mechanism can guarantee feasibility of each chromosome, the resulting individual will also be feasible. Figure 4.4 shows an example of an individual and chromosomes in it. Conflict constraints are from the conflict graph in Figure 4.1. In the figure, the resource allocation matrix (the individual) consists of 6 users and 10 RBs.

4.3.3 Initial Populations

The initial population is generated randomly. Note that the individuals in the initial population must be feasible. To ensure this, we use following steps.

- Step 1: Initialize the selected chromosome (a column in the resource allocation matrix), the set of users, to $1, 2, ..., M + F$
- Step 2: Randomly select a user, f. Set the f^{th} index in the chromosome to 1. Remove f and all user that conflict with f from the set.
- Step 3: If the set is not empty, go to step 2.

We define "retention rate", λ, as the percentage of individuals (in the last population) that will remain in the population. Those retained individuals enter the parent pool to generate offspring by crossover. In this chapter, we define $N_{population}$ as the number of individuals in each population and simply retain the best $\lfloor N_{population}\lambda \rfloor$ individuals on fitness as the parent pool.

4.3.4 Crossover

Before performing a crossover, two parents must be selected from the parent pool, with size $N_{retain} = \lfloor N_{population}\lambda \rfloor$. We use a weighted random pairing algorithm. The probabilities assigned to the individuals in the parent pool are proportional to their fitness. An individual with the highest fitness has the greatest probability to be selected, while the individuals with the lowest fitness is selected with the lowest probability. Particularly, we use rank weighting. First, all individuals in the parent pool are sorted by their fitness and assigned a rank, r, such that the best-fitness individual receives a rank of 1 and the worst-fitness individual receives $r = N_{retain}$. Then the probability with which an individual is selected is assigned to be

$$P_r = \frac{N_{retain} - r + 1}{\sum_{r=1}^{N_{retain}} r}. \tag{4.4}$$

Table 4.1 shows an example.

r	Individual	P_r
1	Individual 1	0.33
2	Individual 2	0.27
3	Individual 3	0.2
4	Individual 4	0.13
5	Individual 5	0.067

Table 4.1: Rank weighted individuals

Another important parameter is the crossover point that separates chromosomes in an individual for crossover. The crossover point of 0.5 is commonly used because it uses a half chromosomes from each parent to form offsprings. In this chapter, we use a randomly selected crossover point, from 0 to 1. Figure 4.5 shows the crossover process in the GA for our resource allocation problem. Again, conflict constraints are from the conflict graph in Figure 4.1 is used as conflict constraints. Note that since each chromosome is a feasible RB allocation, the generated offspring also represent feasible solutions. In the this figure, two parents, with a crossover point between chromosome 4 and chromosome 5, generate two offspring.

4.3.5 Mutation

We use a parameter called the mutation rate, μ, to define the amount of mutation performed in each population. After finishing crossover, mutation is performed by randomly selecting individuals, excluding the ones with the best fitness (these individuals are called elite ones). The number of chromosomes to be mutated is given by:

$$\text{Number of mutations} = \mu(N_{population} - N_{elite})N_{chromosomes}, \tag{4.5}$$

where N_{elite} is the number of elite individuals and $N_{chromosomes}$ is the number of chromosomes in an individual. In our GA, we use an approach called column mutation: We randomly pick

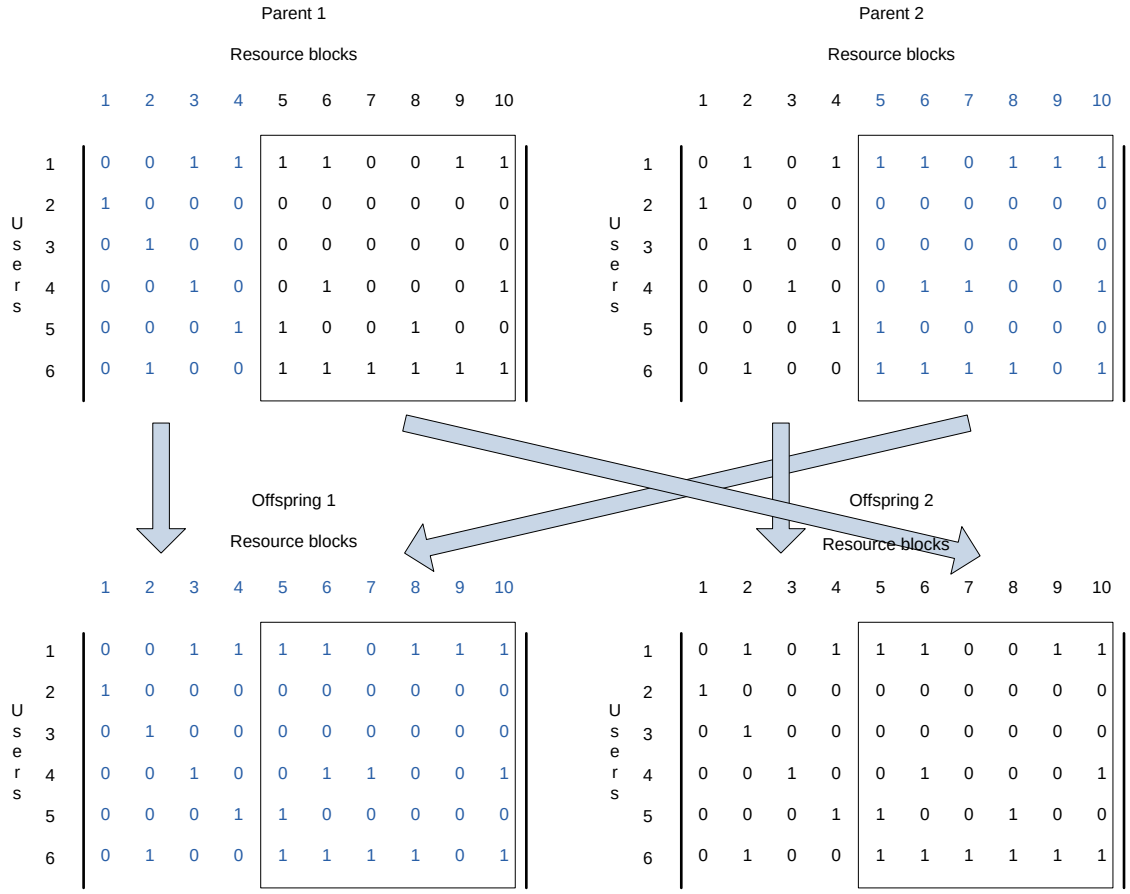

Figure 4.5: A crossover process with a crossover point of 0.4.

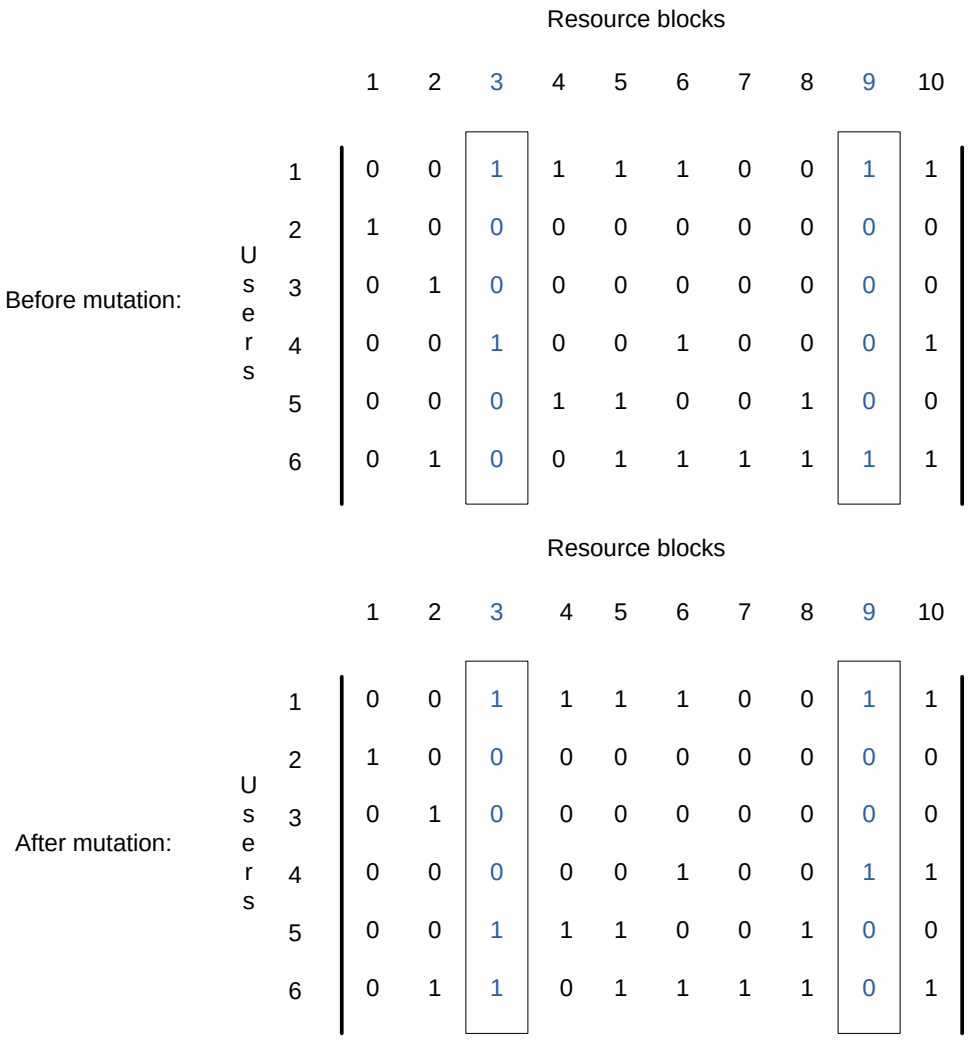

Figure 4.6: A mutation process.

a column in the allocation matrix and replace the entire column with a newly constructed feasible chromosome. This process is shown in Figure 4.6.

4.3.6 The Next Generation and Convergence

After mutation takes place, the process of natural selection, generation of offspring via mating and crossover, and mutation is repeated. The number of generations (iterations of the algorithm) depends on whether an acceptable solution is reached. The current implementa-

tion terminates after a fixed number of iterations or if the maximum fitness does not change for some consecutive number of iterations.

4.4 Numerical Results

4.4.1 A Simple Example

We would like to use a simple example to see how the GA performs in a small network. We still use the interference scenario described in Figure 4.1. Recall that there are 6 users and 10 RBs. The convergence criterion used for this case is to run 200 iterations. Figure 4.7 shows how the maximum fitness of the population evolves as the GA progresses. In this case, the population size is 8. A brute force search is used to find the optimal solution for this simple case and the figure shows the GA reaches the optimum in about 100 iterations. This figure also indicates that the GA is stuck at the fitness of 7.2 for a long time (about 80 iterations) and finally jumps out of this local optimum. If a different convergence criterion is used, the GA might not have been able to reach the optimal solution. However, the GA gives a good fitness (7.2) in a small number of iterations (5).

The optimal resource allocation given by the GA is shown in Figure 4.8.

4.4.2 Large Networks

We now apply the designed GA to obtain proportionally fair resource allocations in larger networks. Three network scenarios are used to evaluate GA's performance. The parameters of the three cases are listed in Table 4.2

Figure 4.9, Figure 4.10, and Figure 4.11 show how the maximum fitness and mean fitness of the population evolve as GA progresses through generations for case I, II, and III, respectively. In all cases, the GA quickly (in about 100 to 200 iterations) reaches a good

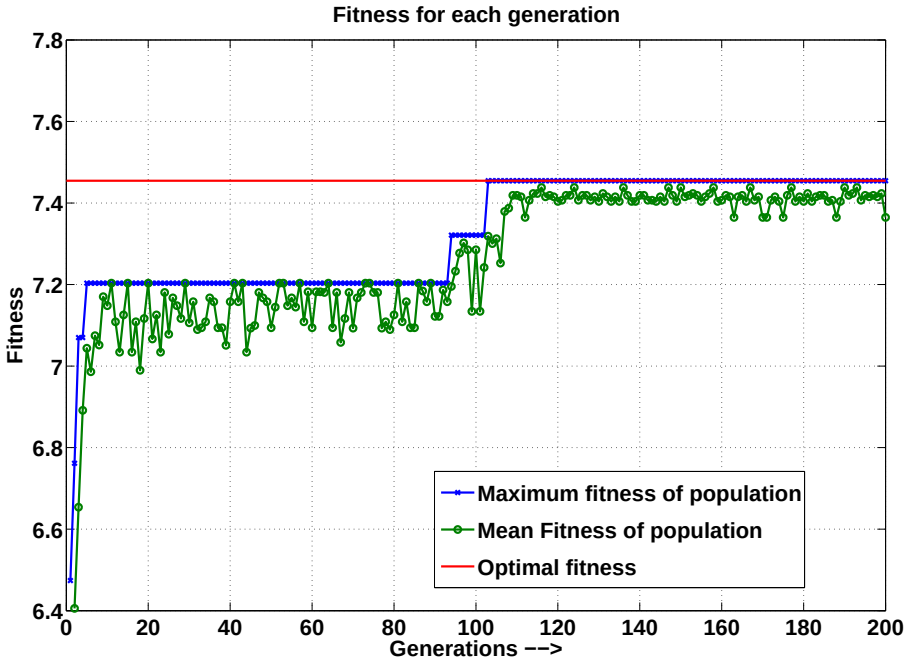

Figure 4.7: Fitness of the population of each iteration in GA.

Resource blocks

Users	1	2	3	4	5	6	7	8	9	10
1	0	1	1	1	0	1	0	1	1	0
2	0	0	0	0	1	0	1	0	0	0
3	1	0	0	0	0	0	0	0	0	1
4	0	1	1	0	0	1	0	0	0	0
5	0	0	0	1	0	0	0	1	1	0
6	1	1	1	1	0	1	0	1	1	1

Figure 4.8: Optimal resource allocation for the simple example

Parameters	Case I	Case II	Case III
Network setup			
Femtocell users	50	75	100
Macrocell users	20	25	30
Resource blocks	100	150	200
p_{ff}	0.2		
p_{mf}	0.2		
GA setup			
Population size	50	50	100
Convergency condition	1000 iterations		2000 iterations
Remain rate, λ	0.5		
Crossover point	Random		
Mutation rate	0.2		
Number of elite users	1		

Table 4.2: Network and GA parameters

level of fitness and then continues exploring better solutions until the convergence condition is met. However, there is no provision to guarantee that the GA has found the optimal solution. The mean fitness of the population tends to follow the maximum fitness, which is expected since the good traits (high fitness) are being propagated in the population.

We would like to compare the performance of the GA and with heuristic algorithm introduced in Chapter 3. Let us recall procedures of the heuristic algorithm. At the beginning, an $(F+M)\times N$ all zero RB allocation matrix is built. The algorithm uses the results obtained from a single coloring algorithm to occupy left columns of the RB allocation matrix, guaranteeing that each user initially receives one RB. Then the algorithm examines each assigned RB, determines if this RB can accommodate more users, and updates the RB allocation matrix. For each remaining all-zero column of the assignment matrix, the algorithm determines which of the previously used column assignments would produce the maximum fitness gain and copies that column to the unassigned column. Four network scenarios are used to compare the two algorithms and their parameters are shown in Table 4.3. Figure 4.12 compares the algorithms under shared reuse (now it is actually universal reuse) and Figure 4.13 shows

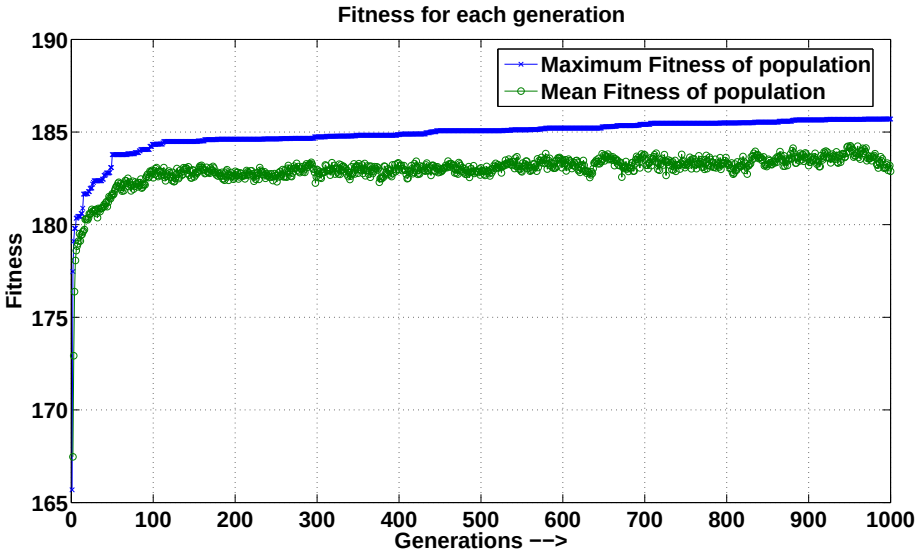

Figure 4.9: Maximum fitness of the population of each iteration in GA for case I.

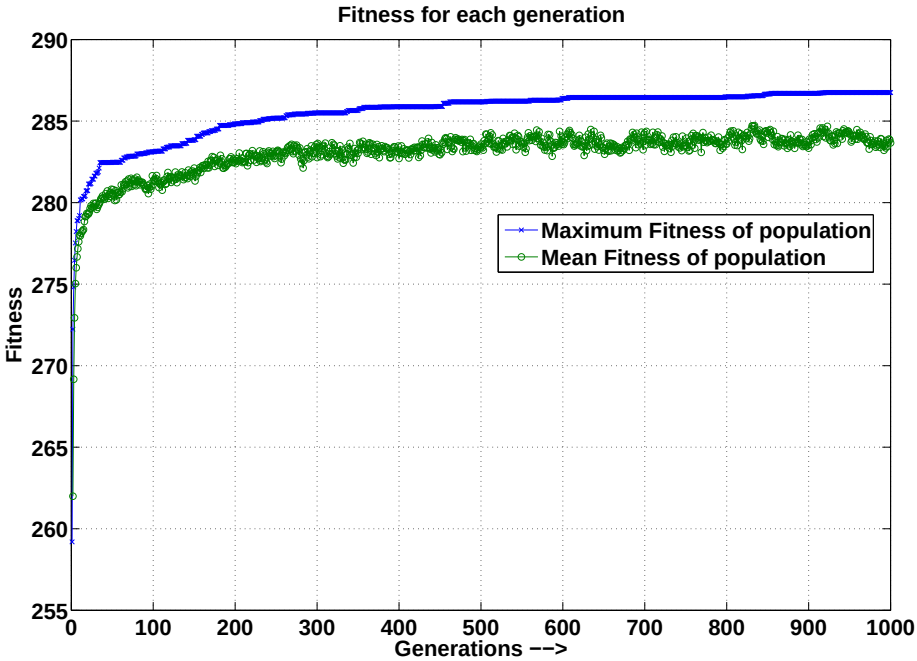

Figure 4.10: Maximum fitness of the population of each iteration in GA for case II.

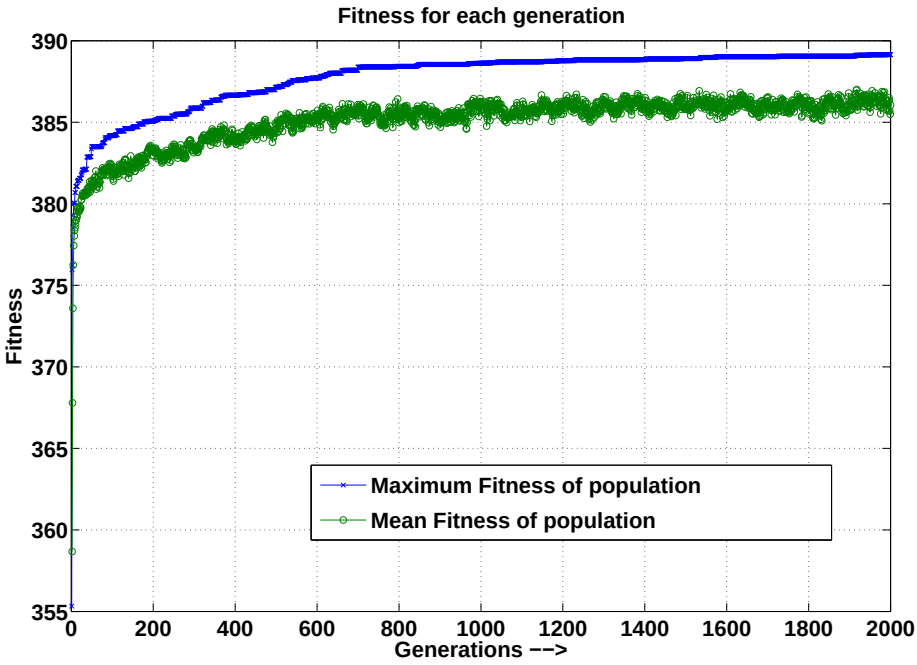

Figure 4.11: Maximum fitness of the population of each iteration in GA for case III.

Parameters	Femtocell users	Macrocell users	p_{ff}	p_{mf}	Number of RBs
Case I	40	15	0.2	0.2	80
Case II	50	20	0.2	0.2	100
Case III	75	25	0.2	0.2	150
Case IV	100	30	0.2	0.2	200

Table 4.3: Network parameters

the results under split reuse. From these two figures, the GA always gives better results than the heuristic algorithm and their the performance gap increases as the network scale become larger. This indicates that the GA will give better fitness in more complex cases, though it comes with the cost of long running time. We also notice that the performance gap in split reuse is smaller than in shared reuse. This can be explained because in split reuse, the complexity of the problem is reduced and thus the heuristic algorithm is able to handle the problem efficiently.

In Chapter 3, we have compared the performance of shared reuse and split reuse and found

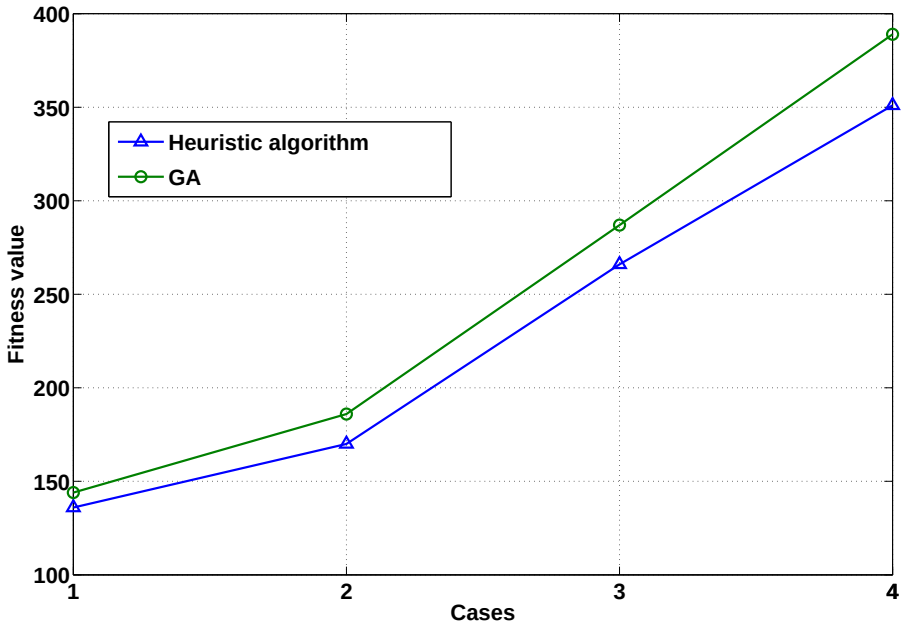

Figure 4.12: Performance comparison between the GA and the heuristic algorithm in different network scenarios for shared reuse.

out that although shared reuse always gives better fitness than split reuse, the performance gap between them is not large, especially when p_{mf} is high and there is a large number of RBs. Recall that there are 500 RBs in the simulation in Chapter 3, which corresponds to a 10MHz LTE system. In this chapter, we would like to compare split reuse and shared reuse using a small number of RBs and users. We expect, in such cases, shared reuse would give larger edges over split reuse because the RB pool is smaller for split reuse and this reduces its efficiency. Figure 4.14 shows their comparison in a network with 75 femtocell users, 15 macrocell users, and 150 RBs. Two sets of results are shown in this figure. Note that for split reuse, we estimate the optimal split point, so there might be better values than what are shown in the figure. Although the performance drop (from shared reuse to split reuse) is about 10% to 15%, which is larger than the drop in Chapter 3 (about 5% to 8%), it is still in an acceptable range. On the other hand, if there are a larger number of macrocell users, comparable to the number of femtocell users, shared reuse will have notable advantages.

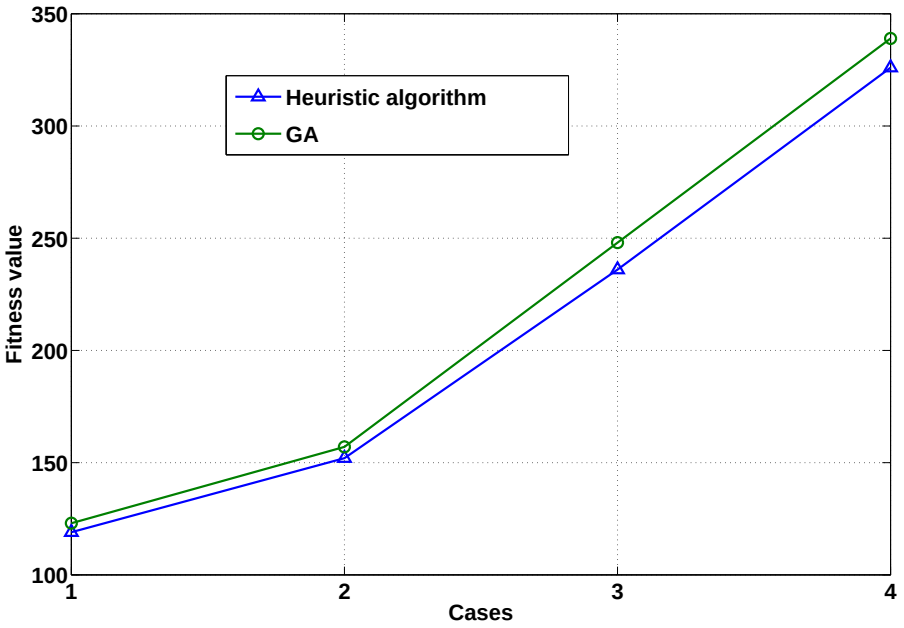

Figure 4.13: Performance comparison between the GA and the heuristic algorithm in different network scenarios for split reuse.

Figure 4.15 shows the comparison for the same network but using 30 macrocell users. From this figure, we can see the gap between shared reuse and split reuse becomes larger than in Figure 4.14.

4.5 Summary

In this chapter, we have introduced a centralized resource allocation algorithm based on genetic algorithms. The results obtained from the GA are compared against the results from the heuristic algorithm developed in Chapter 3. As expected, the GA gives better performance in various network scenarios. Finally, the GA is used compare shared reuse and split reuse, and the simulation results confirm our observations obtained from the heuristic algorithm, that though shared reuse always yields better performance than split reuse, the difference is not large.

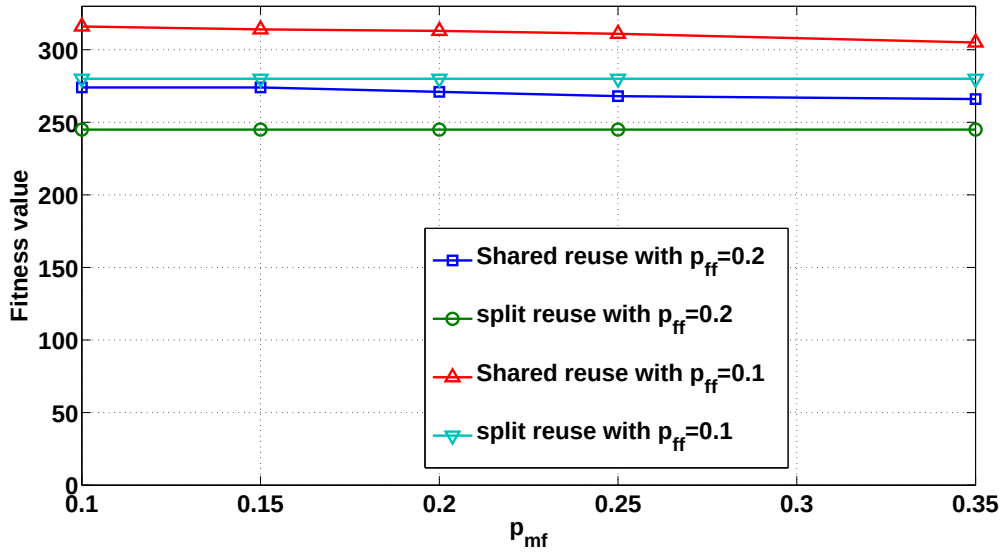

Figure 4.14: Performance comparison between shared reuse and split reuse in a network with 75 femtocell users, 15 macrocell users, and 150 RBs.

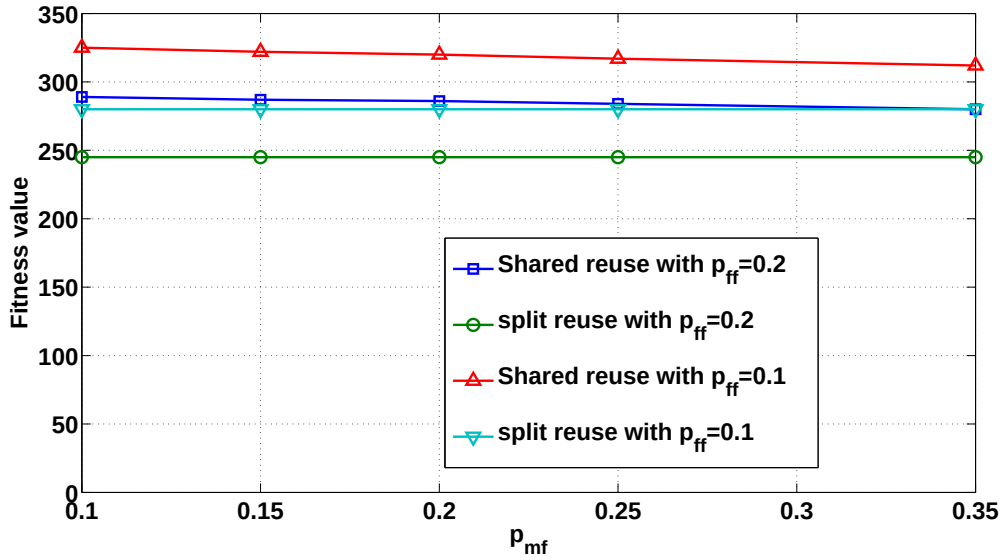

Figure 4.15: Performance comparison between shared reuse and split reuse in a network with 75 femtocell users, 30 macrocell users, and 150 RBs.

Chapter 5

Distributed Algorithms for Resource Allocation

This chapter introduces two practical distributed resource allocation algorithms for cellular networks with coexisting macrocells and femtocells. One algorithm is designed for no communications between the femtocell BSs and the other is designed for the case in which femtocell BSs can exchange information. The developed algorithms are truly distributed, without any central management, and able to adapt to network changes quickly. The results obtained from these two distributed algorithms are compared to the results obtained from the GA and the comparison shows the distributed algorithms have good performance in various network scenarios.

5.1 Introduction

Resource allocation and interference management are often jointly considered as they are clearly related to each other and may be simultaneously addressed. In a centralized resource allocation method, an intelligent allocator gathers information from all network nodes and

finds an optimal or sub-optimal allocation. In a distributed method, the intelligence is distributed among BSs. Femtocell BSs and macrocell BS first acquire needed information, via spectrum sensing or backhaul communications among BSs, and then each BS independently makes decisions on how to use resources, either cooperatively or non-cooperatively. A centralized algorithm potentially gives better performance but may be slow to adapt network changes; a distributed algorithm is able to track network changes promptly but may offer poorer performance than a centralized one. Resource allocation schemes could also depend on resource reuse patterns. In split reuse, resources are separated such that some of them are solely used by femtocell users and others are only for the macrocell users. In shared reuse, both macrocells and femtocells are able to access some resources. Thus, in split reuse, fBSs need only contend for resources with each other; in shared reuse, the coordination is more difficult but the resulting allocation is potentially more efficient.

Femtocells are a natural application area for the idea of self-organizing wireless networks [99]. Femtocell BSs are customer-owned and usually deployed in an ad-hoc fashion. Such deployment makes it is nearly impossible to manage a femtocell network by having a central administrator set most network parameters, as is done in traditional cellular systems. For example, in a macrocell-only cellular network, the interference scenarios are predicable and only cell-edge users are vulnerable to interference caused by a small number of known, neighboring macrocells. Thus, a simple resource partitioning solution can avoid much interference. However, in the femtocell case, there are two aspects of the interference problem. From a femtocell-to-femtocell point of view, a user could experience interference from a large number of neighboring femtocells; at the femtocell-to-macrocell side, femtocells may actually create coverage gaps in the macrocell area if femtocells use the same spectrum as the macrocell. The significant unknown factors and difficulty in predicting femtocell interference renders central resource allocator is impractical.

In previous chapters, we have studied centralized resource allocation for both split reuse and shared reuse. Although central allocation can potentially achieve optimal allocations, it requires global information from the network and significant computational complexity.

These restrictions limit the usage of centralized approaches to small scale and static networks, unlike femtocell networks. This chapter studies distributed algorithms for downlink resource allocation, for both split reuse and shared reuse. We propose two distributed algorithms: the uncoordinated algorithm is designed for a case with no communications between BSs, while the coordinated algorithm is designed to exploit information sharing between BSs.

5.1.1 Related Work

Resource allocation among femtocells shares some similarities with channel allocation in WiFi networks, requiring distributed operations. There are several IEEE 802.11 variants that use control messages to achieve distributed channel management [100–103]. Some work on distributed channel allocation for WLANs does not rely on communications among access points, but is focused on identifying a single orthogonal channel assignment, after which the allocation is static [104]. Though the number of available channels in a WLAN is much smaller than the number of resource blocks in femtocell networks, reducing the complexity of the corresponding resource allocation problem, this work gives useful hints on how to approach our resource allocation problem.

The problem of resource allocation for cellular networks with coexisting femtocells and macrocells has received some attention. Radio resource management considerations within the context of femtocells are outlined in [105]. The authors proposed several ideas on how to negotiate resources so as to mitigate/avoid interference. López-Pérez *et al.* [62] provide an analysis on how the spectrum allocation and interference mitigation problems can be approached. They divide femtocell self-optimization into sensing and tuning phases and provide simulation results on several simple resource assignment schemes. Zhang et al. [30], using a centralized algorithm, study how to allocate spectrum to femtocells and overlaying macrocells subject to QoS requirements. [106] presents a centralized greedy frequency planning algorithm to manage femtocell-to-femtocell interference and the results show that the algorithm is within a factor of two of the optimal solution found by exhaustive search.

A decentralized resource allocation scheme for shared reuse is proposed in [107]. In order to achieve decentralized inter-cell interference avoidance, the algorithm assumes femtocells randomly select a subset of available resources for transmission. Simulation results provide insights into how the resource allocation should take into account the spatial density of femtocells and indoor/outdoor radio propagation conditions. [108] presents two approaches for self-organization of femtocells, in which the femtocell dynamically senses the air interface and tunes its resource assignment to reduce inter-cell interference and enhance system capacity. These approaches rely on message exchange among femtocells or measurement reports from mobiles. Simulation results indicate that it is better to use measurement reports to assign resources.

5.2 Distributed Algorithms

In urban areas, the number of femtocells may be large and there could be hundreds of femtocell users and tens of macrocell users trying to access the network simultaneously. Also, the network interference scenarios may change frequently due to the ad-hoc deployment of femtocells and the nature of the wireless channel. Thus, while designing a distributed algorithm to handle resource allocation for such a large scale and dynamic network, three goals need to be considered:

- Convergence of the algorithm. Convergence to a stable state is more challenging in a distributed algorithm than in a centralized algorithm. Without careful design, a distributed algorithm may end up oscillating between allocations. In this case, a subset of resources might become unusable while several femtocells contended for them. Convergence is more critical if there is no communication between BSs because no one is able to signal others to stop accessing particular resources. This situation is worse when a femtocell has multiple neighbors since the femtocell may not even know which neighbors are causing interference.

- Adaption to the network environment. The interference in femtocell networks is not static. A femtocell may have a changing number of neighboring femtocells in different locations as femtocells become active or idle. Mobility of femtocell and passing macrocell users can also affect the interference. The designed distributed algorithms must adapt to network change and converge to a stable quickly.

- Good performance. When evaluating the performance of an algorithm for resource allocation, various social welfare functions can be used. One common resource allocation objective is proportional fairness, which can obtain good resource reuse efficiency while maintaining fairness.

In the current LTE standard, the X2 interface is defined to support IP connections between BSs. However, initially deployed femtocells may not fully support the X2 interface. This chapter discusses two distributed algorithms: the uncoordinated algorithm is designed without communications between BSs, while the coordinated algorithm takes advantages of communication between BSs, presumably via the X2.

Notation used in the two algorithms is summarized in Table 5.1.

5.2.1 The Uncoordinated Algorithm

In the uncoordinated algorithm, we assume:

- Each femtocell knows the number of femtocells within the macrocell, F, and the empirical probability of interference between any pair of femtocells within the macrocell area, p_{ff}. These statistics are relatively stable with time and can be easily estimated by and obtained from the mobile operator.

- Each femtocell is aware of the identities of neighboring femtocells and which RBs are in use. (These can be tracked by sensing the medium or by obtaining reports from the

Symbol	Definition
$\mathcal{N}$	Set of all RBs, $\{r_1, r_2, ..., r_N\}$
N	Number of RBs.
$\mathcal{F}$	Set of all femtocells, $\{f_1, f_2, ..., f_F\}$.
F	Number of femtocells.
p_{ff}	Probability that two arbitrary femtocells interfere with each other.
N_f	Estimated number of RBs required for F femtocells with interference probability p_{ff} to each receive one RB.
$N_{\max}$	Maximum number of RBs that one femtocell is permitted to use.
T_f	Threshold of femtocell f.
$\mathcal{B}_f$	Set of neighbors of femtocell f.
$\mathcal{R}_f$	Set of RBs that femtocell f uses.
$\mathcal{E}_f$	Set of empty RBs that femtocell f observes.
$\mathcal{C}_f$	Set of conflicted RBs that femtocell f observes.
δ_f	Hungriness factor of femtocell f, i.e. $\delta_i = \max(0, T_f - R_f)$.
$\mathcal{R}$	Set of arbitrary RBs.
$\mathcal{G}_i$	Set of RBs such that in this set, each RB is used by i femtocells, e.g. $\mathcal{G}_1$ represents a set of RBs that each of which is used by one femtocell.
$\mathcal{F}_r$	Set of femtocells that use RB r.
p_r	RB's priority.
$\mathcal{S}_f$	Set of RBs robbed from other femtocells by femtocell f

Table 5.1: Notation

femtocell's mobile). However, femtocells do not know the RB usage pattern of their individual neighbors.

- Femtocells do not know about nearby macrocell users due to the lack of communications between fBSs and the macrocell BS. Simulation results from Chap 2 indicate that the majority of interference ($> 97\%$) between femtocell users and macrocell users is caused by fBSs. Thus we ignore the interference on femtocell users caused by macrocell BS.
- The number of RBs, N is at least as large as the number of femtocells, F. That is $N \geq F$.

Due to asymmetric sensing between fBSs and the macrocell BS, a fBS hardly knows that it is causing interference to nearby macrocell users and hence it is challenging to design an uncoordinated algorithm for shared reuse. We begin by developing an algorithm for a femtocell only network (as in split reuse). However, the macrocell BS can try to avoid interference from femtocells; we will examine if the algorithm is able to accommodate macrocell users in shared reuse in this fashion. The development of the uncoordinated algorithm relies on the results from Chapter 2, which provided theoretical upper and lower bounds on the number of RBs required to assign at least one RB to each user. With F femtocell users and interference probability p_{ff}, the upper and lower bounds on the minimum number of required RBs in a random network is:

$$\frac{F}{\hat{r}_0} \leq N_f \leq \frac{F}{\hat{r}_0}\left(1 + \frac{3\ln\ln F}{\ln F}\right) \tag{5.1}$$

where

$$\begin{aligned}\hat{r}_0 =& \max\left(2, 2\log_b F - 2\log_b\log_b F + 2\log_b\left(\frac{e}{2}\right) + 1\right)\\ b =& 1/(1-p_{ff}).\end{aligned}$$

In this chapter,

$$N_f = \frac{F}{\hat{r}_0}\left(1 + \frac{3\ln\ln F}{\ln F}\right),$$

its upper bound, to estimate the number of RBs required for single coloring. This likely overestimates the number of RBs required to color the network and hence results in a more conservative initial allocation from our algorithms.

With N RBs, each user on average could receive $\bar{n} = N/N_f$ RBs and this would achieve egalitarian (max-min) fairness among users. For proportional fairness, it is natural to assign more RBs to less-interfered users. For the described femtocell network, a femtocell f on average has $(F-1)p_{ff}$ femtocell neighbors. However, the network is dynamic and a femtocell may have different numbers of neighbors at different times. Taking into account the number of current neighbors of a femtocell, we project that the femtocell should receive at least

$$n_f = \left\lfloor \frac{\bar{n}(F-1)p_{ff}}{\max(|\mathcal{B}_f|, 1)} \right\rfloor \tag{5.2}$$

RBs. Recall that $\mathcal{B}_f$ is the set of neighbors of femtocell f. Then n_f is a reasonable target for the number of RBs that femtocell f might expect to obtain. A femtocell will then adapt its RB usage according to its current interference scenario.

Each femtocell dynamically maintains a threshold on the number of RBs that it tries to use; the threshold for femtocell f is T_f, expressed as

$$T_f = \lfloor \min(N_{\max}, n_f) \rfloor,$$

where n_f is from Equation 5.2 and $N_{\max}$ is a cap on the number of RBs that a femtocell may use, preventing a femtocell from taking too many RBs when it has few neighbors. There are two considerations. First, having a small number of neighbors may be temporary and, when new neighbors join, we want to leave them available RBs. Second, even with a $N_{\max} = N/3$ (a typical value that we use), a femtocell can still obtain one-third of all RBs, which is sufficiently large.

In the uncoordinated algorithm, each femtocell is willing to vacate RBs for other femtocells. In the algorithm, a femtocell constantly monitors its current number of neighbors

and voluntarily releases RBs if it detects the presence of a new neighbor. The number of RBs released is equal to the number of RBs that femtocell f has in excess of the new value of its threshold, T_f. In the unlikely event that all of a new femtocell's neighbors are at their thresholds and cannot release any RBs, the new femtocell will be in outage. Thus it is necessary to define a minimum number of RBs that a femtocell uses, $\lfloor N/F \rfloor$. This reflects, the number of RBs that a femtocell could use if all femtocells were fully connected in the conflict graph. Combining this minimum number, we have

$$T_f = \lfloor \max(\min(N_{\max}, n_f), N/F) \rfloor.$$

When femtocell f powers on, it senses the medium to update the current T_f (by knowing the number of its neighbors). At the same time, a neighboring femtocell, j (as well as other neighboring femtocells), becomes aware of a new neighbor and will update its current T_j. If j uses more than T_j RBs, it will release any RBs in excess of T_j. f senses the number of available RBs to see if it can obtain T_f. If so, then all femtocells are satisfied. If not, then f will select and begin using T_f RBs, including all empty ones. In this case, conflicts will be observed at some neighboring femtocells, for example at j. Now j will release the conflicted RBs, provided that after releasing the conflicted RBs it will still have at least N/F RBs. After giving neighbors time to respond, if f still sees conflicts, it releases conflicted RBs. If f still has less than N/F RBs, it will attempt to steal other RBs (other than just released ones) to reach N/F RBs. Again, neighboring femtocells that observe conflicts and follow the above procedure to keep at least N/F RBs. This rob-and-release procedure continues until everyone has at least N/F RBs. Figure 5.1 diagrams the self interference avoidance process.

Theorem 5.2.1. *For a network with F femtocells and N RBs, and $N \geq F$, the algorithm of rob-and-release will guarantee each femtocell to receive at least $\lfloor N/F \rfloor$ RBs.*

Proof. In such a femtocell network, if a femtocell, f, observes $|\mathcal{E}_f| < \lfloor N/F \rfloor$ empty RBs, its $F-1$ neighbors are using $N - |\mathcal{E}_f|$ RBs. We only proof the worst case such that $|\mathcal{E}_f| = 0$.

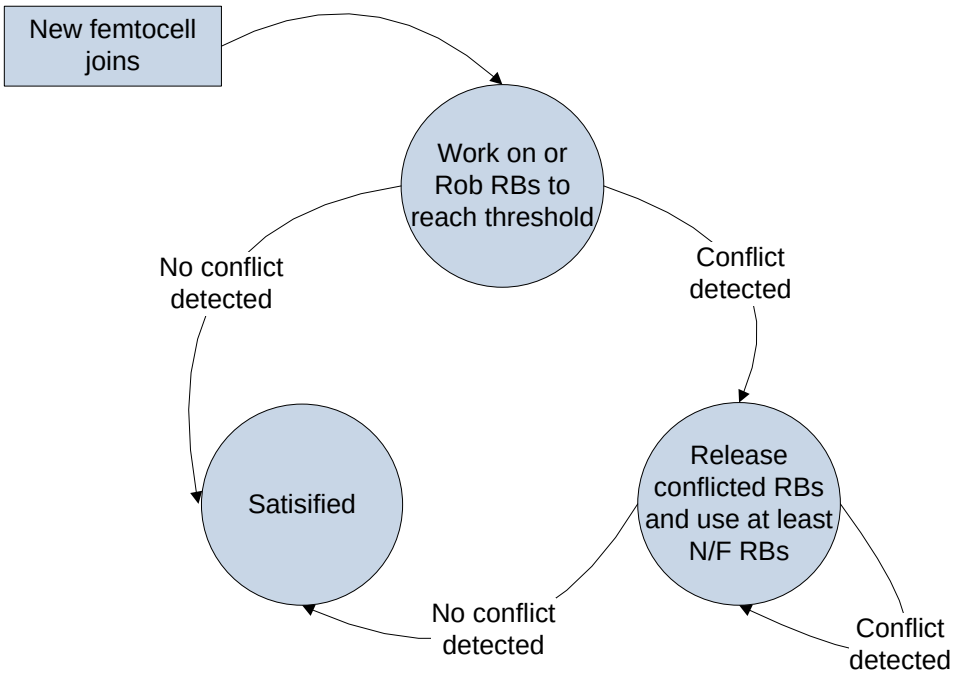

(a) Newly joined femtocell

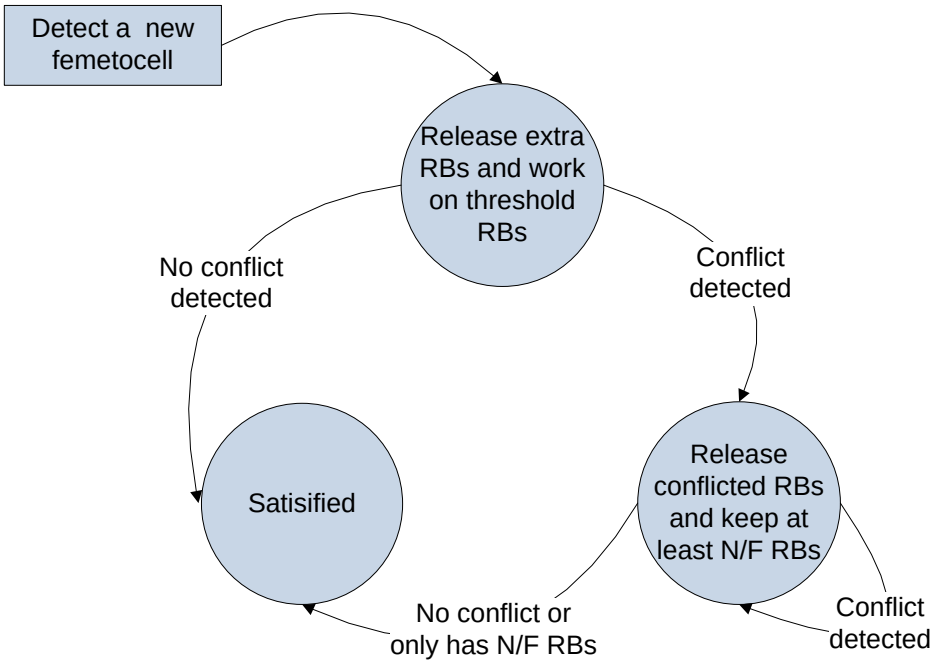

(b) Neighboring femtocells

Figure 5.1: Diagram of self interference avoidance.

There must be at least one neighbor that uses more than $\lfloor N/F \rfloor$ RBs and the following equation holds:

$$\sum_{j \in \mathcal{B}_f} \max(0, |\mathcal{R}_j| - \lfloor N/F \rfloor) \geq \lfloor N/F \rfloor.$$

In rob-and-release, if f tries to take RBs from a neighbor using less than $\lfloor N/F \rfloor$ RBs, the robbery fails since the neighboring femtocells refuses to release this RB. For those femtocells with more than $\lfloor N/F \rfloor$ RBs, in the worst case, f takes one RB each time from one of its neighbors and other $\lfloor N/F \rfloor - 1$ RB robbery fails. Since there are at least $\lfloor N/F \rfloor$ RBs can be released, this femtocell finally will reach $\lfloor N/F \rfloor$ RBs. □

Theorem 5.2.1 shows the uncoordinated algorithm converges.

To use the RBs that remain unused after the rob-and-release process, we define another mechanism, called RB claim to serve two purposes. One, to provide femtocells with less than T RBs an opportunity to obtain T RBs. Two, to allow a femtocell that already has T RBs to claim RBs that are observed to empty in order to maximize RB reuse efficiency. The hungriness factor of f, defined in Table 5.1 as $\delta_f = \max(0, T_f - |\mathcal{R}_f|)$. In the RB claim process, a femtocell, f, that observes empty RBs will randomly pause for a period of time and, if the empty RBs still empty, the femtocell will use $\max(1, \min(\delta_f, |\mathcal{E}_f|))$ of the unoccupied RBs. The random pause time helps reduce the probability that multiple femtocells select the same RBs at the same time, causing a conflict.

Thus far, the uncoordinated algorithm has been presented. The algorithm ensures that each femtocell obtains at least N/F unconflicted RBs. Further, with RB claim, femtocells can use empty RBs to maximize resource reuse efficiency. Pseudocode shown in Algorithm 1, Algorithm 2, and Algorithm 3 reflect algorithms used when a femtocell first joins a network, when a new neighboring femtocell is detected, when a femtocell is otherwise idle. Also though N/F is a pessimistic lower bound, our results show that the uncoordinated algorithm mostly will assign T or almost T RBs to every femtocells.

Algorithm 1 Algorithm used when a femtocell f, first joins a network

f updates neighbor list, $\mathcal{B}_f$ and threshold, T_f
wait for neighbors to respond
if $|\mathcal{E}_f| \geq T_f$ **then**
  randomly select T_f RBs from $\mathcal{E}_f$: $|\mathcal{R}_f| \leftarrow T_f$
  algorithm stops;
else
  use all RBs in $\mathcal{E}_f$ and robs RBs such that: $|\mathcal{R}_f| \leftarrow T_f$
end if
wait for neighbors to release RBs
sense the medium
if $|\mathcal{C}_f| > 0$ **then**
  release $\mathcal{C}_f$: $|\mathcal{R}_f| \leftarrow |\mathcal{R}_f| - |\mathcal{C}_f|$
end if
while $|\mathcal{R}_f| < \lfloor N/F \rfloor$ **do**
  randomly selecl RBs, other than previously released ones, such that $|\mathcal{R}_f| \leftarrow \lfloor N/F \rfloor$
  wait for neighbors to respond
  if $|\mathcal{C}_f| > 0$ **then**
    release $\mathcal{C}_f$: $|\mathcal{R}_f| \leftarrow |\mathcal{R}_f| - |\mathcal{C}_f|$
  end if
end while

Algorithm 2 Algorithm used at femtocell, j, when a new neighboring femtocell is detected

j updates neighbor list, $\mathcal{B}_j$ and threshold, T_j
if $|\mathcal{R}_j| > T_j$ **then**
  randomly release extra RBs and only keeps T_j RBs: $|\mathcal{R}_j| \leftarrow T_j$
end if
sense the medium
while $|\mathcal{C}_j| > 0$ **do**
  if $|\mathcal{R}_j| - |\mathcal{C}_j| \geq \lfloor N/F \rfloor$ **then**
    release $\mathcal{C}_j$: $|\mathcal{R}_j| \leftarrow |\mathcal{R}_j| - |\mathcal{C}_j|$
  else
    randomly release $|\mathcal{R}_j| - \lfloor N/F \rfloor$ RBs from $\mathcal{C}_j$: $|\mathcal{R}_j| \leftarrow \lfloor N/F \rfloor$
  end if
  sense the medium
end while

Algorithm 3 Algorithm of RB claim used in femtocells, k

if k observes empty RBs: $|\mathcal{E}_k| > 0$ **then**
  randomly pause for a period time
  if $|\mathcal{E}_k| > 0$ **then**
    $\delta_k = \max(0, T_k - |\mathcal{R}_k|)$
    randomly use $\max(1, \min(\delta_k, |\mathcal{E}_k|))$ RBs from $\mathcal{E}_k$
  end if
end if

5.2.2 The Coordinated Algorithm

In the coordinated algorithm, femtocells can communicate with one another via the backhaul and share valuable information to aid resource allocation. The coordinated algorithm is expected to give better resource reuse efficiency than the uncoordinated algorithm. Furthermore, this algorithm decreases the likelihood of sensing errors, which can cause interference in the uncoordinated algorithm. Another notable benefit of the coordinated algorithm is that since the macrocell BS can talk to the fBSs, the resource allocation for femtocells can consider nearby macrocell users. Thus, this algorithm can guarantee no outage for macrocell users and can handle both split and shared reuse.

Figure 5.2 diagrams the coordinated algorithm. Femtocell f senses the medium to build a neighbor list and updates T_f. If the number of available RBs is larger than T_f, f uses all these RBs and is satisfied. If not, f will send an RB Request message to its neighbors. The neighbors reply with an RB Reply message to indicate to f their RB usage patterns, current threshold, and their number of neighbors. f will re-shuffle RB usages in its neighborhood (including itself) and send an RB Update message to its neighbors to inform them of the new RB usage patterns. The reshuffling process is a core part of the coordinated algorithm and its pseudocode is shown in Algorithm 4.

f only takes RBs away from neighboring femtocells, rather than assigning RBs to them (otherwise, it may cause interference on the assigned RBs). The first goal of f is to receive T_f RBs while maintaining all neighboring femtocells on their T RBs. f first uses all empty

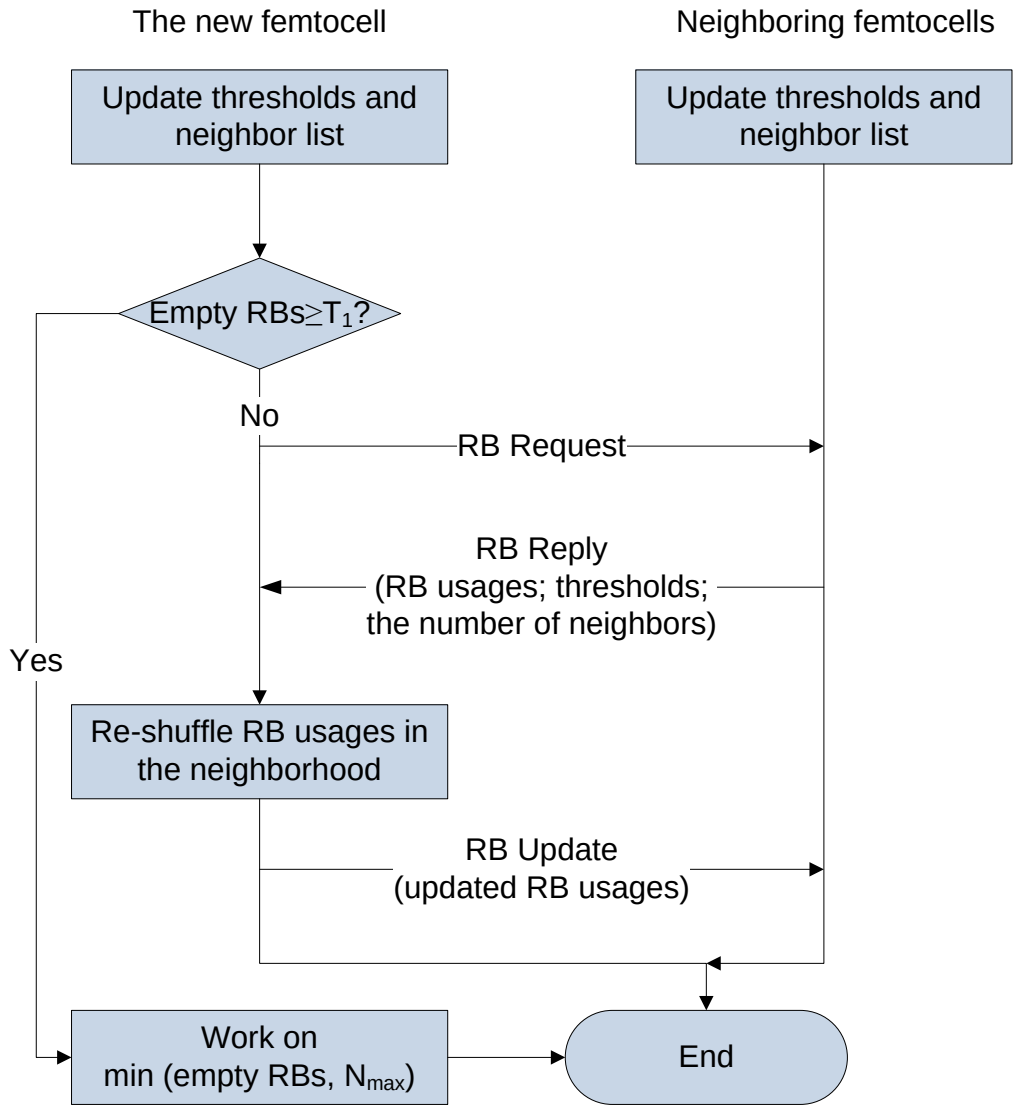

Figure 5.2: Diagram of the coordinated algorithm.

Algorithm 4 Algorithm of RB reshuffling at femtocell f

1: f updates neighbor list, $\mathcal{B}_f$ and threshold, T_f
2: **if** $|\mathcal{E}_f| \geq T_f$ **then**
3: randomly select T_f RBs from $\mathcal{E}_f$: $|\mathcal{R}_f| \leftarrow T_f$
4: **algorithm stops**
5: **else**
6: use all RBs in $\mathcal{E}_f$: $|\mathcal{R}_f| \leftarrow |\mathcal{E}_f|$
7: **end if**
8: collect information from every femtocells in $\mathcal{B}_f$
9: define a set of RBs, $\mathcal{R}$, by removing $\mathcal{R}_f$ from the all RB set, $\mathcal{N}$
10: **for** every j in $\mathcal{B}_f$ **do**
11: **if** $|\mathcal{R}_j| \leq T_j$ **then**
12: remove $\mathcal{R}_j$ from $\mathcal{R}$: $|\mathcal{R}| \leftarrow |\mathcal{R}| - |\mathcal{R}_j|$
13: **end if**
14: **end for**
15: sort RBs in $\mathcal{R}$ according to the number of neighbors using the RB, in an ascending order
16: **for** every $\mathcal{G}_i$ in $\mathcal{R}$ **do**
17: **for** every RB, r, in $\mathcal{G}_i$ **do**
18: $p_r = \sum_{k \in \mathcal{F}_r} |\mathcal{R}_k| - T_k$
19: **end for**
20: sort RBs in $\mathcal{G}_i$ according to p_r, in a descending order
21: **end for**
22: $\mathcal{S}_f = \{\phi\}$
23: **while** $\mathcal{R} \neq \{\phi\}$ **AND** $|\mathcal{S}_f| < T_f - |\mathcal{R}_f|$ **do**
24: pick the first r in $\mathcal{R}$
25: add r to $\mathcal{S}_f$
26: remove r from $\mathcal{R}$
27: **for** each k in $\mathcal{F}_r$ **do**
28: remove r from $\mathcal{R}_k$
29: **end for**
30: **for** every j in $\mathcal{B}_f$ **do**
31: **if** $|\mathcal{R}_j| \leq T_j$ **then**
32: remove $\mathcal{R}_j$ from $\mathcal{R}$: $|\mathcal{R}| \leftarrow |\mathcal{R}| - |\mathcal{R}_j|$
33: **end if**
34: **end for**
35: **end while**
36: add $\mathcal{S}_f$ into $\mathcal{R}_f$
37: **if** $R_f < \lfloor N/F \rfloor$ **then**
38: repeat line 9 to line 36 with replacement of T_f with N/F
39: **end if**

RBs, up to T_f. Starting from the set of all RBs (excluding it already uses), f removes any RB in use by a neighboring femtocell j if $|\mathcal{R}_j| \leq T_j$. f then sorts the remaining RBs. First, RBs are sorted by the number of neighbors using them, in an ascending order. Thus the RB set is divided into several subsets such that each subset contains RBs used by the same number of neighbors. Then, each subset is sorted by priority, in descending order: For each RB, its priority is given by $\sum_{k \in \mathcal{F}_r}(|\mathcal{R}_k| - T_k)$. That is, the RB used by a group of femtocells with the largest total excess RBs will receive the highest priority. f will then take RBs for itself, starting with the first RB in the sorted set. After each RB is taken, if any neighbor j would be left with only T_j RBs, then any RB still used by j, will be removed from the RB set. This process will continue until f reaches T_f or the RB set is empty, meaning that all neighboring femtocells now work on T RBs. If, after this initial reshuffling, $|\mathcal{R}_f| < \lfloor N/F \rfloor$ (though this rarely occurs in our simulations), f will reshuffle again following the same procedure but aiming to obtain $\lfloor N/F \rfloor$ RBs while maintaining neighbors with at least $\lfloor N/F \rfloor$ RBs. f uses the same procedures described above, except for replacing T with $\lfloor N/F \rfloor$, to achieve the second goal. By Theorem 5.2.1, femtocell f can achieve this goal. The coordinated algorithm uses the same RB claim process as in the uncoordinated algorithm to give femtocells the chance to work on additional RBs. In this process, femtocells do not communicate with one another.

In both algorithms, femtocells adjust their RB usage according to the current number of neighbors, i.e. the current interference scenario. This gives the two algorithms the capability to quickly adapt to network changes. We will examine this adaptation capability later.

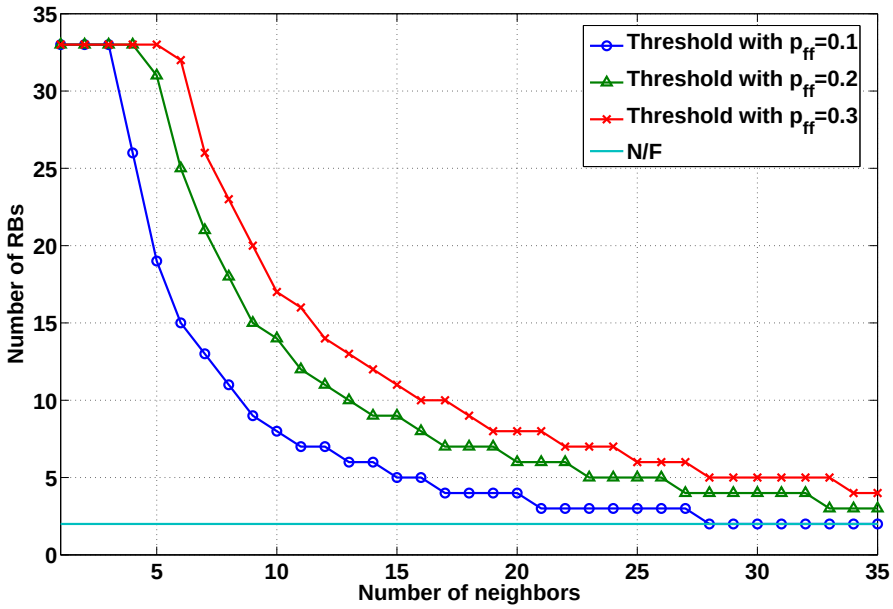

Figure 5.3: Thresholds used in a network with 50 femtocell users, 100 RBs, and various p_{ff}.

5.3 Numerical Results

5.3.1 Thresholds

The curves in Figure 5.3 (50 femtocells and 100 RBs), Figure 5.4 (75 femtocells and 150 RBs), and Figure 5.5 (100 femtocells and 200 RBs) draw threshold T and N/F, which are regarded as indicators of how many RBs that femtocells would work on with different number of neighbors and various p_{ff}. From these figures, we can approximate the number of RBs a femtocell will use.

5.3.2 Performance Comparison

We use proportionally fair fitness (Equation 4.3) to evaluate performance of the uncoordinated and the coordinated algorithms. Figure 5.6, Figure 5.7, Figure 5.8, and Figure 5.9

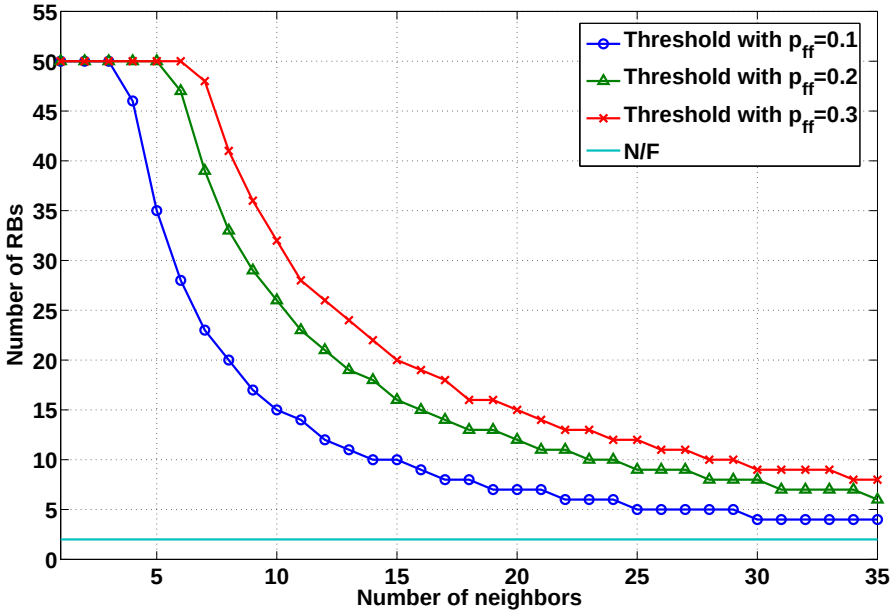

Figure 5.4: Thresholds used in a network with 75 femtocell users, 150 RBs, and various p_{ff}.

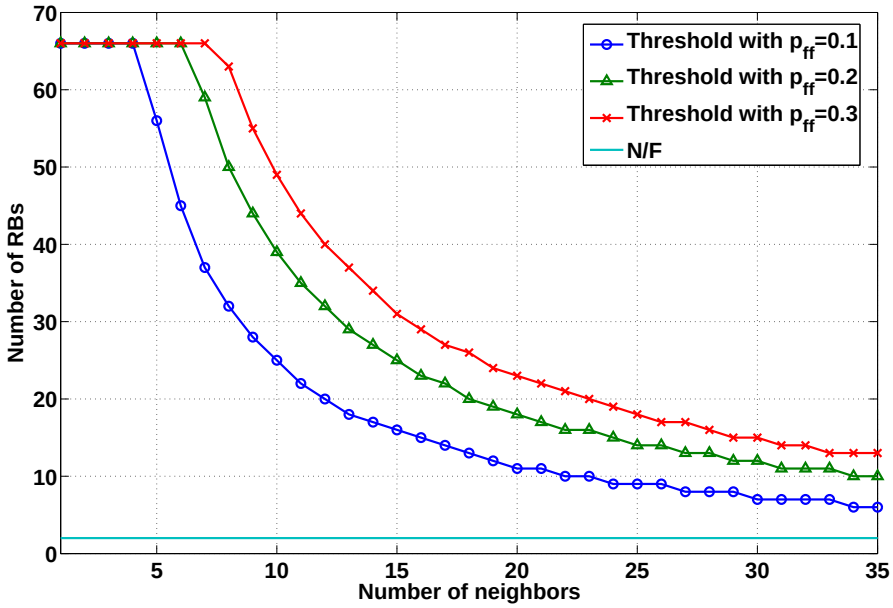

Figure 5.5: Thresholds used in a network with 100 femtocell users, 200 RBs, and various p_{ff}.

compare the two distributed algorithms, the heuristic algorithms developed in Chapter 3, and the GA from Chapter 4. The performance of both distributed algorithms achieves more than 95% of the GA's performance and, in most cases, is better than the heuristic algorithm's performance. Actually, the two distributed algorithms improve their fitness, compared to the GA, as the network scale increases. This is due to their distributed nature, which makes it easier to handle a large network. In the 100 femtocell case, the coordinated algorithm yields fitness close to the GA. Also notable is that although femtocell BSs cannot communicate with each other other under the uncoordinated algorithm, it still generates promising performance, which is not far from the coordinated algorithm's performance. This indicates that the uncoordinated algorithm could be adopted even in femtocell deployments that are not ready to support the X2 interface (which is used to establish an IP connection between any two BSs), without a a significant loss of efficiency. However, we still believe the coordinated algorithm has unique benefits. It works with shared reuse which is not supported by the uncoordinated algorithm, and it avoids the self interference process which may increase the convergence time. Further, perfect sensing is assumed in the uncoordinated algorithm and sensing error may lead to a performance loss.

5.3.3 Distribution of Resource Blocks

We have shown good performance of both distributed algorithms on proportionally fair fitness. We would like to further investigate these two algorithms by observing how RBs are distributed among femtocell users. To do this, we use the thresholds shown in Figures 5.3 to 5.5 as backgrounds and then plot the number of RBs that femtocells actually attain at convergence. Our distributed algorithms follow the principle that the algorithms first guess the number of RBs used in a femtocell, then try to allocate the estimated number of RBs to everyone, and finally allows femtocells to acquire more RBs if available. Thus the feasibility of threshold T plays an important role in the performance of the algorithm. Figures 5.10 to 5.15 show RB distributions obtained by the distributed algorithms for three

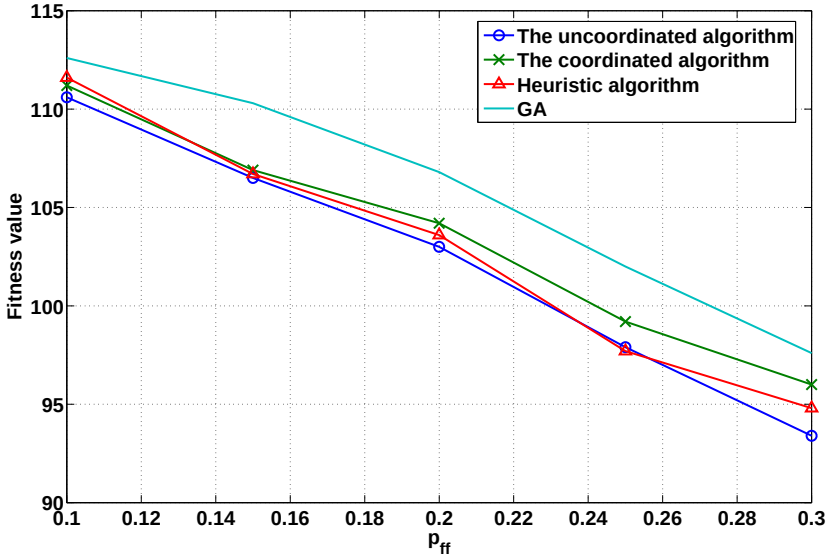

Figure 5.6: Fitness comparison among the distributed algorithms, the heuristic algorithm, and the GA in a network with 30 femtocell users, 100 RBs, and various p_{ff}.

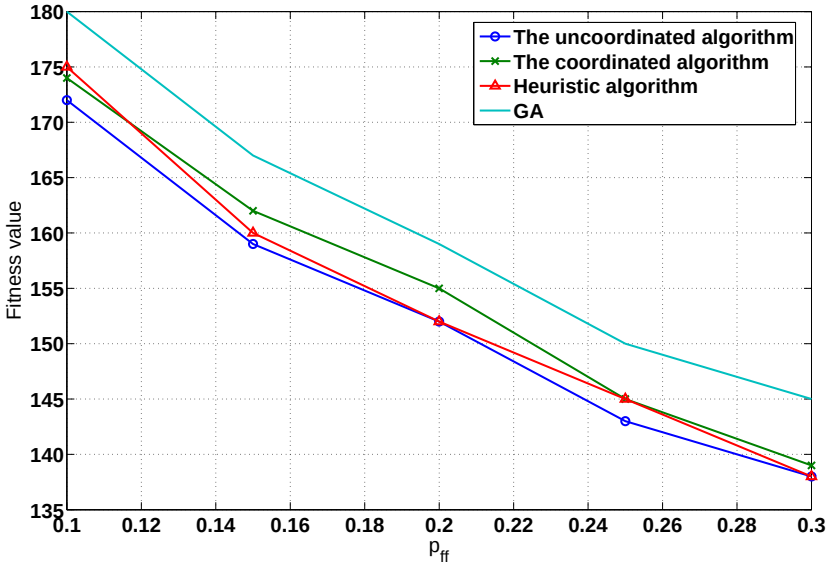

Figure 5.7: Fitness comparison among the distributed algorithms, the heuristic algorithm, and the GA in a network with 50 femtocell users, 100 RBs, and various p_{ff}.

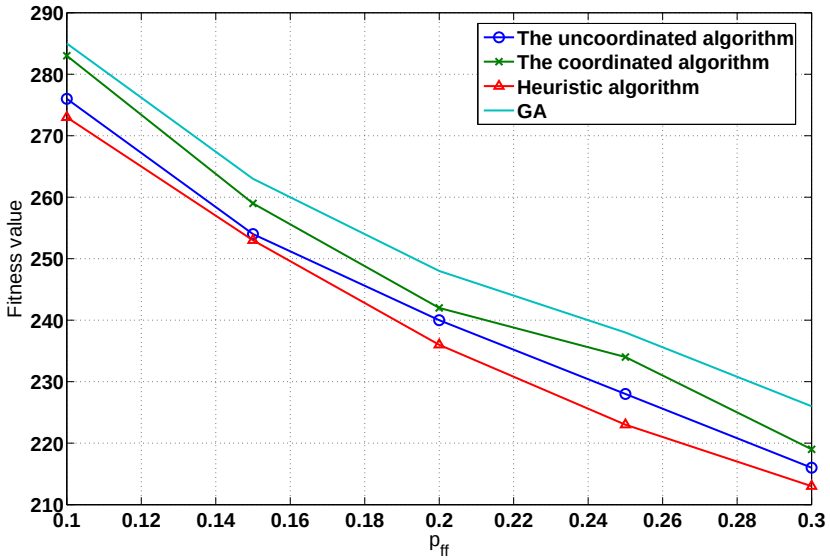

Figure 5.8: Fitness comparison among the distributed algorithms, the heuristic algorithm, and the GA in a network with 75 femtocell users, 150 RBs, and various p_{ff}.

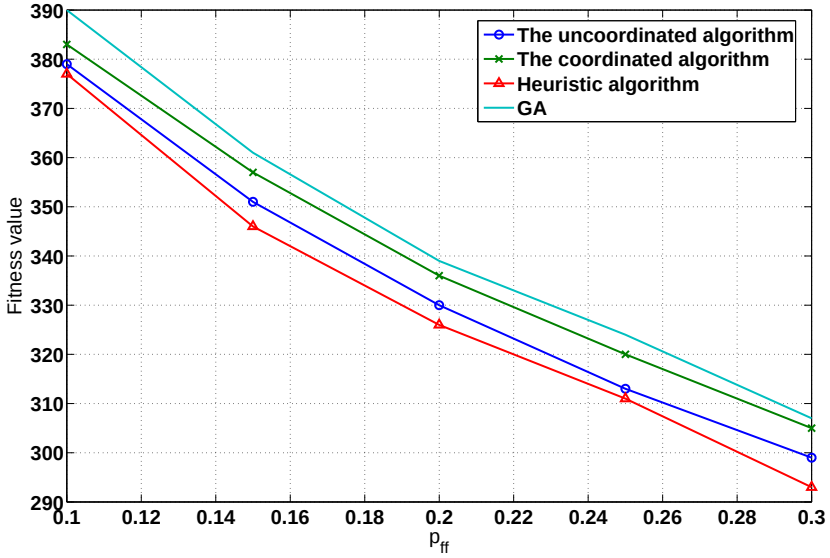

Figure 5.9: Fitness comparison among the distributed algorithms, the heuristic algorithm, and the GA in a network with 100 femtocell users, 200 RBs, and various p_{ff}.

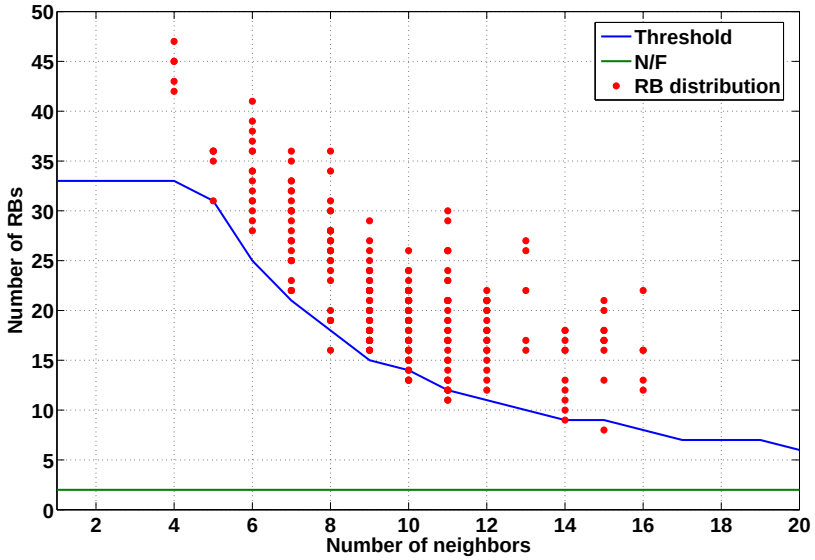

Figure 5.10: RB distribution obtained by the uncoordinated algorithm in a network with 50 femtocell users, 100 RBs, and a p_{ff} of 0.2.

different network settings. All results are based on 5 runs. It is apparent that the majority of femtocells obtain at least T RBs. This is because we are using the upper bound in Equation 5.1 so the average number of RBs for each femtocell is under-estimated, resulting in a conservative T. Thus most femtocells, especially in the uncoordinate algorithm, can easily reach T. Recall that in the uncoordinated algorithm, a femtocell only acquires T RBs at most. The coordinated algorithm does not have the T limit to use RBs. The benefit is that network fitness can be maintained at a level, at the cost of some fairness.

5.3.4 Shared Reuse

So far, all results presented are based on split reuse, but we would also like to investigate the performance of the distributed algorithms under shared reuse. Figure 5.16, Figure 5.17, and Figure 5.18 compare performance between the coordinated algorithm and the GA under three network settings with different number of femtocell users and macrocell users. From

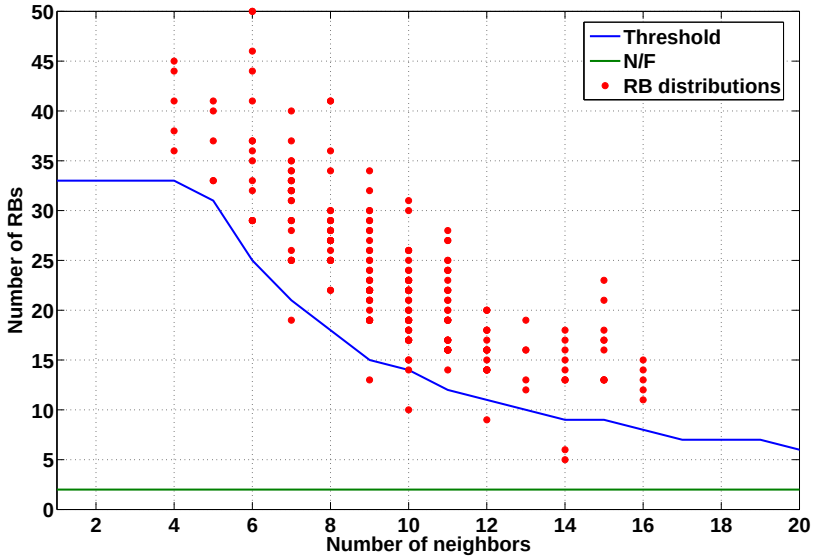

Figure 5.11: RB distribution obtained by the coordinated algorithm in a network with 50 femtocell users, 100 RBs, and a p_{ff} of 0.2.

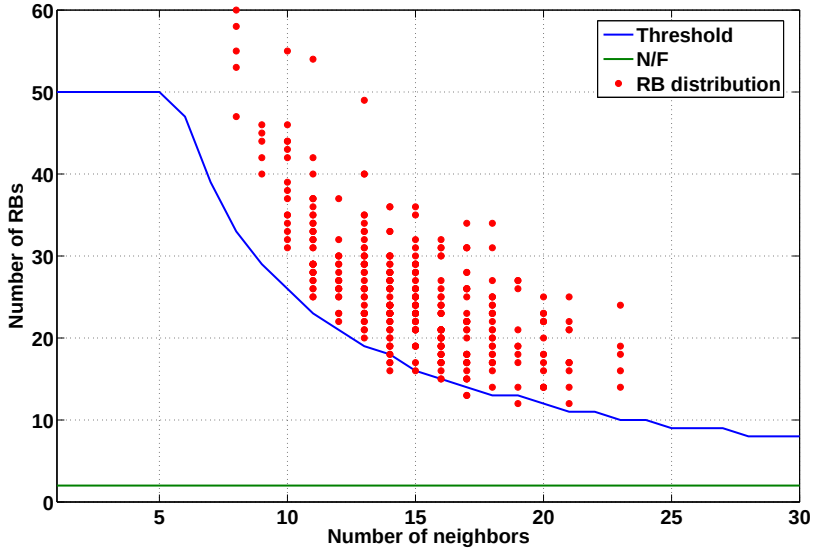

Figure 5.12: RB distribution obtained by the uncoordinated algorithm in a network with 75 femtocell users, 150 RBs, and a p_{ff} of 0.2.

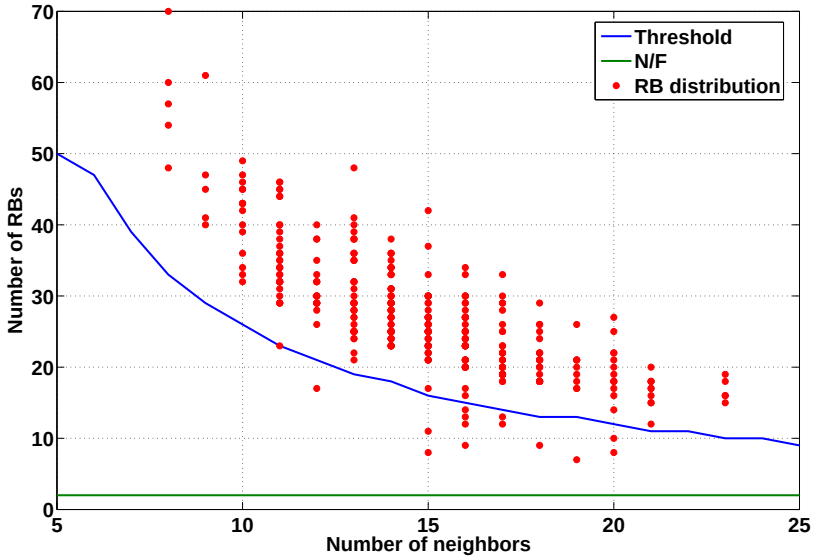

Figure 5.13: RB distribution obtained by the coordinated algorithm in a network with 75 femtocell users, 150 RBs, and a p_{ff} of 0.2.

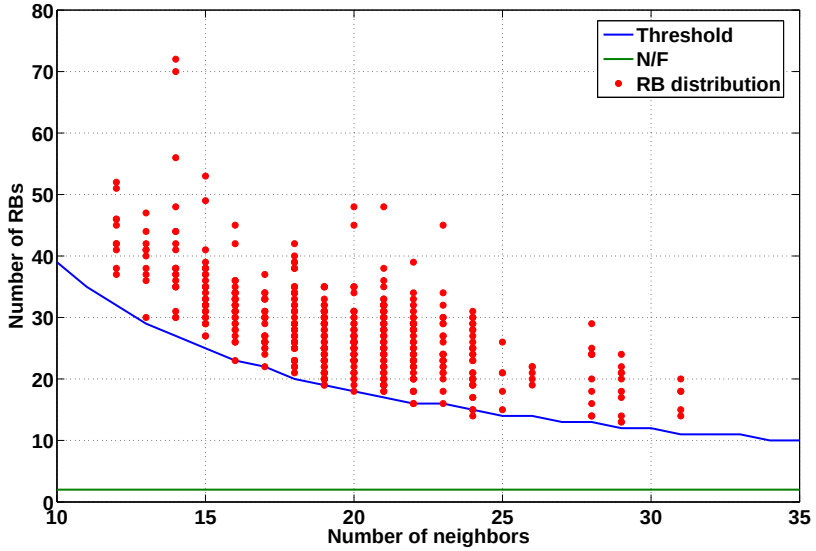

Figure 5.14: RB distribution obtained by the uncoordinated algorithm in a network with 100 femtocell users, 200 RBs, and a p_{ff} of 0.2.

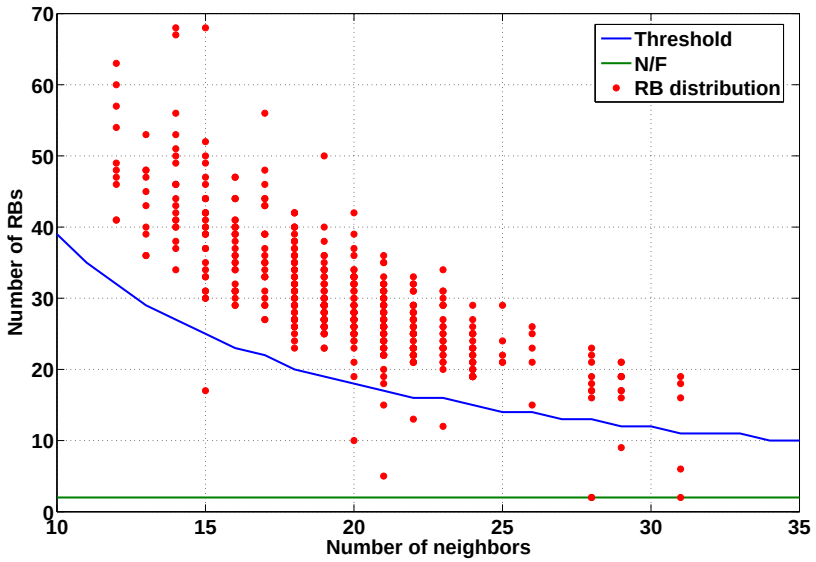

Figure 5.15: RB distribution obtained by the coordinated algorithm in a network with 100 femtocell users, 200 RBs, and a p_{ff} of 0.2.

the figures, the coordinated algorithms have good performance, with only a 10% maximum performance loss.

As mentioned before, the uncoordinated algorithm does not support shared reuse due to the asymmetric sensing between femtocells and macrocells. However, macrocell users may opportunistically access RBs if they observe empty ones. If a macrocell user is not able to work on any RB, this user is said to be in outage. The outage rate is a measure of the probability that a randomly positioned macrocell user will be in outage. Table 5.2 gives outage rates of the uncoordinated algorithm used in shared reuse. Case I represents a network with 50 femtocell users, 20 macrocell users, 100 RBs, and a p_{mf} of 0.2; Case II represents a network with 75 femtocell users, 25 macrocell users, 150 RBs, and a p_{mf} of 0.2; Case III represents a network with 100 femtocell users, 30 macrocell users, 200 RBs, and a p_{mf} of 0.2. Clearly, in most cases, directly applying this algorithm in shared reuse will cause an unacceptable block probability for macrocell users. If the RB claim process is not applied in the algorithm, outage rates are dramatically reduced and in this case, the

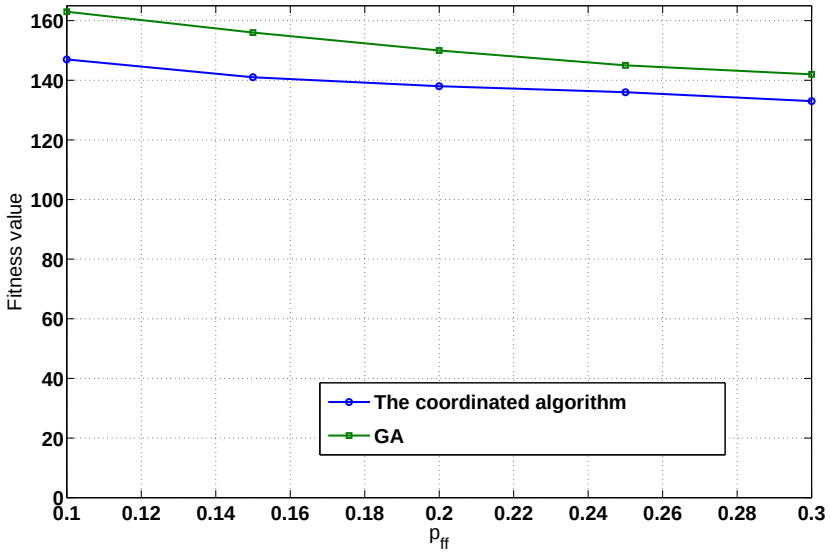

Figure 5.16: Fitness comparison between the coordinated algorithm and the GA for shared reuse in a network with 35 femtocell users, 35 macrocell users, 100 RBs, and a p_{mf} of 0.2.

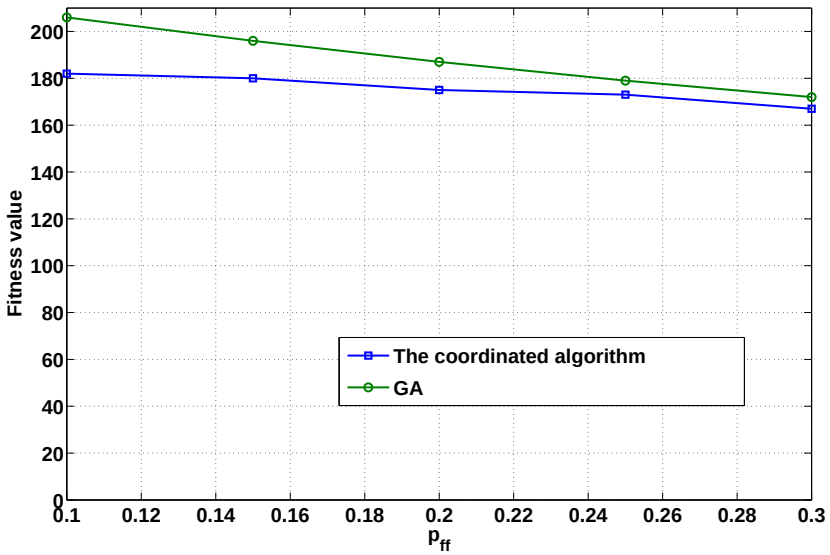

Figure 5.17: Fitness comparison between the coordinated algorithm and the GA for shared reuse in a network with 50 femtocell users, 20 macrocell users, 100 RBs, and a p_{mf} of 0.2.

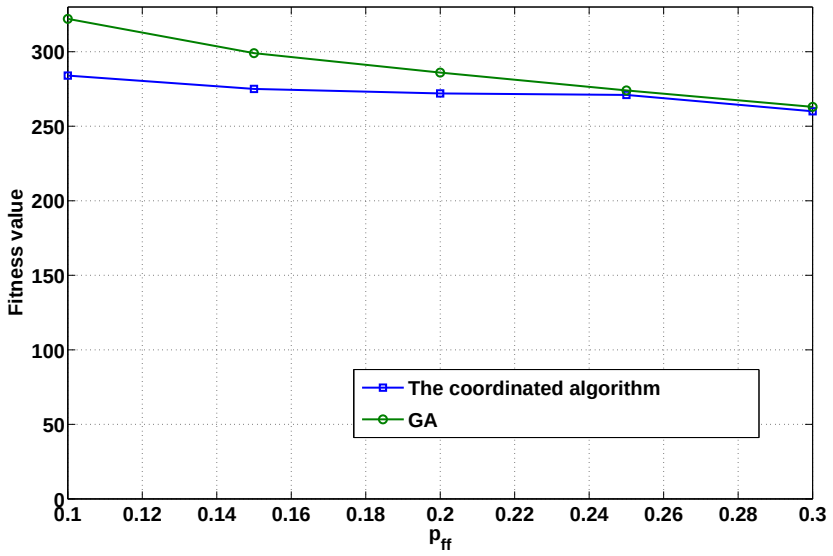

Figure 5.18: Fitness comparison between the coordinated algorithm and the GA for shared reuse in a network with 75 femtocell users, 25 macrocell users, 150 RBs, and a p_{mf} of 0.2.

uncoordinated algorithm can be adopted in shared reuse. However, not using RB claim leads to a large performance loss. The results in this section indicate that if the X2 interface in not available, using split reuse is a better choice because performance lost by not using the RB claim process can be compensated by using a smaller number of RBs for femtocell users with the RB claim process.

p_{ff}		0.1	0.15	0.2	0.25	0.3
Case I	With the RB claim process	52%	23%	16%	8%	4%
	Without the RB claim process	0	0.6%	0.1%	0.3%	0.2%
Case II	With the RB claim process	50%	27%	5%	4%	3%
	Without the RB claim process	0	3.2%	1.5%	0.7%	0.4%
Case III	With the RB claim process	48%	14%	4%	2%	1%
	Without the RB claim process	2%	0	0	0	0

Table 5.2: Outage rates of macrocell users

5.3.5 Adaptation to Network Changes

The coordinated algorithm can catch up to network changes easily. Once a femtocell notices a change in the interference scenario, it will collect the required information from neighboring fBSs and use the described procedures in Section 5.2.2 to re-allocate RBs. For the uncoordinated algorithm, there is no mechanism for a femtocell to collect neighbor information. So a mechanism is needed to enable femtocells to find a new allocation. There are two different cases. If some femtocells leave the network, other femtocells can simply use the RB claim process to use the released RBs. If new conflicts are detected, these femtocells will first release all conflicted RBs, and then the femtocells with less than T RBs will follow the self interference avoidance process to access RBs. To evaluate the ability of the uncoordinated algorithm to adapt, we test the algorithm in an environment in which, the conflict graph is periodically reset. We would like to see how the algorithm perform in such a condition. Figure 5.19 shows the uncoordinated algorithm tracks network changes. The network has 50 femtocell users with varying p_{ff}.

5.4 Map Between Protocol Model and the SINR Model

As previously discussed, the reason we choose a protocol model and conflict graph to analyze the resource allocation problem is that this model makes the problem more analytically tractable. However, as we we present numerical results using the protocol model, a natural question is if these results reflect the real world. In reality, SINR is used to measure the quality of the received signal and determines whether demodulation succeeds or fails. Thus if the protocol-model-based approach does not reflect reality, then our work is less significant. This question motivates us to map our protocol model to the SINR model to see how it accommodates the latter.

In the protocol model, two links either interfere with each other or not. This basically means the two links interfere only if the interference is larger than a threshold; additive

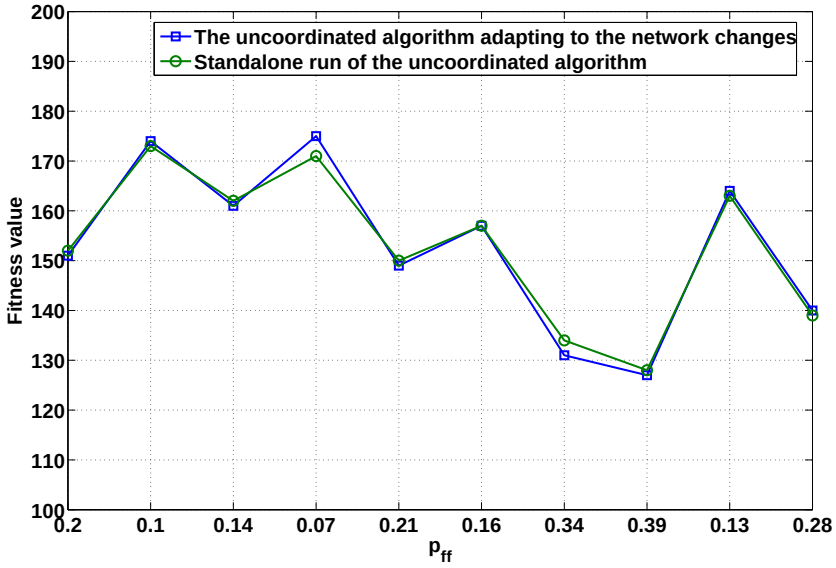

Figure 5.19: Comparison between the adapted uncoordinated algorithm and the standalone uncoordinated algorithm.

interference is not considered. Although one link may not be interfered with any other single link, the sum of interference from several links can still significantly diminish the channel quality. Therefore, if a conflict-free resource allocation generated by the protocol model is applied back to the network and examined under the SINR model, the additivity of interference may make the assignment infeasible or significantly degrade the performance. In this section, we evaluate the performance of a protocol-model-based assignment in the SINR model.

This evaluation follows the following steps:

1. Apply commonly used propagation models to the network and calculate a user's potential SINRs from every other individual link.

2. Define a threshold such that SINR values lower than this threshold will result in declaring a conflict between the two links.

3. Build a conflict graph based on the conflicts identified in the previous step and apply

our distributed algorithms to solve the resource allocation problem.

4. Apply the resulting RB allocation to the network and examine its performance under the SINR model with additive interference.

While evaluating a RB allocation (obtained from the protocol model) under the SINR model, an important metric is the percentage of users who are blocked. Normally 5% blocking rate is the maximum acceptable number. Let define a SINR value S_1 indicating a threshold for successful demodulations of the received signal. Clearly, if S_1 is used to determine a conflict between two links, most likely the additive interference will result in the SINR value of the received signal lower than S_1. Thus, the threshold, denoted as S_2, declaring a conflict must be larger than S_1. We would like to see the SINR margin, denoted $\delta_s = S_2 - S_1$, required to make a RB allocation feasible under the SINR model.

In choosing a network size to do our simulations, we use the same estimates introduced in Chapter 2. With an inter-site (macrocell BS) distance of 1 km, the area of a sector of a hexagon macrocell will be 0.289 km^2. In this section, we will refer this sector as a macrocell. Population density in dense urban areas is $10,000$ to $20,000$ per km^2. We take the upper bound of $20,000$ and assume there are 7692 household units (2.6 persons per household) per km^2. This corresponds to 2223 household units per macrocell. Furthermore, we assume cellular phone penetration of 80%, operator penetration of 40%, and femtocell penetration of 30%. Thus we have approximately 213 femtocells in one macrocell located in dense urban areas.

Suppose 200 femtocell users and 50 macrocell users are uniformly distributed in a macrocell. Femtocell users are dropped as described in Section 2.5.2. Each femtocell is given a 100m^2 area and a fBS and a user are randomly dropped in this area. Macrocell users are dropped outside this area. The propagation models described in Section 2.4.3 are used to model the path loss from a BS to a mobile user, with respect to their geographical locations. The transmit power is 43 dBm for macrocell BS and 20 dBm for femtocell BS. For simplicity, we do not apply power control and thus BSs always use full power. Figure 5.21 shows

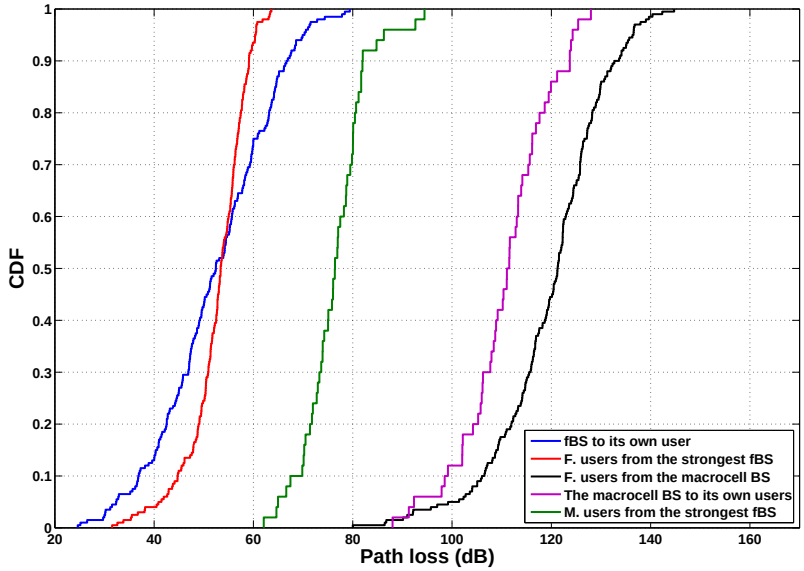

Figure 5.20: CDF of path losses in a network with 200 femtocell users and 50 macrocells.

CDF of path losses for different transmitter-receiver pairs. Clearly, femtocell-to-femtocell and femtocell-to-macrocell interference consist of most interference occurred in the network. In figure **??**, we use 50 femtocell users and 50 macrocell users and the figure indicates a similar interference scenario.

We evaluate two cases. The first one is for a single RB allocation. Once a conflict matrix is generated by using the SINR model and a S_2, the single coloring algorithm is applied to obtain a single RB allocation matrix such that each user receives only one RB. In this allocation, if the RB used by a user has a SINR value lower than S_1, this user is blocked. In the second case, we evaluate a multiple RB allocation. Here, since each user will have multiple RBs, the definition of blocking probability is different. First, we assume a user's received power is distributed over all of its RBs equally. Then by observing the RB allocation matrix (250 users $\times$ 500 RBs), we denote the block probability as the ratio between the number of RBs with SINR less than S_1 and the number of total assigned RBs (all 1s in the matrix). Our preliminary results suggest a $\delta_s = 5$ dB is a good estimate to achieve the acceptable blocking probability. Table 5.3 shows the blocking probabilities of the above two

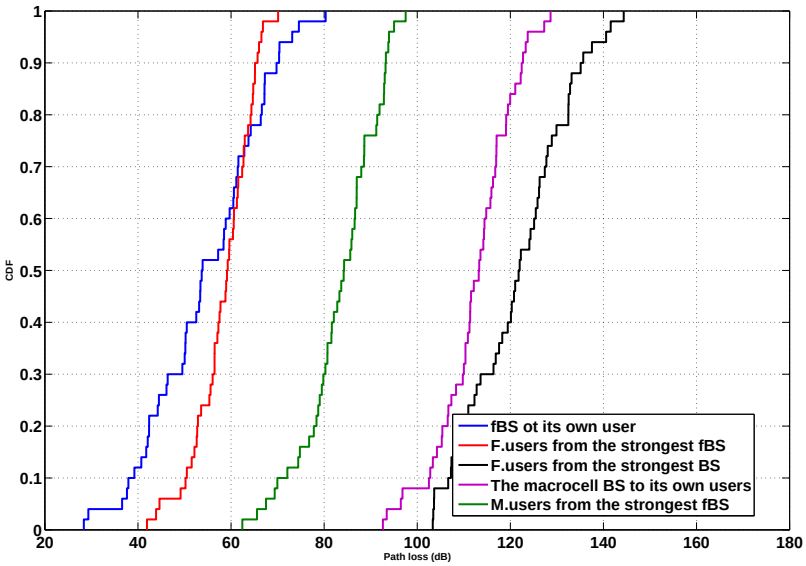

Figure 5.21: CDF of path losses in a network with 50 femtocell users and 50 macrocells.

cases. The blocking probabilities in the multiple RB allocation case are generally larger than the single RB allocation because in the latter, the single coloring algorithm only assigns one RB to each user, resulting in the average received interference is smaller. And this situation is more apparent when S_1 uses a larger number since most potential interfering links are already excluded (due to a large S_1). In the multiple RB allocation case, the coordinated algorithm tends to heavily reuse RBs so the average interference measured at RBs is bigger, leading to high blocking probabilities. If the shown blocking probabilities are not satisfied, we can increase the SINR margin to achieve lower blocking probabilities, at the cost of lower RB reuse efficiency. Table 5.4 shows the blocking probabilities with a $\delta_s = 6$ dB.

We also run simulations on a smaller network with less number of femtocell users. Table 5.5 shows the blocking probabilities with a $\delta_s = 5$ dB in a network with 50 femtocell users and 50 macrocell users. Due to the small number of users, the interference is reduced and thus a 5 dB SINR margin gives satisfactory blocking probability.

S_1 (dB)	5	10	15
Blocking probability of a single RB allocation, with $\delta_s = 5$ dB	6%	4%	0.8%
Blocking probability of a multiple RB allocation, with $\delta_s = 5$ dB	6.2%	8%	7%

Table 5.3: Blocking probability of a single RB allocation and a multiple RB allocation with various S_1 and $\delta_s = 5$ dB in a network with 200 femtocell users and 50 macrocell users.

S_1 (dB)	5	10	15
Blocking probability of a single RB allocation, with $\delta_s = 6$ dB	2%	1.6%	0
Blocking probability of a multiple RB allocation, with $\delta_s = 6$ dB	3.7%	3%	2.8%

Table 5.4: Blocking probability of a single RB allocation and a multiple RB allocation with various S_1 and $\delta_s = 6$ dB in a network with 200 femtocell users and 50 macrocell users.

S_1 (dB)	5	10	15
Blocking probability of a single RB allocation, with $\delta_s = 5$ dB	0	0	0
Blocking probability of a multiple RB allocation, with $\delta_s = 5$ dB	6%	4%	4.3%

Table 5.5: Blocking probability of a single RB allocation and a multiple RB allocation with various S_1 and $\delta_s = 5$ dB in a network with 50 femtocell users and 50 macrocell users.

5.5 Summary

In this chapter, we have proposed two distributed algorithms to allocate resources for cellular networks with coexisting femtocells and macrocells. The uncoordinated algorithm is designed for the case without backhaul connections between BSs. This algorithm uses a self interference avoidance process to allocate resources for femtocells. Another process, called the RB claim process, is used to improve RB reuse efficiency. The coordinated algorithm uses shared information between neighboring BSs to aid resource allocation. We have compared these distributed algorithms to the GA from Chapter 4 and the heuristic algorithm developed in Chapter 3. The results show both the uncoordinated algorithm and the coordinated algorithm give comparable performance to the GA and, in most cases, beat the heuristic algorithm. We then compare the coordinated algorithm to the GA in shared reuse and see that is also gives promising performance. We also evaluate the uncoordinated algorithm in a highly dynamic network in which the interference scenarios are constantly changing. The results show that the algorithm can quickly track network changes and converge to a new resource allocation without losing RB reuse efficiency. Finally, the obtained resource allocations from our protocol-model-based algorithms are applied to simulated networks and examined under the SINR model. This evaluation shows that, with a small adjustment, our algorithms offer reasonable performance under the SINR model.

Chapter 6

Conclusions

This dissertation addresses fundamental aspects of resource allocation and interference management in cellular networks with coexisting femtocells and macrocells. In Chapter 2, we addressed the impact of femtocell deployment in current cellular networks on resource requirements. To investigate this question, two resource reuse schemes are presented. In shared reuse, femtocells share some of the resources used by macrocells; in split reuse, femtocells and macrocells use different resource pools. We determine the minimum number of resource blocks required to support a femtocell/macrocell network with respect to the two resource reuse schemes using a random graph model of interference.

The choice between shared reuse and split reuse is one that faces the mobile operators when they deploy femtocells. Therefore, in Chapter 3, we attempt to compare the two reuse schemes. We evaluate the performance of split reuse and shared reuse using three social welfare functions, denoted utilitarian fitness, egalitarian fitness, and proportionally fair fitness. Numerical results confirm our analysis and indicate that in the case of heavy interference between femtocell and macrocell users, split reuse may be preferable to shared reuse because of easier interference control and lower computational complexity with comparable performance. In the case of lighter interference between femtocell users and macrocell users, our results are less stark. Shared reuse can provide significant fitness benefits, but at potentially

high computational and informational cost.

Another important issue is identifying optimal resource allocations. Utilitarian fitness and egalitarian fitness are rarely used in practice because the former tends to result in unfair allocations while the latter, in most cases, suffers from resource reuse inefficiency. Thus we focus on proportional fairness. Due to the computational complexity of maximizing proportional fairness, we use a genetic algorithm-based centralized algorithm to generate sub-optimal solutions. The results from Chapter 4, indicate the best known resource allocation with respect to proportionally fair fitness and offer a baseline to be compared with the later developed distributed algorithms.

A centralized resource allocation algorithm usually relies on global information and a central entity. However, in practical networks, global information is difficult or sometimes is impossible to acquire. In Chapter 5, we propose two practical distributed algorithms, used in different network conditions. Their performance is comparable to the performance from the GA, especially in large network. In addition, the distributed algorithms show great capability in adapting to network changes.

All of the work reviewed thus far is based on the protocol model. However, in Section 5.4 we evaluated the performance of our allocation algorithms, developed under the protocol model, in the SINR model.

Overall, the research of this dissertation provides guidance to cellular operators in handling the resource allocation in a cellular network with femtocells and macrocells. This dissertation clearly bounds the resources required to accommodate femtocells, and thus the number of femtocells that can be added into a current network under different interference scenarios could be obtained. Tradeoffs between shared reuse and split reuse are also presented. In addition, two adaptive distributed algorithms are developed to allocate resources among network users and their achieved social welfare is promising. Finally, the SINR evaluation study justifies a key assumption of our work.

Bibliography

[1] *Regulatory Aspects of Femtocells*. Femto Forum, 2008. [Online] Available at `http://www.femtoforum.org/femto/Files/File/FFRegulatoryAspectsofFemtocells.pdf`.

[2] Y. Shi, A. B. MacKenzie, L. A. DaSilva, K. Ghaboosi, and M. Latva-aho, "On resource reuse for cellular networks with femto- and macrocell coexistence," in *IEEE Global Communications Conference (GLOBECOM)*, Dec. 2010.

[3] G. Mansfield, "Femtocells in the US market - business drivers and consumer propositions," in *FemtoCells Europe*, June 2008.

[4] *Femtocells Challenges and Opportunities*. GENBAND, Oct. 2008.

[5] J. Mitola, *Cognitive Radio: An Integrated Agent Architecture for Software Defined Radio*. Ph.D. dissertation, Royal Institute of Technology, 2000.

[6] V. Chandrasekkhar, J. G. Andrews, and A. Gatherer, "Femotocell networks: A survey," *IEEE Communications Magazine*, vol. 46, no. 9, pp. 59–67, 2008.

[7] D. Niyato and E. Hossain, "Call admission control for QoS provisioning in 4G wireless networks: issues and approaches," *IEEE Network*, vol. 19, no. 5, pp. 5–19, 2005.

[8] K. Yang, Y. Wu, and H.-H. Chen, "QoS-aware routing in emerging heterogeneous wireless networks," *IEEE Communications Magazine*, vol. 45, no. 2, pp. 74–80, 2007.

[9] K. Yeung and S. Nanda, "Channel management in microcell/macrocell cellular radio systems," *IEEE Transactions on Vehicular Technology*, vol. 45, no. 4, pp. 601–612, 1996.

[10] Z. Shen and S. Kishore, "Optimal multiple access to data access points in tiered CDMA systems," in *IEEE Vehicular Technology Conference*, pp. 719–723, 26-29 Sept. 2004.

[11] T. E. Klein and S.-J. Han, "Assignment strategies for mobile data users in hierarchical overlay networks: performance of optimal and adaptive strategies," *IEEE Journal on Selected Areas in Communication*, vol. 22, no. 5, pp. 849–861, 2004.

[12] Y. Liang, R. Valenzuela, G. Foschini, D. Chizhik, and A. Goldsmith, "Interference suppression in wireless cellular networks through picocells," in *IEEE Asilomar Conference on Signals, Systems and Computers (ACSSC)*, pp. 1041–1045, 2007.

[13] Y. Yang, H. Hu, J. Xu, and G. Mao, "Relay technologies for WiMax and LTE-advanced mobile systems," *IEEE Communications Magazine*, vol. 47, no. 10, pp. 100–105, 2009.

[14] R. Schoenen, R. Halfmann, and B. Walke, "An FDD multihop cellular network for 3GPP-LTE," in *IEEE Vehicular Technology Conference (VTC)*, pp. 1990–1994, May 2008.

[15] R. Schoenen, R. Halfmann, and B. Walke, "MAC performance of a 3GPP-LTE multihop cellular network," in *IEEE International Conference on Communications (ICC)*, pp. 4819–4824, May 2008.

[16] R. Irmer and F. Diehm, "On coverage and capacity of relaying in LTE-advanced in example deployments," in *IEEE International Symposium on Personal, Indoor and Mobile Radio Communications (PIMRC)*, pp. 1–5, Sept. 2008.

[17] S. W. Peters and R. W. Heath, "The future of WiMAX: Multihop relaying with IEEE 802.16j," *IEEE Communications Magazine*, vol. 47, no. 1, pp. 104–111, 2009.

[18] *Measuring the Information Society: The ICT Development Index*. International Telecommunication Union, 2009. [Online] Available at `http://www.itu.int/ITU-D/ict/publications/idi/2009/material/IDI2009\_w5.pdf`.

[19] S.-P. Yeh, S. Talwar, S.-C. Lee, and H. Kim, "WiMAX femtocells: a perspective on network architecture, capacity, and coverage," *IEEE Communications Magazine*, vol. 46, no. 10, pp. 58–65, 2008.

[20] V. Chandrasekhar and J. G. Andrews, "Uplink capacity and interference avoidance for two-tier cellular networks," in *IEEE Global Telecommunications Conference (GLOBECOM)*, pp. 3322–3326, Nov. 2007.

[21] *Navigating Operator Business Model Concerns for Femtocells*. Motorola. [Online] Available at `http://www.motorola.com/web/Business/Solutions/Technologies/Femtocells/_Documents/Staticfiles/Navigating_Operator_Bus_Model_Femtocell_558186-001-a.pdf`.

[22] M. Singh, "Top ten challenges to femtocell deployment," 2008. [Online] Availalbe at `http://www.itu.int/ITU-D/ict/publications/idi/2009/material/IDI2009\_w5.pdf`.

[23] V. Chandrasekhar, J. Andrews, T. Muharemovic, Z. Shen, and A. Gatherer, "Power control in two-tier femtocell networks," *IEEE Transactions on Wireless Communications*, vol. 8, no. 8, pp. 4316–4328, 2009.

[24] M. Yavuz, F. Meshkati, S. Nanda, A. Pokhariyal, N. Johnson, B. Raghothaman, and A. Richardson, "Interference management and performance analysis of UMTS/HSPA+ femtocells," *IEEE Communications Magazine*, vol. 47, no. 9, pp. 102–109, 2009.

[25] H.-S. Jo, J.-G. Yook, C. Mun, and J. Moon, "A self-organized uplink power control for cross-tier interference management in femtocell networks," in *IEEE Military Communications Conference (MILCOM)*, pp. 1–6, Nov. 2008.

[26] R. Kim, J. S. Kwak, and K. Etemad, "WiMAX femtocell: requirements, challenges, and solutions," *IEEE Communications Magazine*, vol. 47, no. 9, pp. 84–91, 2009.

[27] A. Golaup, M. Mustapha, and L. Patanapongpibul, "Femtocell access control strategy in umts and lte," *IEEE Communications Magazine*, vol. 47, no. 9, pp. 117–123, 2009.

[28] D. Lopez-Perez, A. Valcarce, G. De La Roche, E. Liu, and J. Zhang, "Access methods to WiMAX femtocells: A downlink system-level case study," in *IEEE Communication Systems (ICCS)*, pp. 1657–1662, Nov. 2008.

[29] M. Chowdhury, W. Ryu, E. Rhee, and Y. M. Jang, "Handover between macrocell and femtocell for UMTS based networks," in *IEEE Advanced Communication Technology (ICACT)*, pp. 237–241, Feb. 2009.

[30] H. Zhang, X. Wen, B. Wang, W. Zheng, and Y. Sun, "A novel handover mechanism between femtocell and macrocell for LTE based networks," in *International Conference on Communication Software and Networks*, Feb. 2010.

[31] G. Joshi, M. Yavuz, and C. Patel, "Performance analysis of active handoff in CDMA2000 femtocells," in *IEEE National Conference on Communications (NCC)*, pp. 1–5, Jan. 2010.

[32] J. Zhang and G. de la Roche, *Femtocells: Technologies and Deployment*. Wiley, Hoboken, NJ, Mar. 2010.

[33] D. H. Friend, *Cognitive Networks: Foundations to Applications*. Ph.D. dissertation, Virginia Polytechnic Institute and State University, 2009.

[34] L. Song and J. Shen, *Evolved Cellular Network Planning and Optimization for UMTS and LTE*. CRC Press (1st edition), Aug. 2010.

[35] L. Narayanan and S. M. Shende, "Static frequency assignment in cellular networks," *Algorithmica*, vol. 29, no. 3, pp. 396–409, 2001.

[36] J. Janssen, D. Krizanc, L. Narayanan, and S. Shende, "Distributed online frequency assignment in cellular networks," in *Symposium on Theoretical Aspects of Computer Science*, pp. 3–13, Feb. 1998.

[37] T. Nielsen, J. Wigard, and P. Mogensen, "On the capacity of a GSM frequency hopping network with intelligent underlay-overlay," in *IEEE Vehicular Technology Conference (VTC)*, pp. 1867–1871, May. 1997.

[38] H. Olofsson, J. Naslund, and J. Skold, "Interference diversity gain in frequency hopping GSM," in *IEEE Vehicular Technology Conference (VTC)*, pp. 102–106, Jul. 1995.

[39] J. Wigard, P. Mogensen, J. Johansen, and B. Vejlgaard, "Capacity of a GSM network with fractional loading and random frequency hopping," in *IEEE Personal, Indoor and Mobile Radio Communications (PIMRC)*, pp. 723–727, Oct. 1996.

[40] C. Carneheim, S.-O. Jonsson, M. Ljungberg, M. Madfors, and J. Naslund, "FH-GSM frequency hopping GSM," in *IEEE Vehicular Technology Conference (VTC)*, pp. 1155–1159, Jun. 1994.

[41] M. Buehrer and W. Tranter, *Code Division Multiple Access (CDMA)*. Morgan & Claypool Publishers (1st edition), Jul. 2006.

[42] A. Sampath, P. Sarath Kumar, and J. Holtzman, "Power control and resource management for a multimedia CDMA wireless system," in *IEEE Personal, Indoor and Mobile Radio Communications (PIMRC)*, pp. 21–25, Sept. 1995.

[43] L. Jorguseski, E. Fledderus, J. Farserotu, and R. Prasad, "Radio resource allocation in third generation mobile communication systems," *IEEE Communications Magazine*, vol. 39, no. 2, pp. 117–123, 2001.

[44] L. Ortigoza-Guerrero and A. Aghvami, "A distributed dynamic resource allocation for a hybrid TDMA/CDMA system," *IEEE Transactions on Vehicular Technology*, vol. 47, no. 4, pp. 1162–1178, 1998.

[45] K. Begain, G. I. Rozsa, A. Pfening, and M. Telek, "Performance analysis of GSM networks with intelligent underlay-overlay," in *International Symposium on Computers and Communications (ISCC)*, pp. 135–141, Sept. 2002.

[46] *3GPP TSG RAN WG1#42 R1-050764. Inter-cell interference handling for E-UTRA. Technical report.* Ericsson, 2005.

[47] M. C. Necker, "Coordinated fractional frequency reuse," in *ACM Symposium on Modeling, Analysis, and Simulation of Wireless and Mobile Systems*, pp. 296–305, 2007.

[48] S. Ali and V. Leung, "Dynamic frequency allocation in fractional frequency reused OFDMA networks," *IEEE Transactions on Wireless Communications*, vol. 8, no. 8, pp. 4286–4295, Aug. 2009.

[49] H. Jia, Z. Zhang, G. Yu, P. Cheng, and S. Li, "On the performance of IEEE 802.16 OFDMA system under different frequency reuse and subcarrier permutation patterns," in *IEEE International Conference on Communications (ICC)*, pp. 5720–5725, Jun., 2007.

[50] H. Lei, L. Zhang, X. Zhang, and D. Yang, "A novel multi-cell OFDMA system structure using fractional frequency reuse," in *IEEE International Symposium on Personal, Indoor and Mobile Radio Communications (PIMRC)*, pp. 1–5, Sept., 2007.

[51] A. Stolyar and H. Viswanathan, "Self-organizing dynamic fractional frequency reuse in OFDMA systems," in *IEEE International Conference on Computer Communications (INFOCOM)*, pp. 691–699, Apr., 2008.

[52] A. Stolyar and H. Viswanathan, "Self-organizing dynamic fractional frequency reuse for best-effort traffic through distributed inter-cell coordination," in *IEEE International Conference on Computer Communications (INFOCOM)*, pp. 1287–1295, Apr., 2009.

[53] Y.-J. Choi, C. S. Kim, and S. Bahk, "Flexible design of frequency reuse factor in OFDMA cellular networks," in *IEEE International Conference on Communications (ICC)*, pp. 1784–1788, Jun., 2006.

[54] H. Fujii and H. Yoshino, "Theoretical capacity and outage rate of ofdma cellular system with fractional frequency reuse," in *IEEE Vehicular Technology Conference*, pp. 1676–1680, May, 2008.

[55] B. Korte and J. Vygen, *Combinatorial Optimization: Theory and Algorithms, Second Edition*. Springer-Verlag, 2002.

[56] C. Weeraddana, W. Li, M. Codreanu, and M. Latva-aho, "Weighted sum-rate maximization for downlink OFDMA systems," in *Asilomar Conference on Signals, Systems and Computers*, pp. 990–994, Oct., 2008.

[57] Z. Mao and X. Wang, "Efficient optimal and suboptimal radio resource allocation in OFDMA system," *IEEE Transactions on Wireless Communications*, vol. 7, no. 2, pp. 440–445, Feb. 2008.

[58] S. Pietrzyk and G. Janssen, "Radio resource allocation for cellular networks based on OFDMA with qos guarantees," in *IEEE Global Telecommunications Conference (GLOBECOM)*, pp. 2694–2699, Nov., 2004.

[59] G. Li and H. Liu, "Downlink radio resource allocation for multi-cell OFDMA system," *IEEE Transactions on Wireless Communications*, vol. 5, no. 12, pp. 3451–3459, Dec. 2006.

[60] M. Yavuz, F. Meshkati, S. Nanda, A. Pokhariyal, N. Johnson, B. Raghothaman, and A. Richardson, "Interference management and performance analysis of UMTS/HSPA+ femtocells," *IEEE Communications Magazine*, vol. 47, no. 9, pp. 102–109, Sept. 2009.

[61] P. Humblet, B. Raghothaman, A. Srinivas, S. Balasubramanian, C. Patel, and M. Yavuz, "System design of cdma2000 femtocells," *IEEE Communications Magazine*, vol. 47, no. 9, pp. 92–100, Sept. 2009.

[62] D. López-Pérez, A. Valcarce, G. de la Roche, and J. Zhang, "OFDMA femtocells: A roadmap on interference avoidance," *IEEE Communications Magazine*, vol. 47, no. 9, pp. 41–48, Sept. 2009.

[63] R. Kim, J. S. Kwak, and K. Etemad, "WiMAX femtocell: requirements, challenges, and solutions," *IEEE Communications Magazine*, vol. 47, no. 9, pp. 84–91, Sept. 2009.

[64] P. Kulkarni, W. H. Chin, and T. Farnham, "Radio resource management considerations for LTE femto cells," in *ACM SIGCOMM Computer Communication Review*, pp. 26–30, Jan. 2010.

[65] K. Sundaresan and S. Rangarajan, "Efficient resource management in OFDMA femto cells," in *International Symposium on Mobile Ad Hoc Networking & Computing*, pp. 33–42, 2009.

[66] G. de la Roche, A. Valcarce, D. Lépez-Pérez, and J. Zhang, "Access control mechanisms for femtocells," *IEEE Communications Magazine*, vol. 48, no. 2, pp. 33–39, Feb. 2010.

[67] C.-Y. Oh, M. Y. Chung, H. Choo, and T.-J. Lee, "A novel frequency planning for femtocells in OFDMA-based cellular networks using fractional frequency reuse," *Computational Science and Its Applications (Lecture Notes in Computer Science)*, vol. 6018, pp. 96–106, Sept. 2010.

[68] V. Chandrasekhar and J. G. Andrews, "Spectrum allocation in tiered cellular networks," *IEEE Transactions On Communications*, vol. 57, no. 10, pp. 3059–3068, Oct. 2009.

[69] A. Simonsson, "Frequency reuse and intercell interference co-ordination in E-UTRA," in *IEEE Vehicular Technology Conference*, pp. 3091–3095, Apr. 2007.

[70] B. Fan, Y. Qian, K. Zheng, and W. Wang, "A dynamic resource allocation scheme based on soft frequency reuse of ofdma systems," in *IEEE International Symposium on Microwave, Antenna, Propagation and EMC Technologies for Wireless Communications*, pp. 1–4, Aug. 2007.

[71] S. H. Won, H. J. Park, J. O. Neel, and J. H. Reed, "Inter-cell interference coordination/avoidance for frequency reuse by resource scheduling in an ofdm-based cellular system," in *IEEE Vehicular Technology Conference*, pp. 1722–1725, Oct. 2007.

[72] L. T. W. Ho and H. Claussen, "Effects of user-deployed, co-channel femtocells on the call drop probablity in a residential scenario," in *IEEE Internaional Symposium on Personal, Indoor and Mobile Radio Communications*, Sept. 2007.

[73] H. Claussen, "Performance of macro-and co-channel femtocells in a hierarchical cell structure," in *IEEE Internaional Symposium on Personal, Indoor and Mobile Radio Communications*, Sept. 2007.

[74] R. Giuliano, P. Loreti, F. Mazzenga, and G. Santella, "Planning and performance evaluation of OFDM/OFDMA multi-carrier cellular systems with femto cells," in *International Conference on Wireless Communications and Mobile Computing*, pp. 1478–1482, 2009.

[75] P. Gupta and P. R. Kumar, "The capacity of wireless networks," *IEEE Transactions On Information Theory*, vol. 46, no. 2, pp. 388–404, Feb. 2000.

[76] S. Schmid and R. Wattenhofer, "Algorithmic models for sensor networks," in *Parallel and Distributed Processing Symposium, 2006. IPDPS 2006. 20th International*, p. 11 pp., 2006.

[77] E. Lebhar and Z. Lotker, "Unit disk graph and physical interference model: Putting pieces together," *Parallel and Distributed Processing Symposium, International*, vol. 0, pp. 1–8, 2009.

[78] D. B. West, *Introduction to Graph Theory*. Prentice Hall, second ed., 2000.

[79] B. Bollobás, *Random Graphs*. Cambridge University Press, second ed., 2001.

[80] D. W. Matula, "The employee party problem," *Notice of the American Mathematical Society*, vol. 19, no. 7, p. A382, 1972.

[81] C. McDiarmid, "On the chromatic number of random graphs," *Random Structures and Algorithms*, vol. 1, no. 4, pp. 435–442, 2006.

[82] *3GPP Technical Specification Group Radio Access Networks; Radio Frequency (RF) system scenarios (Release 7)*. 3GPP, 2007. [Online] Available at `http://www.3gpp.org/ftp/Specs/archive/25_series/25.942/25942-700.zip`.

[83] J. Keenan and A. J. Motley, "Radio coverage in buildings," *British Telccom Technology*, vol. 8, no. 1, pp. 19–24, 1990.

[84] *3GPP Technical Specification Group Radio Access Networks; FDD Base Station(BS) classification (Release 7)*. 3GPP, 2007. [Online] Available at `http://www.3gpp.org/ftp/Specs/archive/25_series/25.951/25951-700.zip`.

[85] P. Mani and D. Petr, "Clique number vs. chromatic number in wireless interference graphs: Simulation results," *IEEE Communication Letters*, vol. 11, no. 7, pp. 592–594, 2007.

[86] R. Schoenen, R. Halfmann, and B. H. Walke, "MAC performance of a 3GPP-LTE multihop cellular network," in *IEEE International Conference on Communications*, pp. 4819–4824, May. 2008.

[87] G. Li and H. Liu, "Downlink radio resource allocation for multi-cell OFDMA system," *IEEE TRANSACTIONS ON WIRELESS COMMUNICATIONS*, vol. 5, no. 12, pp. 3451–3459, 2006.

[88] B. Korte and J. Vygen, *Combinatorial Optimization: Theory and Algorithms*. Springer-Verlag, second ed., 2002.

[89] S. Ramanathan, "A unified framework and algorithm for channel assignment in wireless networks," *Wireless Networks*, vol. 5, no. 2, pp. 81–94, 1999.

[90] A. Federgruen and H. Groenevelt, "The greedy procedure for resource allocation problems: Necessary and sufficient conditions for optimality," *Operations Research*, vol. 34, no. 6, pp. 909–918, Nov. - Dec. 1986.

[91] J. Alcaraz and C. Maroto, "A robust genetic algorithm for resource allocation in project scheduling," *Annals of Operations Research*, vol. 102, no. 4, pp. 83–109, 2001.

[92] Y. Dai and X. Wang, "Optimal resource allocation on grid systems for maximizing service reliability using a genetic algorithm," *Reliability Engineering & System Safety*, vol. 91, no. 9, pp. 1071–1082, Sept. 2006.

[93] C. Ngo and V. Li, "Fixed channel assignment in cellular radio networks using a modified genetic algorithm," *IEEE Transactions on Vehicular Technology*, vol. 47, no. 1, pp. 163–172, Feb. 1998.

[94] A. Zomaya and M. Wright, "Observations on using genetic-algorithms for channel allocation in mobile computing," *IEEE Transactions on Parallel and Distributed Systems*, vol. 13, no. 9, pp. 948–962, Sept. 2002.

[95] D. H. Friend, M. Y. ElNainay, Y. Shi, and A. B. MacKenzie, "Architecture and performance of an island genetic algorithm-based cognitive network," in *IEEE Consumer Communications and Networking Conference (CCNC)*, pp. 993–997, Jan. 2008.

[96] R. L. Haupt and S. E. Haupt, *Practical Genetic Algorithms, Second Edition*. Wiley-Interscience, 2004.

[97] J. H. Holland, *Adaptation in Natural and Artificial Systems*. The University of Michigan Press, 1975.

[98] D. E. Goldberg, *Genetic Algorithms in Search, Optimization, and Machine Learning*. Addison-Wesley Professional, 1989.

[99] H. Claussen, "Distributed algorithms for robust self-deployment and load balancing in autonomous wireless access networks," in *IEEE International Conference on Communications (ICC)*.

[100] S. Kumar, V. Raghavan, and J. Deng, "Medium access control protocols for ad hoc wireless networks: A survey," *Elsevier Ad Hoc Networks*, vol. 4, no. 3, pp. 326–358, May. 2006.

[101] B. Raman, "Channel allocation in 802.11-based mesh networks," in *IEEE International Conference on Computer Communications (INFOCOM)*, pp. 1–10, Apr. 2006.

[102] W. R. da Silva and J. F. de Rezende, "A dynamic channel allocation mechanism for IEEE 802.11 networks," in *Internatonal Telecommunications Symposium*, pp. 225–230, Sept. 2006.

[103] K. K. Leung and B.-J. J. Kim, "Frequency assignment for IEEE 802.11 wireless networks," in *IEEE Vehicular Technology Conference*.

[104] D.Malone, P. Clifford, D.Reid, and D.J.Leith, "Experimental implementation of optimal WLAN channel selection without communication," in *IEEE International Symposium on New Frontiers in Dynamic Spectrum Access Networks (DySPAN)*, pp. 316–319, Apr. 2007.

[105] P. Kulkarni, W. H. Chin, and T. Farnham, "Radio resource management considerations for LTE femto cells," *ACM SIGCOMM Computer Communication Review*, vol. 40, no. 1, pp. 26–30, Jan. 2010.

[106] J. Ling, D. Chizhik, and R. Valenzuela, "On resource allocation in dense femto-deployments," in *IEEE International Conference on Microwaves, Communications, Antennas and Electronics Systems*, pp. 1–6, Nov. 2009.

[107] X. Chu, Y. Wu, Benmesbah, L. Benmesbah, and W.-K. Ling, "Resource allocation in hybrid macro/femto networks," in *IEEE Wireless Communication and Networking Conference Workshops*, pp. 1–5, Nov. 2010.

[108] D. López-Pérez, Ákos Ladányi, A. Júttner, and J. Zhang, "OFDMA femtocells: A self-organizing approach for frequency assignment," in *IEEE International Symposium on Personal, Indoor and Mobile Radio Communications (PIMRC)*, pp. 2202–2207, Sept. 2009.